ROLE OF END PEELING IN BEHAVIOR OF REINFORCED CONCRETE BEAMS WITH EXTERNALLY BONDED REINFORCEMENT

A Thesis
Presented to
The Academic Faculty

by

Christine L. Allen

In Partial Fulfillment
of the Requirements for the Degree
Master of Science in Civil Engineering in the
School of Civil and Environmental Engineering

Georgia Institute of Technology
May 2010

ROLE OF END PEELING IN BEHAVIOR OF REINFORCED CONCRETE BEAMS WITH EXTERNALLY BONDED REINFORCEMENT

Approved by:

Dr. Abdul-Hamid Zureick, Advisor
School of Civil and Environmental Engineering
Georgia Institute of Technology

Dr. Bruce R. Ellingwood, Advisor
School of Civil and Environmental Engineering
Georgia Institute of Technology

Dr. Rami M. Haj-Ali
School of Civil and Environmental Engineering
Georgia Institute of Technology

Date Approved: April 1, 2010

ACKNOWLEDGEMENTS

I wish to thank my advisors, Dr. Abdul-Hamid Zureick and Dr. Bruce R. Ellingwood, for their guidance throughout my research and in developing this thesis. I would also like to thank my father and mother for their continuous support.

TABLE OF CONTENTS

LIST OF TABLES

LIST OF FIGURES

LIST OF SYMBOLS

a = length of shear span (Eq. 2.7)

A = axial (tension) force in the externally bonded plate

A_s = cross-sectional area of flexural tension reinforcement (Eq. 2.8)

A_{se} = $\frac{1}{2}A_s$ = effective area of flexural tension reinforcement (Eq. 2.8)

A_v = cross-sectional area of the transverse reinforcement (Eq. 2.7)

b = width of the reinforced concrete beam (Eq. 2.8)

b_m = $\left(b + b_p\right)/2$ = effective width of plate-adhesive interface (Eq. 2.8)

b_p = width of external reinforcement (Eq. 2.8, 5.6)

c = depth of the compression zone in the reinforced concrete beam (Eq. 2.1, 2.3)

c_c = cover distance from the extreme concrete tension surface to the centroid of the flexural tension reinforcement (Eq. 2.8)

C = resultant compression force

d = $0.9h$ = effective depth of the reinforced concrete beam (Eq. 2.7)

d_b = diameter of flexural tension reinforcement (Eq. 2.8)

d_s = depth of the flexural tension reinforcement (Eq. 2.1, 2.3)

E_a = elastic modulus of the adhesive (Eq. 2.4, 2.6, 5.1, 5.3)

E_c = elastic modulus of the concrete

E_f = tensile modulus of elasticity of FRP (Eq. 2.2)

E_p = elastic modulus of the external reinforcement (Eq. 2.4, 2.5, 5.1, 5.2)

E_s = elastic modulus of the flexural tension reinforcement

f_c = concrete compressive stress

f'_c = compressive strength of concrete (Eq. 2.2, 2.8, 2.9, 5.5)

f''_c = maximum concrete compressive stress

f_{ce} = $\nu_c f'_c$ = effective compressive strength of concrete (Eq. 2.9)

f_{peel} = normal peeling stress in the adhesive (Eq. 2.4, 5.1, 5.4)

f_s = stress in the flexural tension reinforcement

f'_t = concrete tensile strength (Eq. 2.8, 2.9)

f_{yp} = yield strength of external steel reinforcement

f_y = yield strength of flexural tension reinforcement

f_{yt} = yield strength of the transverse reinforcement (Eq. 2.7)

G_a = shear modulus of the adhesive (Eq. 2.5, 2.6, 5.2, 5.3)

h = depth of the reinforced concrete beam (Eq. 2.1, 2.3, 2.5, 2.7, 5.2)

I_T = moment of inertia of an equivalent external reinforcement transformed section, neglecting any contribution of concrete in tension (Eq. 2.5, 5.2)

k = multiplier for locating the resultant compression force (Eq. 2.3)

k_1 = 0.8 = coefficient for crack spacing size (Eq. 2.8)

k_2 = 0.5 = coefficient for crack spacing size (Eq. 2.8)

l_a = length of the external reinforcement from the location of maximum moment into the shear span (Eq. 2.7)

l_c = crack spacing size (Eq. 2.6)

L = beam span length

L_d = minimum development length of external FRP reinforcement (Eq. 5.6)

M = bending moment

$M_{\exp}$ = experimental ultimate moment at the point of external reinforcement termination (Eq. 2.5)

M_n = nominal flexural strength (Eq. 2.1)

M_{th} = theoretical flexural capacity (Eq. 2.3)

M_u = factored moment at the point of external plate termination (Eq. 5.2)

n = number of plies of FRP reinforcement (Eq. 2.2)

p_y = $A_v f_{yt} / s$ = strength of the transverse reinforcement (Eq. 2.7)

P = applied load

$P_{\exp}$ = experimental load at ultimate failure

s = spacing of the transverse reinforcement (Eq. 2.7)

t_a = thickness of the adhesive (Eq. 2.4, 2.5, 5.1, 5.2)

t_f = nominal thickness of one ply of FRP reinforcement (Eq. 2.2)

t_p = thickness of the external reinforcement (Eq. 2.4, 2.5, 5.1, 5.2)

T = resultant tensile force from flexural tension reinforcement and external reinforcement

T_{FRP} = tensile force in the external FRP reinforcement corresponding to an FRP strain of 0.005 (Eq. 5.6)

T_p = tensile force in the external reinforcement (Eq. 2.1, 2.3)

T_s = tensile force in the flexural tension reinforcement (Eq. 2.1, 2.3)

U_y = bond strength (Eq. 2.7, 2.8)

V = shear force

$V_{\exp}$ = experimental ultimate shear force at the point of external reinforcement termination (Eq. 2.5)

V_{th} = theoretical shear force at the point of external reinforcement termination (Eq. 2.7)

V_u = factored shear force at the point of external reinforcement termination (Eq. 5.2)

y = distance from the extreme compression surface to the neutral axis of an equivalent concrete transformed section, neglecting any contribution of concrete in tension (Eq. 2.5, 5.2)

α = a/d = ratio of shear span to effective beam depth (Eq. 2.7)

β = l_a/d = ratio of plate length in shear span to effective beam depth (Eq. 2.7)

β_1 = factor for determining the concrete compression force (Eq. 2.1)

δx = length of an element of external reinforcement

ε_c = concrete strain

ε_{fd} = debonding strain of externally bonded FRP (Eq. 2.2)

ε_{fu} = design rupture strain of FRP reinforcement (Eq. 2.2)

ε_p = strain in the external reinforcement

ε_s = strain in the flexural tension reinforcement

ε_{ult} = ultimate concrete strain

ε_{yp} = strain in external steel plate at yield

ε_{ys} = strain in flexural tension reinforcement at yield

ε_0 = concrete strain corresponding to the maximum concrete stress

θ = angle between the concrete strut and the longitudinal axis of the beam

ν_a = Poisson's ratio of the adhesive, which may be taken as 0.35 (Eq. 2.6, 5.3)

ν_c = 0.7 = effectiveness factor for concrete (Eq. 2.9)

ρ_r = $A_{se}/(2.5bc_c)$ = effective tensile steel reinforcement ratio (Eq. 2.8)

τ = shear force per unit length in the adhesive layer

τ_a = shear stress in the adhesive (Eq. 2.4, 2.5, 5.1, 5.2)

τ_{int} = interfacial shear transfer strength (Eq. 5.4, 5.5, 5.6)

ϕ = U_y/p_y = ratio of bond strength to stirrup strength (Eq. 2.7)

ψ_f = strength reduction factor for external FRP reinforcement (Eq. 2.1)

SUMMARY

Aging bridges in the United States demand effective, efficient, and economical strengthening techniques to meet future traffic requirements. One such technique is to bond steel or fiber reinforced polymer (FRP) plates to the tension faces of reinforced concrete bridge beams with adhesives to strengthen them in flexure. However, beams that have been flexurally strengthened in this manner often fail prematurely, in particular by plate end peeling.

The benefits of flexural strengthening by externally bonded reinforcement can only be fully realized by preventing premature failure modes so as to allow the development of composite action between the beam and the external reinforcement. With this goal in mind, several critical limit states of externally reinforced beams are examined in this thesis. Models developed by Roberts (1989) and by Colotti, Spadea, and Swamy (2004) that predict premature plate end debonding are examined in depth using data from previously conducted experimental programs that employed both steel and FRP external reinforcement. In addition, various parameters of the concrete beam, adhesive, and external reinforcement are analyzed in each model to determine the role of each parameter in failure prediction.

A critical appraisal of the performance of the models using existing experimental data leads to the selection of the Roberts (1989) model. This model is used to develop recommended design guidelines for flexurally strengthening reinforced concrete bridge beams with externally bonded FRP plates and for preventing premature plate peeling.

CHAPTER 1

INTRODUCTION

1.1 Background

Transportation infrastructure in the United States is aging due to increasing traffic demands and deferred maintenance, leading to structural deterioration that may impair its function or, in extreme cases, endanger the public. Concrete bridge structures deteriorate for numerous reasons including corrosion of steel reinforcement, freeze-thaw action, expansive aggregate reactions, excessive loading and poor initial design and construction. In addition, many existing bridge structures have been designed to codes which are now outdated and have been in service for 50 (or more) years, during which time design loads have increased and design and construction practices have changed. For these reasons, many bridge structures are no longer considered adequate in terms of their load carrying capacity. If replacement is not practical or feasible, such bridges must be either be strengthened or posted to maintain highway service at an appropriate level of safety. Posting is undesirable because of its significant economic impact on the area served by the bridge. In the State of Georgia, for example, approximately 3800 bridges on the primary and secondary state system that were designed for archaic H15 or H20 loads and were constructed between 1945 and 1975 remain functional as of 2005. Approximately 2000 out of 9000 bridges in the state inventory have been posted.[1] Structural

[1] Wang, N. et al. (2009). "Condition assessment of existing bridge structures: Report of Task 1 – Appraisal of state-of-the-art of bridge condition assessment." GDOT Project RP05-01. (ftp://ftp.dot.state.ga.us/DOTFTP/Anonymous-Public/Research_Projects/)

strengthening is an attractive alternative to posting if the bridge is in otherwise good condition.

Structural strengthening generally is significantly more affordable than replacement and is environmentally preferable, particularly if rapid, effective and simple strengthening methods are available. The choice between upgrading and replacement is based on factors specific to each individual case, but certain issues are considered in every case. Such issues include the length of time during which the bridge will be out of service or will provide reduced service and the relative costs of upgrading and replacement in terms of labor and materials. The need to upgrade bridges is worldwide, placing considerable importance on upgrading techniques.

One of several available rehabilitation practices for flexural strengthening is to bond external reinforcement to the soffits of reinforced concrete beams. The bonding of external reinforcement, either steel or fiber reinforced polymer (FRP) plates, to increase the flexural capacity of a reinforced concrete beam is an ideal retrofit method because it is simple, can be applied quickly, does not significantly alter the height of the structure, and can be performed while the structure is still in service.

Steel plates were the first to be used as external reinforcement to flexurally strengthen reinforced concrete bridge beams. While flexural strengthening using externally bonded steel plates has been successful in practice, the technique also has disadvantages. Because the steel plates are exposed to the external environment, the possibility of corrosion exists. Corrosion can adversely affect bond strength and durability, leading to failure of the strengthening system. In addition, steel plates are difficult to form to intricate girder profiles. Because steel plates tend to be heavy, they

are troublesome to transport and handle on site, especially in areas of limited access. Extensive shoring is required to hold the steel plates in the position while the adhesive cures. When beam spans are greater than the length of the steel plates, plate joints are required. Welding at the joints would destroy the adhesive bond. Consequently, lapped joints have to be formed. Therefore, the application of steel plates for strengthening can be labor intensive.

Fiber reinforced polymer reinforcement was introduced to overcome some of the disadvantages of steel plates in strengthening applications. Because FRP reinforcement is versatile and lightweight, it is easier to handle than steel reinforcement and may be placed without the use of extensive formwork. As a result, the application of FRP plates for flexural strengthening is less labor intensive, reducing labor costs and time. Unlike steel plates, FRP plates with great lengths are available and can be cut to size in the field. Finally, the critical advantage of FRP reinforcement over steel reinforcement is corrosion resistance. Exposed external reinforcement is highly susceptible to deterioration due to chloride from deicing salts and marine environments. FRP has been demonstrated in research and field applications to have superior resistance to corrosion when compared to steel.

1.2 Research Objectives and Scope

The research described herein investigates the performance of reinforced concrete beams which have been strengthened through externally bonded reinforcement, consisting of either fiber reinforced polymers or steel plates. To ensure adequate flexural strengthening, premature failure modes must be prevented to achieve full flexural capacity. The research herein examines models to predict premature plate end peeling,

which is known to be a significant consideration in the proper design of externally bonded strengthening systems. The formulations for predicting plate end peeling are evaluated using previous studies that have been conducted with external reinforcement. The effects of various parameters such as the concrete, adhesive, and external reinforcement which influence peeling behavior will be investigated. A model will be selected to recommend design guidelines to prevent plate end peeling failure of reinforced concrete beams flexurally strengthened with externally bonded FRP reinforcement.

1.3 Organization of Thesis

The remainder of this thesis is organized into five chapters. Chapter 2 presents the governing limit states for beams that have been flexurally strengthened with externally bonded reinforcement and introduces models which have been developed for failure prediction. Chapter 3 provides an overview of relevant literature which will be used in data analysis to critically evaluate the failure prediction models introduced in Chapter 2. Chapter 4 provides a detailed description of the data analysis, leading to a recommended model for design to prevent premature plate end debonding of external FRP reinforcement. Chapter 5 outlines guidelines for the Georgia Department of Transportation (GDOT) to use for design of externally bonded FRP reinforcement for flexural strengthening of simple-span reinforced concrete bridge beams and slabs. Lastly, Chapter 6 summarizes the conclusions and recommendations resulting from this research.

CHAPTER 2

BEHAVIOR OF REINFORCED CONCRETE MEMBERS STRENGTHENED WITH EXTERNALLY BONDED REINFORCEMENT

The limit states of reinforced concrete members that have been flexurally strengthened using externally bonded FRP or steel plates will be reviewed in this chapter. Members that have been strengthened in flexure with external reinforcement may fail prematurely, most commonly by debonding and sometimes by FRP failure prior to developing their intended flexural capacity. Recent research has focused on the use of external reinforcement for the rehabilitation of reinforced concrete members to anticipate and suppress premature failure modes.

2.1 Current Practices using Externally Bonded Reinforcement

Current guidelines for flexural strengthening with FRP are provided by the American Concrete Institute (ACI) Committee 440 report (2008), *Guide for the Design and Construction of Externally Bonded FRP Systems for Strengthening Concrete Structures*. The *Guide* is based on the notions of strength-design, similar to ACI Standard 318-05 (2005), which requires that the design flexural strength of a member exceed its required flexural strength. The *Guide* recommends using load factors as outlined by ACI 318-05 (2005) in computing the required flexural strength. In computing the design flexural strength, the nominal flexural strength is multiplied by a strength-reduction factor for conservatism. An additional strength reduction factor, ψ_f, is applied to the contribution of the FRP reinforcement to achieve the desired reliability

in strength and to account for premature failure modes, such as end peeling. Using this additional reduction factor, the nominal flexural strength of a reinforced concrete beam with externally bonded FRP reinforcement is given by

$$M_n = T_s\left(d_s - \frac{\beta_1 c}{2}\right) + \psi_f T_p\left(h - \frac{\beta_1 c}{2}\right) \tag{2.1}$$

in which

c = depth of the compression zone in the reinforced concrete beam, mm (in.)

d_s = depth of the flexural tension reinforcement, mm (in.)

h = depth of the reinforced concrete beam, mm (in.)

M_n = nominal flexural strength, N-mm (k-in.)

T_p = tensile force in the external reinforcement, N (kips)

T_s = tensile force in the flexural tension reinforcement, N (kips)

β_1 = factor for determining the concrete compression force

ψ_f = strength reduction factor for external FRP reinforcement

The strength reduction factor is intended to reflect the contribution of the FRP reinforcement to the reliability of the beam in flexure, and it accounts for the premature delamination failure observed for FRP strengthened members. The *Guide* recommends a reduction factor of $\psi_f = 0.85$ to be used for design.

In order to prevent premature FRP debonding failure, the *Guide* recommends that the strain of the FRP reinforcement be limited to the following value (in SI units):

$$\varepsilon_{fd} = 0.41\sqrt{\frac{f'_c}{nE_f t_f}} \le 0.9\varepsilon_{fu} \qquad (2.2)^{2}$$

in which

E_f = tensile modulus of elasticity of FRP, MPa (psi)

f'_c = compressive strength of concrete, MPa (psi)

n = number of plies of FRP reinforcement

t_f = nominal thickness of one ply of FRP reinforcement, mm (in.)

ε_{fd} = debonding strain of externally bonded FRP, mm/mm (in./in.)

ε_{fu} = design rupture strain of FRP reinforcement, mm/mm (in./in.)

The debonding strain equation proposed by Teng et al. (2003, 2004) was modified to generate Equation (2.2) above. The *Guide* also notes that composite behavior of the beam and FRP reinforcement is improved with end anchorage. Greater strains in the FRP reinforcement are reached at the point of debonding failure, provided that the plate ends have been anchored.

Research has been ongoing since the publication of the *Guide* to attain a better understanding of beam behavior with externally bonded reinforcement. While most failure mechanisms had been identified at the time when the guidelines were drafted, further research was needed to reasonably predict premature failure, especially plate end delamination.

---

[2] In English units: $\varepsilon_{fd} = 0.083\sqrt{\frac{f'_c}{nE_f t_f}} \le 0.9\varepsilon_{fu}$

The behavioral limit states of concrete members flexurally strengthened with externally bonded reinforcement will be discussed in the subsequent sections. Prediction models for premature failure modes will be presented and then evaluated using the experimental test programs detailed in Chapter 3.

2.2 Behavior of Beams with Externally Bonded Reinforcement

Classical beam theory, reflected in the Euler-Bernoulli Beam model, provides a simplified means of calculating the load and deflection characteristics of beams under externally applied load. Classical beam theory can be extended to the analysis of beams with externally bonded reinforcement, using the underlying assumption of the theory: that transverse plane sections remain plane and normal to the longitudinal axis of the beam during and after bending. However, if composite action between the concrete and the internal or external reinforcement is not maintained, then classical beam theory can no longer be applied to predict the behavior of the beam.

The flexural behavior of reinforced concrete beams with externally bonded steel or FRP plates can be described by the following limit states:

1. Concrete crushing in compression
2. Plate debonding between the plate ends
3. Plate end delamination with or without concrete cover separation
4. Interlaminar failure of an FRP plate with multiple reinforcement layers
5. Failure of the FRP plate in tension

The distinctive features of these five limit states are summarized in the following sections.

2.2.1 Concrete Crushing in Compression

Concrete crushing in compression occurs when the concrete reaches an ultimate compressive strain, which can range from values of 0.003 to 0.008 (ACI 318-05 Commentary Section R10.2.6); however, the maximum usable strain specified by ACI 318-08 (2008) for design is 0.003. This flexural failure may be preceded by yielding of the tension and/or compression reinforcement, as well as yielding of the external reinforcement if steel plates have been used. In order for an externally reinforced concrete beam to fail in this mode, composite action of the concrete beam with the external reinforcement must be maintained. In this case, plate debonding from the adhesive and/or concrete does not occur, and the beam may undergo large deflections with considerable strain in the external reinforcement. This is the ideal situation where the externally reinforced concrete beams behave in a ductile fashion and achieve full flexural capacity.

The member flexural strength can be calculated from the stress distribution shown in Figure 2.1a using a linear distribution of strain. This is a realistic stress distribution that can be used when the compressive strain in the concrete compression zone falls below the limiting design strain of 0.003. The stress-strain curve which has been adopted (Todeschini et al., 1964) is illustrated in Figure 2.1b. This nonlinear model is given by one continuous function which uses the following notation for stress and strain:

f_c = concrete compressive stress

f'_c = compressive strength of concrete

f''_c = maximum concrete compressive stress

ε_c = concrete strain

ε_0 = concrete strain corresponding to the maximum concrete stress

ε_{ult} = ultimate concrete strain

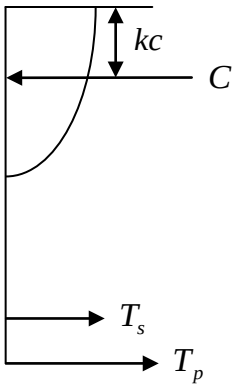

Figure 2.1a. Compressive Stress Distribution and Resultant Compression Force

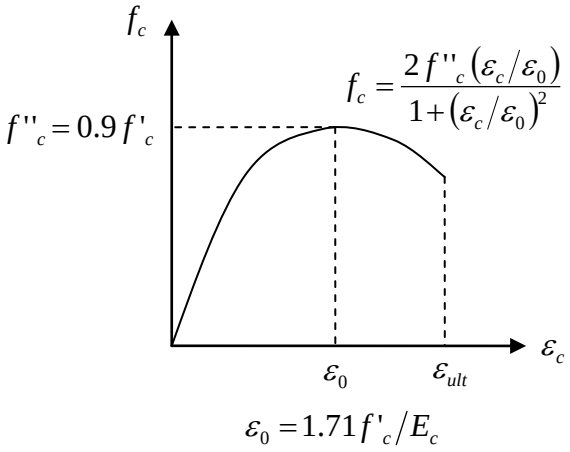

Figure 2.1b. Nonlinear Compressive Stress-Strain Curve for Concrete

At the highest point of the stress-strain curve, when $f''_c = 0.9 f'_c$, the stress-block properties are similar to that of the rectangular stress-block when $\varepsilon_{ult} = 0.003$.

Assuming composite action, the flexural strength of an externally reinforced concrete beam can be calculated using force equilibrium and strain compatibility, resulting in the equation:

$$M_{th} = T_s(d_s - kc) + T_p(h - kc) \tag{2.3}$$

in which

c = depth of the compression zone in the reinforced concrete beam, mm (in.)

d_s = depth of the flexural tension reinforcement, mm (in.)

h = depth of the reinforced concrete beam, mm (in.)

k = multiplier for locating the resultant compression force

M_{th} = theoretical flexural capacity, N-mm (kip-in.)

T_p = tensile force in the external reinforcement, N (kips)

T_s = tensile force in the flexural tension reinforcement, N (kips)

2.2.1.1 Jones, Swamy, and Charif (1988) Study

The importance of composite action when determining the flexural capacity of an externally reinforced concrete beam using force equilibrium has been demonstrated by Jones et al. (1988), who tested seven reinforced concrete beams with steel plates bonded to their soffits. The results of the test program are summarized in Table 2.1 on the following page. The beams had simple spans of 2300 mm (90.55 in.). They were tested in four-point bending, with loads at one-third and two-thirds span length. The externally bonded steel plates were terminated 50 mm (1.97 in.) from the supports. Four of the test specimens, specimens F34 through F37, used end anchorage for the external

reinforcement to prevent premature failure by debonding. The remaining three, specimens F31, F32, and F33, did not use any end anchorage and experienced plate end debonding before their full flexural capacity was reached. The ratio of the ultimate experimental moment, $M_{\exp}$, to the theoretical flexural capacity, M_{th}, at the point of external reinforcement termination was much less than 1.0, ranging from 0.66 to 0.75, for these three specimens. Appendix A supplies sample calculations for computing the theoretical flexural strength using equation (2.2).

Specimens F34 and F35 used steel bolts for end anchors, which enabled composite action of the reinforced concrete beam with the steel plate to be maintained up to approximately 90% of the ultimate experimental load. At this point, sudden plate end debonding took place over a length of approximately 12 inches (305 mm) within the shear span. The anchor bolts prevented complete plate separation, allowing the beams to carry more load. Ultimate failure occurred by crushing of the concrete without yielding of the external steel plate. The ratios of experimental to theoretical ultimate moment of 0.8 for these two specimens were markedly greater than the ratios for the specimens without end anchorage.

In contrast, specimens F36 and F37 used steel anchor plates at the ends of the external reinforcement. The steel anchor plates were bent in an L-shape and adhered to the sides of the beam and the bottom of the external reinforcement. Two anchor plates were used at each end of the external reinforcement, one on either side of the specimen. Specimens F36 and F37 reached their full flexural capacity, maintaining composite beam action and undergoing concrete crushing without yielding of the external steel

reinforcement. The experimental to theoretical ultimate moment ratios were slightly greater than 1.0 for specimens F36 and F37.

Table 2.1. Experimental vs. Theoretical Moment Capacity (Jones et al., 1988)

Specimen Number	M_{exp} *@ Pl End (kip-in.)*	M_{th} *@ Pl End (kip-in.)*	$\frac{M_{exp}}{M_{th}}$	*End Anchorage*	*Failure Mode*
F31	40.3	61.0	0.66	None	Peel
F32	46.0	61.6	0.75	None	Peel
F33	42.3	61.0	0.69	None	Peel
F34	48.9	61.0	0.80	Bolts	Peel/Crush
F35	50.2	61.6	0.81	Bolts	Peel/Crush
F36	63.1	61.0	1.03	Steel Plates	Crush
F37	62.6	61.0	1.03	Steel Plates	Crush

2.2.1.2 Duthinh and Starnes (2004) Study

Like the study by Jones et al. (1988), the experimental program conducted by Duthinh and Starnes (2004) utilized plate end anchorage to prevent premature peeling failure. The program consisted of eight specimens; however, only six of the eight were flexurally strengthened and tested. These six specimens were strengthened with carbon FRP plates and tested in four-point bending. The length between simple supports was 2750 mm (108.3 in.). The shear spans were 815 mm (32.09 in.). The external reinforcement was terminated in the shear spans, 50 mm (1.97 in.) from the supports. Specimens 4a, 6, and 7N were clamped at the plate ends, while specimens 4b, 5, and 6 used carbon FRP U-wraps as end anchors.

The results from the experimental program are summarized in Table 2.2. Although the carbon FRP plate ends were anchored, specimens 4a and 5 failed prematurely due to plate end peeling without concrete cover separation. In both cases,

the failure was abrupt with no signs of concrete crushing. The experimental moments at the plate end when debonding failure occurred were approximately 80% of the beams' theoretical flexural strength.

Specimens 4b, 7N, and 8N all failed due to crushing of the concrete. Although shear cracking and localized plate debonding was observed with specimens 7N and 8N, complete debonding was prevented and the intended flexural capacity was achieved. The ratio of experimental to theoretical ultimate moment at the plate end was slightly greater than 1.0 for specimens 4b, 7N, and 8N.

Specimen 6 was unique in that it failed due to interlaminar slip within the thickness of the carbon FRP plate; however, the experimental moment at failure was slightly greater than theoretical ultimate moment. The test description noted that the compression face concrete at the midspan was spalling and severely distressed just before failure. When the specimen was removed from the test rig, two parallel vertical cracks at the load points and a horizontal crack at the level of the longitudinal reinforcement connected, causing a large rectangular section of the beam to fall off. Based on this test description, the specimen may have been near the concrete crushing limit state before interlaminar failure of the FRP occurred.

Table 2.2. Experimental vs. Theoretical Moment Capacity (Duthinh and Starnes, 2004)

Specimen Number	M_{exp} *@ Pl End (kip-in.)*	M_{th} *@ Pl End (kip-in.)*	$\frac{M_{exp}}{M_{th}}$	*End Anchorage*	*Failure Mode*
4a	50.8	64.0	0.79	Clamps	Peel
4b	82.0	81.6	1.01	FRP Wraps	Crush
5	63.5	75.2	0.84	FRP Wraps	Peel
6	80.4	79.8	1.01	Clamps	FRP Slip
7N	97.2	93.4	1.04	Clamps	Crush
8N	110.8	109.1	1.01	FRP Wraps	Crush

2.2.2 Plate Debonding between Plate Ends

Plate debonding between plate ends is typically induced by a shear crack or notch forming in the beam soffit at the concrete/adhesive interface at a location along the length of the beam. A redistribution of strain in the plate occurs to cause peeling of the plate (Hollaway and Leeming, 1999). Peeling can then continue along the length of the plate toward the supports. Similar to concrete crushing in compression, this limit state can be analyzed using classical beam theory, which assumes strain compatibility and equilibrium of forces.

2.2.3 Plate End Debonding with or without Concrete Cover Separation

The plate end debonding limit state is the primary focus of this research, as this failure mode is sudden and can be catastrophic. Many parameters, including the geometry of the beam, material properties, and properties of the internal and external reinforcement, affect plate end debonding failure. Peeling is induced by areas of high stress concentrations, some normal to the plate, at the point of termination of the external reinforcement (Hollaway and Leeming, 1999) and may occur with or without concrete cover separation.

Plate end peeling with concrete cover separation has been observed in experimentation with both steel (Jones et al., 1988; Oehlers and Moran, 1990) and FRP external reinforcement (Malek et al., 1998; Yao and Teng, 2007). Cracking at the ends of the external reinforcement initiates this failure mode. Once the cracks in the concrete cover have reached the level of the longitudinal reinforcement, they may propagate toward the beam midspan causing bond loss between the concrete and longitudinal reinforcement. When the distance from the support to the plate end is great, such as

when the external reinforcement is terminated in the constant moment region, plate end peeling with concrete cover separation is likely to occur (Oehlers and Moran, 1990; Yao and Teng, 2007).

Like debonding with concrete cover separation, plate end interfacial debonding begins with cracking at the plate ends. The cracks instead propagate along the interface of the concrete and the plate, never reaching the level of the longitudinal reinforcement. According to Yao and Teng (2007), plate end debonding without concrete cover separation is most likely to occur when the width of the plate is significantly less than the width of the beam.

Plate end debonding is an abrupt failure mechanism that must be prevented. Two models which have been developed for peeling failure prediction are presented in the following sub-sections

2.2.3.1 Roberts (1989)

The model by Roberts (1989) is based on partial interaction theory. Because stress concentration at the external plate ends can lead to plate end debonding, Roberts aimed to develop approximate formulae for computing the plate end shear and normal stresses at the point of peeling failure. Roberts' analysis considered composite action of the reinforced concrete beam with external steel reinforcement (Figure 2.2a) and the boundary conditions where the external reinforcement terminates. Figure 2.2b depicts the internal forces in the flexurally strengthened beam used in analysis, where

A = axial (tension) force in the externally bonded plate

M = bending moment

V = shear force

δx = length of an element of external reinforcement

τ = shear force per unit length in the adhesive layer

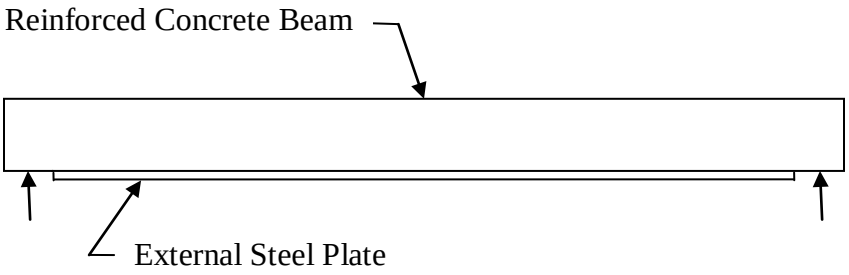

Figure 2.2a. Reinforced Concrete Beam with Bonded Steel Plate

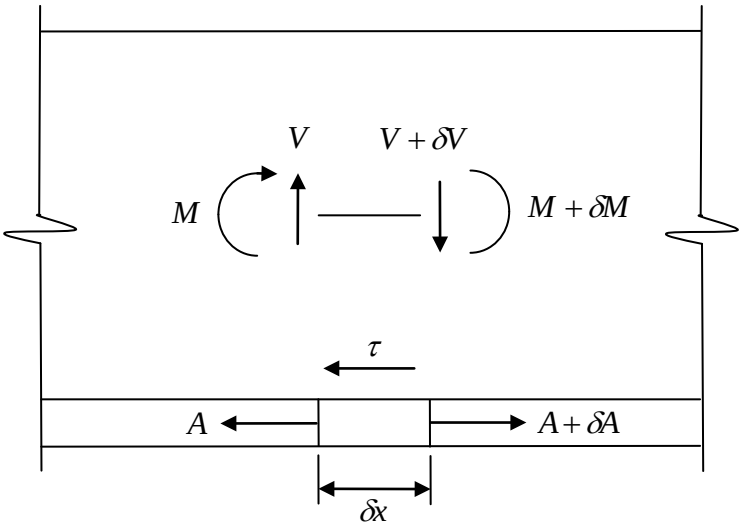

Figure 2.2b. Resultant Forces in Plated Concrete Beam

The derivation of the prediction formulae assumed linearly elastic behavior of materials up to the point of failure, and the contribution of the internal steel reinforcement was ignored. Finally, tension forces within the external reinforcement were assumed to vanish at the points of termination. Equations adopted from Roberts

(1989) model for computing the normal and shear peeling stresses (f_{peel} and τ_a) at the point of termination of the external reinforcement are

$$f_{peel} = \tau_a \left[\left(\frac{3E_a}{E_p} \right) \frac{t_p}{t_a} \right]^{1/4} \tag{2.4}$$

$$\tau_a = \left[V_{\exp} + \left(\frac{G_a}{E_p t_p t_a} \right)^{1/2} M_{\exp} \right] \frac{t_p \left[h + \left(t_p / 2 \right) - y \right]}{I_T} \tag{2.5}$$

in which

$$E_a = 2G_a(1+\nu_a) \tag{2.6}$$

and

E_a = elastic modulus of the adhesive, MPa (ksi)

E_p = elastic modulus of the external reinforcement, MPa (ksi)

f_{peel} = normal peeling stress in the adhesive, MPa (ksi)

G_a = shear modulus of the adhesive, MPa (ksi)

h = depth of the reinforced concrete beam, mm (in.)

I_T = moment of inertia of an equivalent external reinforcement transformed section, neglecting any contribution of concrete in tension, mm^4 ($in.^4$)

$M_{\exp}$ = experimental ultimate moment at the point of external plate termination, N-mm (kip-in.)

t_a = thickness of the adhesive, mm (in.)

t_p = thickness of the external reinforcement, mm (in.)

$V_{\exp}$ = experimental ultimate shear force at the point of external reinforcement termination, N (kips)

y = distance from the extreme compression surface to the neutral axis of an equivalent concrete transformed section, neglecting any contribution of concrete in tension, mm (in.)

ν_a = Poisson's ratio of the adhesive, which may be taken as 0.35

τ_a = shear stress in the adhesive, MPa (ksi)

2.2.3.2 Colotti, Spadea, and Swamy (2004)

The model presented by Colotti, Spadea, and Swamy (Colotti and Spadea, 2001; Colotti et al., 2004) idealizes the mechanism of bond transfer at the plate/concrete interface. The model relates force transfer, equilibrium, and plasticity conditions to attain the ultimate shear force corresponding to plate end peeling failure. The theoretical shear force, V_{th}, at which premature plate delamination occurs is given by the equation

$$V_{th} = p_y d\left[\phi + \alpha - \sqrt{(\phi+\alpha)^2 - 2\phi\beta}\right];\ p_y > 0 \tag{2.7a}$$

where

$$p_y = A_v f_{yt}/s \tag{2.7b}$$

$$d = 0.9h \tag{2.7c}$$

$$\phi = U_y/p_y \tag{2.7d}$$

$$\alpha = a/d \tag{2.7e}$$

$$\beta = l_a/d \tag{2.7f}$$

and the bond strength, U_y, is the minimum of (2.8a) and (2.8b)

$$U_y = b_m\left[2.77 + 0.06\left(f'_c - 20\right)\right];\ f'_c > 20MPa \tag{2.8a}$$ [3]

[3] In English units: $U_y = b_m\left[0.40175 + 0.06\left(f'_c - 2.9\right)\right];\ f'_c > 2.9ksi$

$$U_y = \frac{f'_t \, l_c b}{6 c_c} \tag{2.8b}$$

where

$$b_m = \left(b + b_p\right)/2 \tag{2.8c}$$

$$l_c = 50 + 0.25 k_1 k_2 d_b / \rho_r \tag{2.8d}$$ [4]

$$\rho_r = A_{se} / \left(2.5 b c_c\right) \tag{2.8e}$$

$$A_{se} = \frac{1}{2} A_s \tag{2.8f}$$

in which

a = length of shear span, mm (in.)

A_s = cross-sectional area of flexural tension reinforcement, mm^2 (in.^{2})

A_{se} = effective area of flexural tension reinforcement, mm^2 (in.^{2})

A_v = cross-sectional area of the transverse reinforcement, mm^2 (in.^{2})

b = width of the reinforced concrete beam, mm (in.)

b_m = effective width of plate-adhesive interface, mm (in.)

b_p = width of external reinforcement, mm (in.)

c_c = cover distance from the extreme concrete tension surface to the centroid of the flexural tension reinforcement, mm (in.)

d = effective depth of the reinforced concrete beam, mm (in.)

d_b = diameter of flexural tension reinforcement, mm (in.)

f'_c = compressive strength of concrete, MPa (ksi)

[4] In English units: $l_c = 1.9685 + 0.25 k_1 k_2 d_b / \rho_r$

f'_t = concrete tensile strength, MPa (ksi)

f_{yt} = yield strength of the transverse reinforcement, MPa (ksi)

h = depth of the reinforced concrete beam, mm (in.)

k_1 = 0.8 = coefficient for crack spacing size

k_2 = 0.5 = coefficient for crack spacing size

l_a = length of the external reinforcement from the location of maximum moment into the shear span, mm (in.)

l_c = crack spacing size, mm (in.)

p_y = strength of the transverse reinforcement, N/mm (kips/in.)

s = spacing of the transverse reinforcement, mm (in.)

U_y = bond strength, N/mm (kips/in.)

V_{th} = theoretical shear force at the point of external reinforcement termination, N (kips)

ρ_r = effective tensile steel reinforcement ratio

If the concrete tensile strength, f'_t, is unknown, it may be taken as (in SI units)

$$f'_t = 1.3 * 0.3 f_{ce}^{2/3} \qquad (2.9a)$$ [5]

where

$$f_{ce} = \nu_c f'_c \qquad (2.9b)$$

in which

f_{ce} = effective compressive strength of concrete, MPa (ksi)

ν_c = 0.7 = effectiveness factor for concrete

[5] In English units: $f'_t = 0.2049 * f_{ce}^{2/3}$

The bond transfer mechanism is characterized by slippage of the plate within the shear span. The bond strength is assumed to have reached its ultimate value at the point of slippage, while the stirrups at the crack locations have reached their yield strength. Two equations to determine the limiting bond strength are provided in the model. They characterize the two types of debonding failure, with and without concrete cover separation.

The failure mechanism of plate end interfacial debonding depends on the aspects of the adhesive-concrete interface. The limiting bond strength without concrete cover separation proposed by Colotti et al. (2004) is derived from experimental results obtained from a series of pull-out tests (Swamy et al., 1986) and is given by Equation (2.8a).

For the limiting bond strength of end-plate delamination with concrete cover separation, a simple strut-and-tie model was adopted. Analysis of the concrete behavior begins in the region between the external plate and the internal reinforcement, which allows the evaluation of the tangential interface stress using a strut-and-tie schematic, as seen in Figure 2.3 under an applied load, P. The idealized plane truss consists of an upper chord (compression concrete), lower chord (internal and external flexural reinforcement assuming perfect bonding), and web elements in compression (concrete struts) and tension (shear reinforcement assuming closely spaced stirrups). The concrete compression struts form an angle, θ, with respect to the longitudinal axis of the beam. The contribution of the internal longitudinal reinforcement at the ultimate state is neglected when plate end debonding is the failure mode.

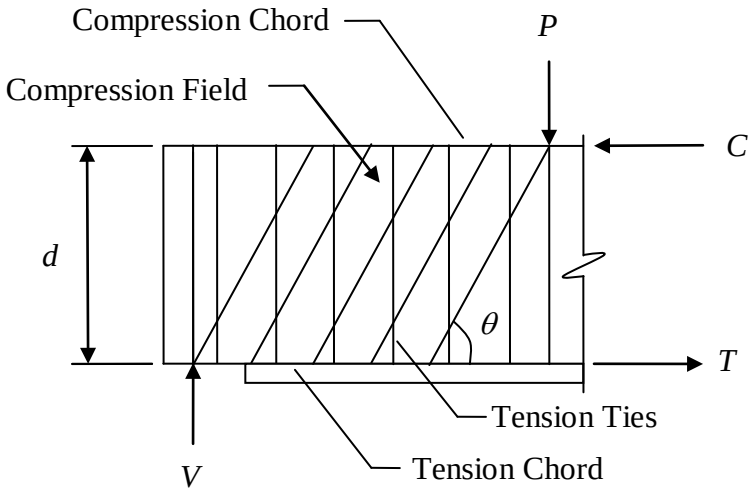

Figure 2.3. Strut-and-Tie Schematic for Flexurally Strengthened Beams

Considering a concrete element within the cover as a portion of plate subjected to in-plane shear forces along its boundary, the limiting bond strength for plate end debonding with concrete cover separation is given by Equation (2.8b).

2.2.4 Interlaminar Failure of an FRP Plate

Section 2.2.1.2 noted that specimen 6, which was strengthened with an externally bonded carbon FRP plate, of the study by Duthinh and Starnes (2004) failed due to interlaminar slip. Interlaminar failure of an FRP plate is a shear failure, causing slippage between layers of a multiple layer FRP plate. Unlike external steel plates, FRP plates have through-thickness material properties that are different from their in-plane properties. This failure mode is greatly influenced by the properties of the plate resin, but the strengths between fiber reinforcement layers can be lower than the strengths of the resin alone due to stress concentrations around the fibers.

2.2.5 Failure of an FRP Plate in Tension

Failure of an externally bonded FRP plate in tension occurs when the strain in the FRP plate reaches its limiting rupture strain. The rupture strain for FRP plates varies and is dependent upon fiber type. For carbon fiber FRP, the rupture strain is typically between 0.01 and 0.015 (GangaRao et al., 2007). This failure mode occurs when the concrete beam is under-reinforced and is likely to be preceded by yielding of the flexural steel reinforcement.

2.3 Summary

Guidelines currently in place in the U.S. for flexural strengthening with FRP systems must account for uncertainties in strength prediction due to premature failure modes, particularly plate end peeling. As the studies by Jones et al. (1988) and Duthinh and Starnes (2004) have shown, maintaining composite beam action is crucial for achieving the full flexural capacity of an externally reinforced concrete beam. Because plate end peeling is a likely premature failure mode that is abrupt, two models have been proposed for its prediction. The plate end debonding models proposed by Roberts (1989) and Colotti et al. (2004) will be assessed using the studies detailed in Chapter 3.

CHAPTER 3

EXPERIMENTAL STUDIES ON EXTERNALLY BONDED REINFORCEMENT

Beams can be strengthened with externally bonded steel plates or fiber-reinforced polymeric plates. A review of the literature on both strengthening methods was performed. Test data from the literature was used to evaluate the behavioral models from Chapter 2 and to identify their advantages and limitations as design tools. Brief descriptions of the test data from the literature are provided in the following sections; Appendix B tabulates the test data used in the model examination and validation.

3.1 Strengthening with Externally Bonded Steel Plates

3.1.1 Swamy, Jones, and Bloxham (1987)

Twenty-four rectangular reinforced concrete beams were tested in four-point bending. The beams spanned 2300 mm (90.55 in.) between simple supports, and the shear spans were 767 mm (30.20 in.) in length. A diagram of the experimental set-up is shown in Figure 3.1a. All beams had cross-sectional dimensions of 155 x 255 mm (6.10 x 10.04 in.) and were 2500 mm (98.43 in.) in length. Three 20 mm (0.79 in.) bars were used as flexural tension reinforcement. They were placed at a depth of 220 mm (8.66 in.). Closed stirrups, 6 mm (0.24 in.) in diameter, were spaced at 75 mm (2.95 in.) in the shear spans. Figure 3.1b shows a typical cross-section. Test data for the beams are summarized in Table B.1 of Appendix B.

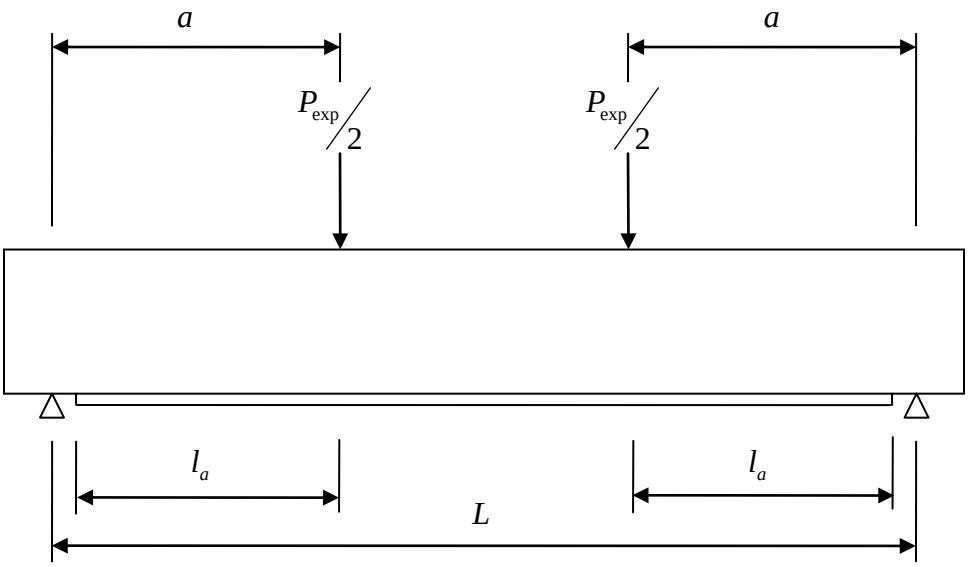

Figure 3.1a. Experimental Set-up used by Swamy et al. (1987)

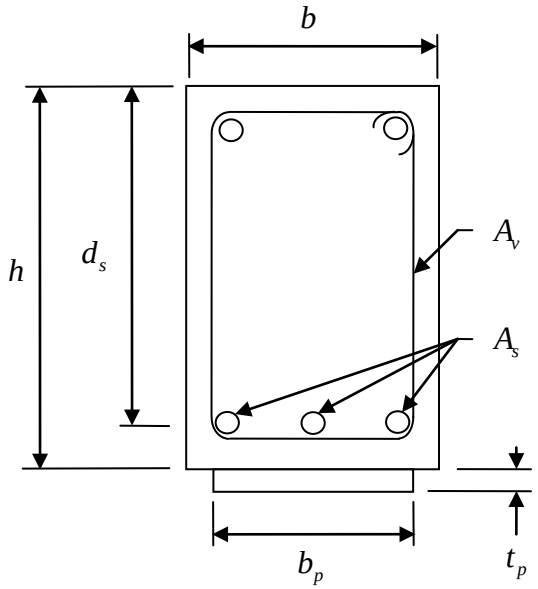

Figure 3.1b. Typical Specimen Cross-Section used by Swamy et al. (1987)

Two of the twenty-four beams, specimens 201 and 202, were used as control beams. Specimen 201 did not have any external reinforcement or adhesive, while specimen 202 had only an adhesive layer 3 mm (0.12 in.) in thickness. All other beams

were externally reinforced with steel plates bonded to the beam soffits. The plates terminated 50 mm (1.97 in.) from the supports. All steel plates were 125 mm (4.92 in.) in width but varied in thickness: 1.5 mm (0.06 in.), 3 mm (0.12 in.), and 6 mm (0.24 in.). The adhesive thickness varied, as well: 1.5 mm (0.06 in.), 3 mm (0.12 in.), and 6 mm (0.24 in.). Two 1.5 mm (0.06 in.) plates were layered when bonded to beams 206, 213, and 214. These beams were used for comparison with beams that had a single 3 mm (0.12 in.) plate. Five beams, 211 to 215, had lapped plates, either at the midspan or load points to simulate field application. Three beams, 222 to 224, were pre-cracked and then unloaded before the external steel plates were applied. The adhesive layer on beam 220 varied in thickness along its length from 3 mm to 8 mm (0.12 in. to 0.31 in.). Finally, areas of stress concentration were created at the load points by cutting v-notches into the soffit of beam 221.

The 28-day cube compressive strength of the concrete ranged from 63 to 73 MPa (cylinder strength of 7.7 to 9.1 ksi). The relation between cube and cylinder concrete compressive strengths is shown in Table 3.1. The concrete tensile strength ranged from 4.19 to 4.37 MPa (0.61 to 0.63 ksi). The flexural tension reinforcement had a yield strength of 425 MPa (61.64 ksi), while the shear reinforcement was made of mild steel with a yield strength of 250 MPa (36.26 ksi). The 1.5 mm, 3 mm, and 6 mm external steel plates had yield strengths of 236, 258, and 248 MPa (34.23, 37.42, and 35.97 ksi), respectively. The modulus of elasticity of the longitudinal, shear, and external reinforcement was 200 GPa (29000 ksi). The elastic modulus of the adhesive was 2100 MPa (304.6 ksi), while its Poisson's ratio was 0.33.

Table 3.1. Conversion between Cube and Cylinder Strengths[6]

Cube Strength		*Cylinder Strength*	
(MPa)	*(psi)*	*(MPa)*	*(psi)*
15	2175	12	1740
20	2900	16	2320
25	3625	20	2900
30	4350	25	3625
37	5365	30	4350
45	6525	35	5075
60	8700	50	7250

This experimental program revealed that beams that were externally reinforced with steel plates had higher cracking loads than those of the two control beams. Beams with the thinnest adhesive layers performed the best. The effect of plate thickness on the failure mechanism was apparent. Beams with the thinnest plates (1.5 mm) experienced plate yielding followed by concrete crushing, while beams with the thickest plates (6 mm) experienced premature failure with plate peeling and concrete cover separation. Beams that were strengthened in flexure using plates of moderate thickness (3 mm) experienced a combined shear/bond failure, with concrete cover separation and peeling, in which failure was initiated by a crack propagating from the point at which the steel plate terminated. Finally, specimens which had irregularities commonly found in practice, often due to the field application process, behaved similarly to beams without such irregularities. Thus, irregularities such as stress concentrations, varying glue thickness, and lapped plates did not appear to adversely affect the capacities of the retrofitted beams.

[6] "Conversion between Cube and Cylinder Strengths." Retrieved May 18, 2009, from http://www.logicsphere.com/products/firstmix/hlp/html/stre4s9w.htm

Swamy et al. (1987) noted the importance of composite action in order for beams to reach their full flexural capacity after retrofit. The specimens that failed in flexure maintained composite action between the plate, adhesive, and concrete up to the point of failure. Examination of these specimens after failure revealed that rupture occurred in the concrete cover, rather than in the plate/adhesive or adhesive/concrete interfaces.

3.1.2 Jones, Swamy, and Charif (1988)

Seven rectangular reinforced concrete beams flexurally strengthened using externally bonded steel plates were tested in four-point bending. Test data for this beam series are summarized in Table B.2. The beams were simply-supported. The length between the supports was 2300 mm (90.55 in.), while the overall beam length was 2500 mm (98.43 in.). The shear spans were 767 mm (30.20 in.), and the externally bonded steel plates extended 717 mm (28.23 in.) into the shear spans. Figure 3.2a shows the experimental test set-up.

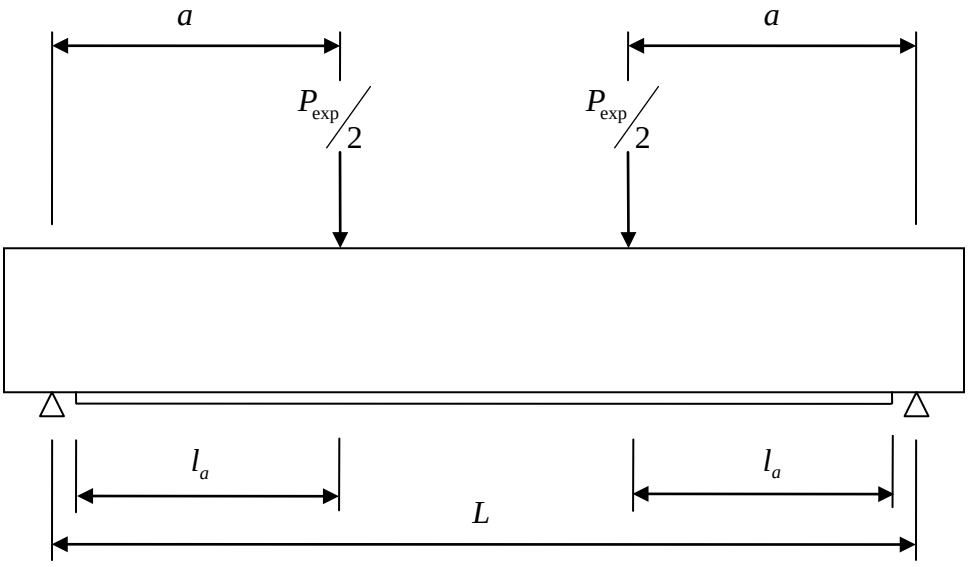

Figure 3.2a. Experimental Set-up used by Jones et al. (1988)

All specimens were designed to have the same cross section. Thus, they would also have the same theoretical flexural capacity. Cross-sectional dimensions were 155 x 255 mm (6.10 x 10.04 in.).[7] The cover distance from the extreme concrete tension surface to the centroid of the flexural reinforcement was reported to be 35 mm (1.38 in.). The flexural tension reinforcement consisted of three 20 mm (0.79 in.) diameter bars with yield strengths of 430 MPa (62.37 ksi). The shear reinforcement consisted of 6 mm (0.24 in.) diameter closed stirrups with yield strengths of 324 MPa (46.99 ksi) spaced at 75 mm (2.95 in.). Both the longitudinal and shear reinforcement had an elastic modulus of 200 GPa (29000 ksi). The average 28-day cube concrete compressive strength was 53.6 MPa (cylinder strength of 6.32 ksi), while the average tensile splitting strength was 3.55 MPa (0.51 ksi). Figure 3.2b shows a typical beam cross-section.

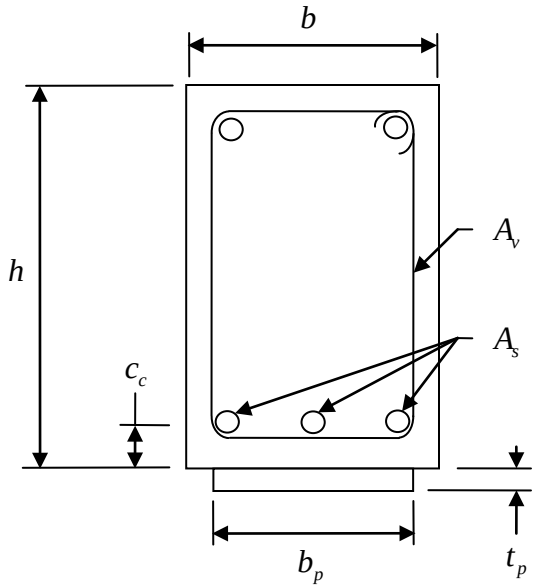

Figure 3.2b. Typical Specimen Cross-Section used by Jones et al. (1988)

[7] On page 88, line 6 of Jones et al. (1988), the beam dimensions are listed as 155 x 255 x 2500 mm; however, cross-sectional diagrams shown in Figures 5 and 6 on pages 87 and 88 depict the beam height to be 225 mm. Email correspondence with Professor R. N. Swamy verified that the experimental depth was 255 mm.

The beams were flexurally strengthened with mild steel plates. An adhesive with thickness of 1.5 mm (0.06 in.) was used for bonding the steel plates to the soffits of the beams. The adhesive had an elastic modulus of 278.9 MPa (40.45 ksi). The total thickness of the external reinforcement for all specimens was 6 mm (0.24 in.); however, two beams, F32 and F35, were plated with two 3 mm (0.12 in.) plates. The remaining five used one 6 mm (0.24 in.) plate. The yield strengths of the 3 mm and 6 mm external steel plates were 263 MPa (38.14 ksi) and 246 MPa (35.68 MPa). The external reinforcement had an elastic modulus of 200 GP (29000 ksi).

Different methods were used to anchor the ends of the externally bonded steel plates in areas of high stress concentrations and peeling forces. Four of the seven beams (F34 through F37) were anchored at the plate ends. Beams F34 and F35 had anchor bolts, while beams F36 and F37 used bonded steel anchor plates. Additionally, the outer external plates of beams F32 and F35 were curtailed at the ends, so the plates terminated 358.5 mm (14.1 in.) before the termination of the inner plates. The ends of both the inner and outer plates were bolted on beam F35. The 6 mm (0.24 in.) steel plate of specimen F33 was tapered to 2 mm (0.08 in.) at its point of termination. These anchorage methods were intended to prevent the premature peeling failure of strengthened beams. All beams without end anchorage (F31 through F33) experienced this type of premature failure.

The effectiveness of the different end anchorage systems (anchor bolts and bonded anchor plates) was assessed, and additional steel end anchor plates yielded the best results. While anchor bolts improved only the ductility of the plated beam, anchor plates improved both the plated beam's strength and ductility. The full theoretical flexural strength of the strengthened beam was achieved using this anchorage technique.

3.1.3 Oehlers and Moran (1990)

This research utilized an extensive specimen database, consisting of 57 rectangular reinforced concrete beams to determine the effects of curvature, geometry and material properties, and pre-cracking and pre-cambering on plate peeling. Test data are summarized in Table B.3 of Appendix B. Beams were tested in both three-point bending and four-point bending. The beams were simply-supported with spans varying from 1650 to 2500 mm (65.96 to 98.43 in.). Experimental set-ups are depicted in Figure 3.3a and Figure 3.3b.

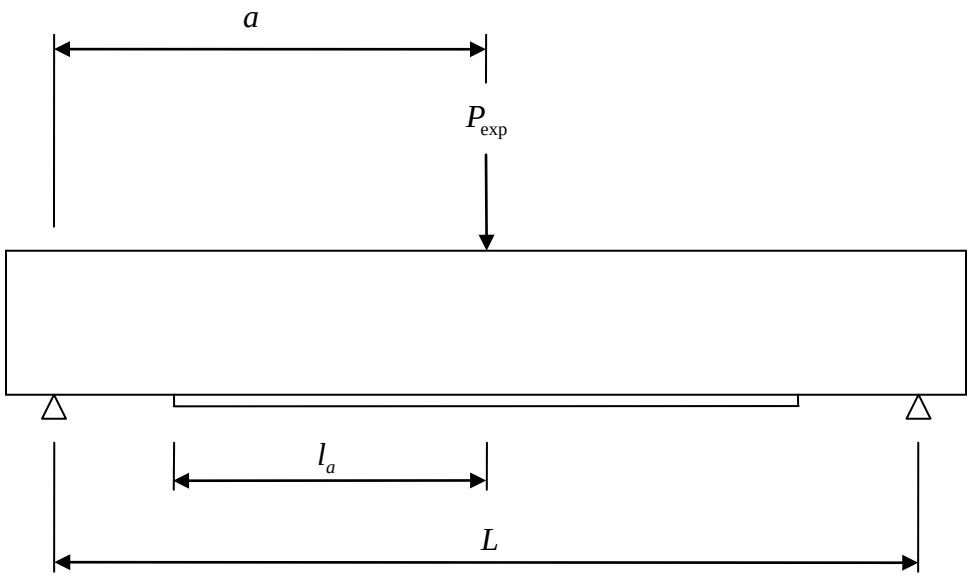

Figure 3.3a. Three-Point Bending Experimental Set-up by Oehlers and Moran (1990)

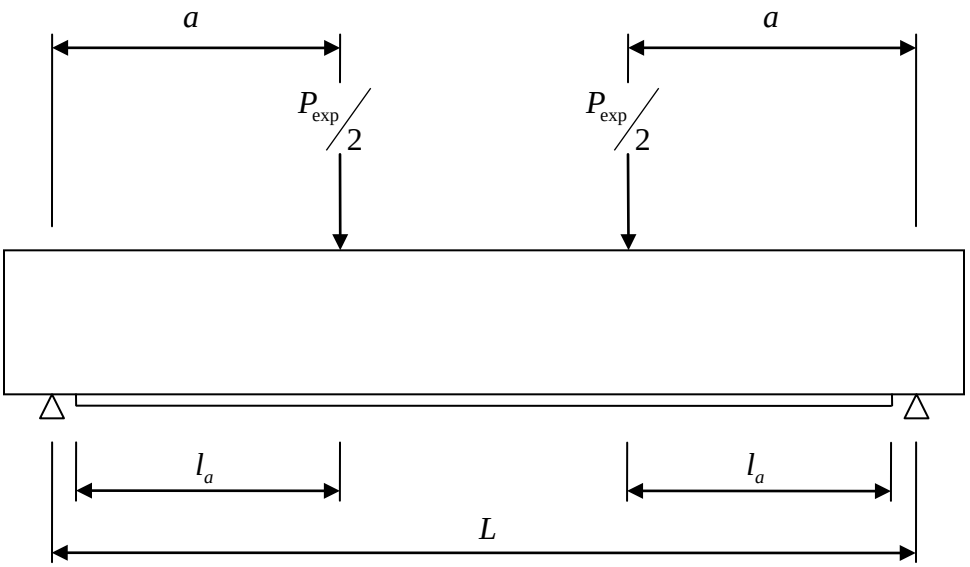

Figure 3.3b. Four-Point Bending Experimental Set-up by Oehlers and Moran (1990)

Two beam widths were used: 120 and 125 mm (4.72 and 4.92 in.). Overall beam depths varied from 150 to 240 mm (5.91 to 9.45 in.). The cover distance from the extreme tension surface to the centroid of the flexural tension reinforcement varied from 18 to 58 mm (0.71 to 2.28 in.). Two bars were used as tension reinforcement, varying in diameter from 12 to 20 mm (0.47 to 0.79 in.). The cube concrete compression strength varied from 28 to 48 MPa (cylinder strength of 3.34 to 5.51 ksi). The concrete tensile strength varied from 2.7 to 4.9 MPa (0.39 to 0.71 ksi). A typical specimen cross-section is shown Figure 3.3c.

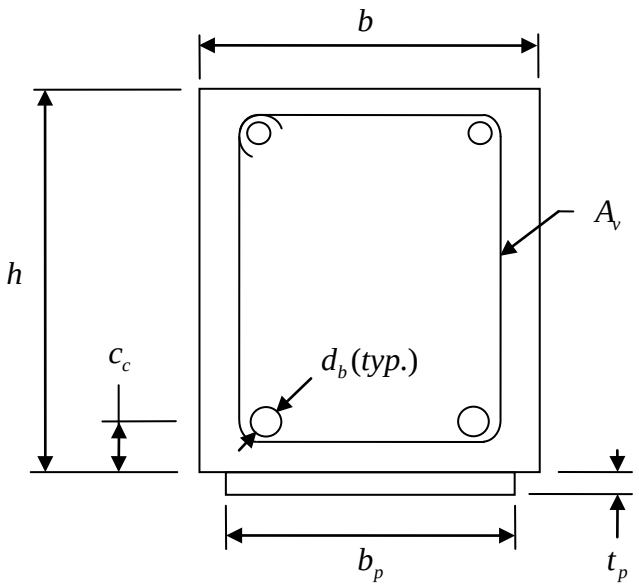

Figure 3.3c. Typical Specimen Cross-Section used by Oehlers and Moran (1990)

All test specimens were flexurally strengthened with externally bonded steel plates. The plates varied in thickness from 2.0 to 15 mm (0.08 to 0.59 in.). The steel plates matched the widths of the beams, except for four steel plates of beam series 12. The widths of these four plates were less than the beam widths with the narrowest plate being 25 mm (0.98 in.).

The shear reinforcement, the yield strengths of the reinforcing bars, the yield strengths of the steel plates, the shear spans, and the plate end locations were not reported in this study, but were provided in a Master's Thesis[8] on which the journal article was based. The reported shear reinforcement is outlined in Table B.3b. For all test specimens, the yield strength of the longitudinal reinforcement was taken as 460 MPa (66.72 ksi). The yield strength of the shear and external reinforcement was reported to be

[8] Moran, John P. (1988, June). "Separation of Externally Bonded Steel Plates from Reinforced Concrete Beams in Flexure." A thesis submitted to the National University of Ireland in candidature for the degree of Master of Engineering Science, University College Cork, Cork, Ireland.

250 MPa (36.26 ksi). The shear spans of the beams varied from 350 to 825 mm (13.78 to 32.48 in.). With the exception of the external reinforcement for beam series 7 and 8, all steel plates terminated in the constant moment region of the beams. For beam series 7 and 8, the plate termination points varied within shear span, as shown in Table B.3c. Unfortunately, the properties of the adhesive were not reported in the journal article or in the Master's Thesis.

3.1.4 Oehlers (1992)

Oehlers tested 26 reinforced concrete specimens in both three-point bending and four-point bending. However, definitive descriptions of the shear reinforcement were provided for just eight of the 26 specimens. Only these specimens, which were all tested in three-point bending, were analyzed in the literature review and will be discussed herein. Test data are summarized in Table B.4 of Appendix B. The span lengths of the beams were not reported, but the lengths of the shear spans were reported to be 550 mm (21.65 in.). A diagram of the experimental set-up is shown in Figure 3.4a.

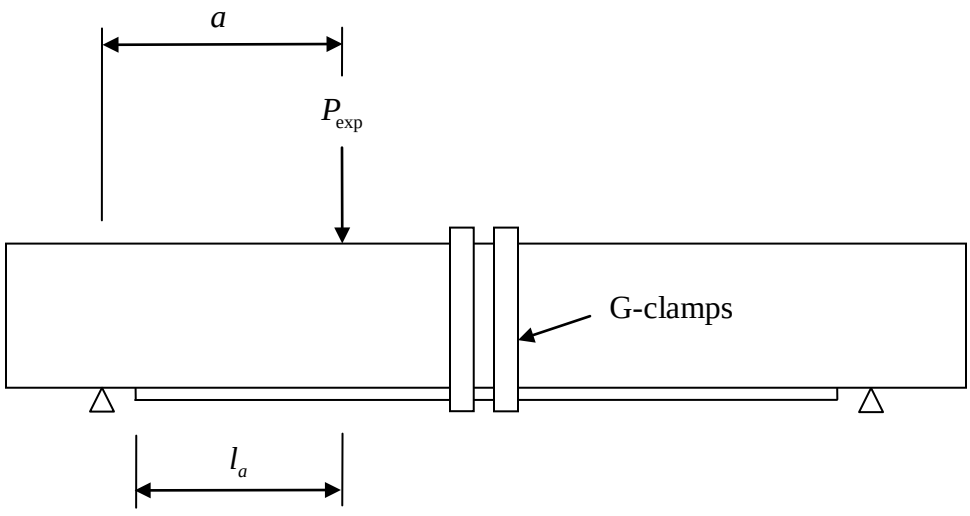

Figure 3.4a. Experimental Set-up used by Oehlers (1992)

Figure 3.4b shows a cross-section of a typical specimen. The beams had cross-sectional dimensions of 130 x 175 mm (5.12 x 6.89 in.). Two bars, 16 mm (0.63 in.) in diameter, with a yield strength of 444 MPa (64.40 ksi) were used as flexural tension reinforcement. The depth to the flexural tension reinforcement was 147 mm (5.79 in.). For shear reinforcement, either 4 or 6 mm (0.16 or 0.24 in.) closed stirrups were used. Stirrup spacing was either 45 or 75 mm (1.77 or 2.95 in.). The yield strength of the 4 mm stirrups was 568 MPa (82.38 ksi), and the yield strength of the 6 mm stirrups was 511 MPa (74.11 ksi). The cylinder compressive strength of the concrete was 47 MPa (6.82 ksi) for beam series 2 and 49 MPa (7.11 MPa) for beam series 5. The tensile strength of the concrete was 4.3 MPa (0.62 ksi) for beam series 2 and 4.7 MPa (0.68 ksi) for beam series 5.

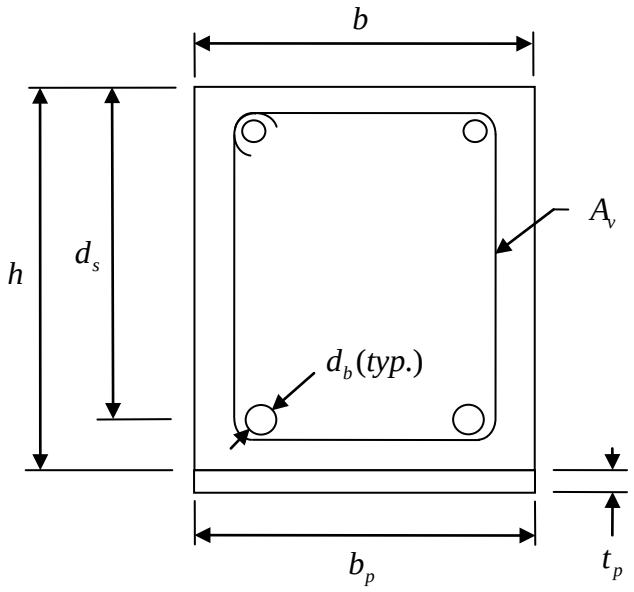

Figure 3.4b. Typical Specimen Cross-Section used by Oehlers (1992)

Each specimen was externally reinforced with a steel plate that was 5 mm (0.20 in.) in thickness. The plates were as wide as the beams and had yield strengths of 272 MPa (39.45 ksi). The points of termination of the external reinforcement varied within the shear spans of the beams. The lengths of the steel plates from the location of maximum moment into the shear span are shown in Table B.4c. The properties of the adhesive used to bond the external reinforcement to the beam soffits were not reported.

3.2 Strengthening with Externally Bonded Fiber Reinforced Polymer Plates

3.2.1 Duthinh and Starnes (2004)

This experimental study consisted of eight specimens as summarized in Table B.5 of Appendix B. One of the beams (Beam 10) was a theoretical beam that was used in calculations but was not actually fabricated. The fabricated beams were tested in four-point bending, as shown in the experimental set-up in Figure 3.5a.

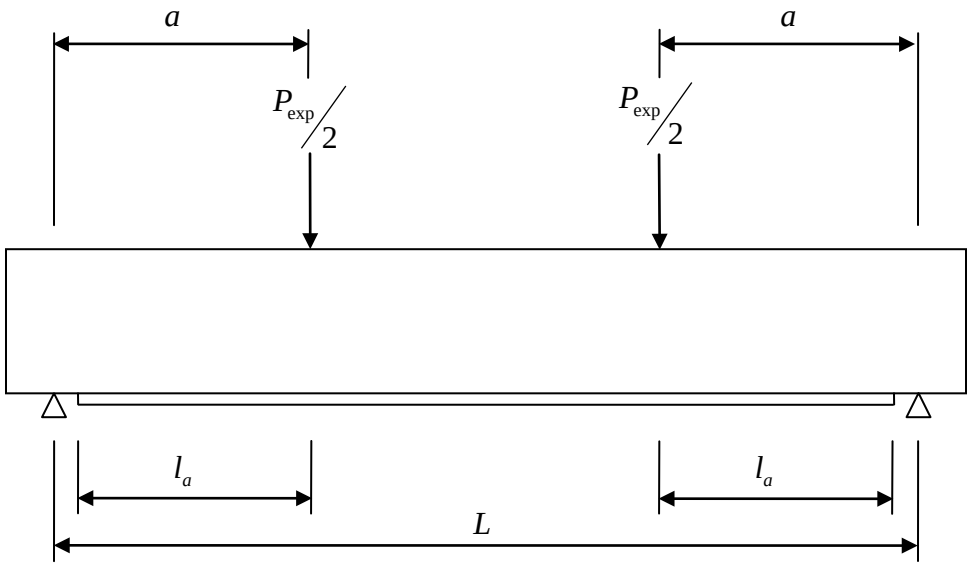

Figure 3.5a. Experimental Set-up used by Duthinh and Starnes (2004)

All beams had the same nominal dimensions: 150 x 460 mm (5.91 x 18.11 in.). The span length was 2750 mm (108.27 in.), and the shear span was 815 mm (32.09 in.). The cylinder compressive strength of the concrete for each specimen is shown in Table B.5a. The area of flexural tension reinforcement varied by specimen. Two bars were used as flexural tension reinforcement in each specimen, and the specimen number indicated the U.S. size of rebar used. The depth and the yield strength of the longitudinal reinforcement are outlined in Table B.5a and Table B.5b, respectively. The shear reinforcement consisted of U.S. #3 vertical stirrups with a yield strength of 415 MPa (60 ksi) spaced at 100 mm (3.94 in.). Figure 3.5b shows a typical beam cross-section.

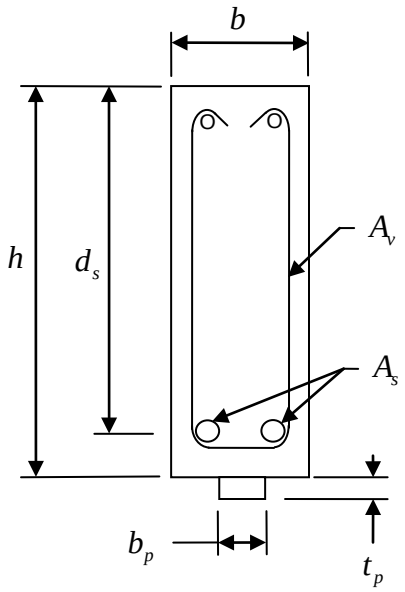

Figure 3.5b. Typical Specimen Cross-Section used by Duthinh and Starnes (2004)

Six test specimens were externally reinforced with carbon FRP plates. Beam 9 was not externally reinforced, and Beam 10 was the theoretical specimen. The plates were applied to the six specimens shortly after the first flexural cracks appeared at about

one-third of the calculated ultimate moment capacity of all beams except 4a and4b (before the application of external reinforcement). The plates were applied at 68% and 52% of the ultimate moment capacities for beams 4a and 4b because they were lightly reinforced. The load was maintained during application and curing of all plated test specimens.

The carbon FRP plates were 1.2 mm (0.05 in.) and 50 mm (1.97 in.) wide for all specimens except beam 4b whose plate was 100 mm (3.94 in.) wide. The elastic modulus specified by the manufacturer of the carbon FRP plates was 155 GPa (22481 ksi). The adhesive was applied with a thickness of 1.5 mm (0.06 in.) to the beam soffits. Another layer of adhesive was applied to the FRP plates with the same thickness. Thus, the total thickness of the adhesive layer was assumed to be 3 mm (0.12 in.). All plated specimens were anchored at the external reinforcement point of termination 50 mm (1.97 in.) from the supports. Beams 4a, 6, and 7N were clamped at the plate ends. Carbon fiber U-shaped wraps were used as end anchors on all other specimens. The wraps were 200 mm (7.87 in.) in width and placed on both sides of the specimen.

3.2.2 Yao and Teng (2007)

Yao and Teng investigated the behavior and failure mechanisms of reinforced concrete beams with externally bonded FRP plates using the results of three-point and four-point bending tests, conducting a total of 21 tests total with 11 different specimens (summarized in Table B.6 of Appendix B). One specimen, SP-A/B, was retrofitted using steel plates instead of FRP for comparative purposes. A wide range of geometric and material parameters were investigated.

Test series A consisted of ten four-point bending tests, as shown in Figure 3.6a. In this test series, the beams were simply-supported over a span of 1500 mm (59.06 in.) with loads at one-third points of the span length. The external reinforcement terminated in the constant moment region, and clamps were used to prevent failure at the opposite plate end. This test series was designed to investigate flexural debonding failure mechanisms. In test series B, eleven three-point bending tests were conducted, as shown in Figure 3.6b. This test series aimed to investigate shear debonding failure mechanisms. A beam without stirrups was included in this test series. The failed plate end in the constant moment region from test series A was clamped, and the opposite plate end terminated 50 mm (1.97 in.) from the support. With the same span length, the beams were loaded only at the third point near the opposite plate end.

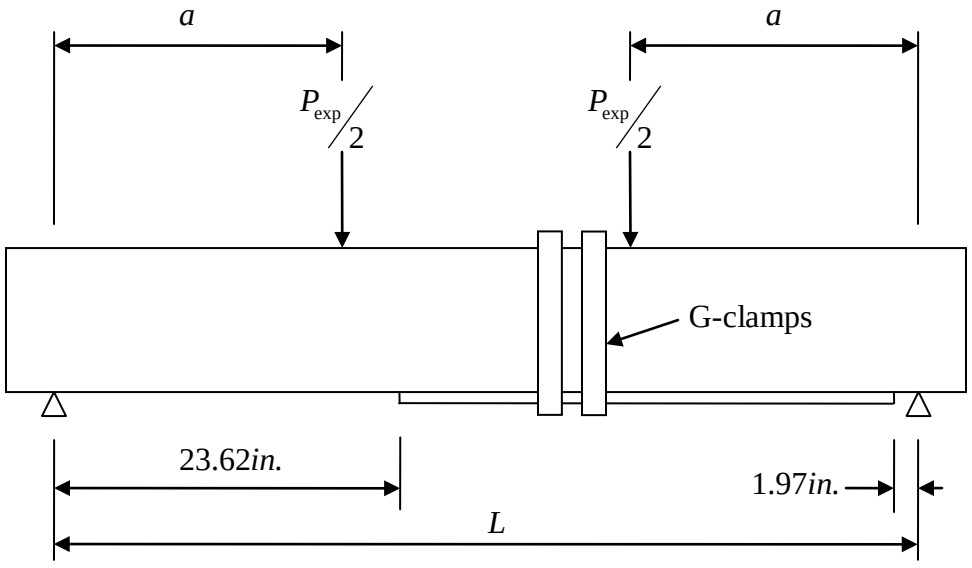

Figure 3.6a. Series A Experimental Set-up used by Yao and Teng (2007)

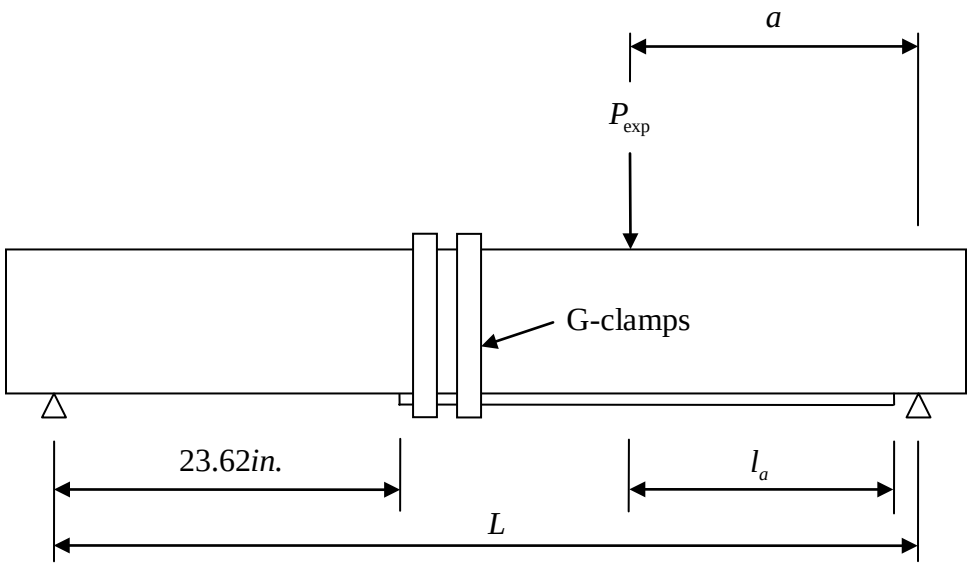

Figure 3.6b. Series B Experimental Set-up used by Yao and Teng (2007)

A typical specimen cross-section is shown in Figure 3.6c. All of the test specimens had the same nominal dimensions. The beams were 150 mm (5.91 in.) wide and 250 mm (9.84 in.) deep. They were designed to be under-reinforced, using only two 10 mm (0.39 in.) diameter bars for flexural tension reinforcement. The cover distance from the extreme tension surface to the centroid of the flexural tension reinforcement was approximately 35 mm (1.38 in.) for each specimen except specimens CS-C10-A/B and CS-C50-A/B, which had cover distances of 17 and 56.5 mm (0.67 and 2.22 in.), respectively. All beams had 10 mm (0.39 in.) closed stirrups spaced at 100 mm (3.94 in.) except for beam CS-NS-B which only used three stirrups, one at each end and one at the midspan.

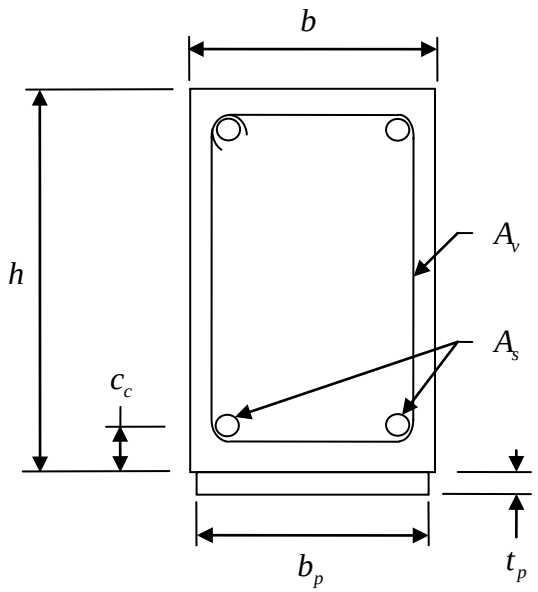

Figure 3.6c. Typical Specimen Cross-Section used by Yao and Teng (2007)

The cube compressive strength of the concrete ranged from 27.3 to 39.5 MPa (cylinder strength of 3.24 to 4.58 ksi). The concrete tensile strength for each specimen is listed in Table B.6a, and the yields strengths and elastic modulus of the reinforcing bars are listed in Table B.6b.

The width of the composite FRP plate was 148 mm (5.83 in.) for all specimens except CS-W50-A/B and CS-W100-A/B, which had plate widths of 50 and 100 mm (1.97 and 3.94 in.), respectively. The average plate thickness, along with the elastic modulus of the FRP fibers and the steel plate, are listed in Table B.6c. The material properties of the composite FRP plate are unknown and the type of FRP (i.e. the manufacturer) was not reported. The thesis research (Yao, 2004)[9] on which the Yao/Teng paper is based

[9] Yao, Jian. (2004, October). "Debonding Failures in RC Beams and Slabs Strengthened with FRP Plates." A thesis submitted in partial fulfillment of the requirements for the degree of Doctor of Philosophy, The Hong Kong Polytechnic University, Hong Kong, China.

does not provide any further information. The type of adhesive, Sikadur-30 Normal, and an adhesive thickness of 2 mm (0.08 in.) was reported for each specimen.

3.3 Summary

The severity of premature failure due to plate end delamination became apparent from the literature review. In some experimental programs, such as Oehlers and Moran (1990), all specimens experienced end delamination failure. Warning signs of impending plate end delamination were not always discernible. Furthermore, some strengthened specimens achieved less than 50% of their theoretical ultimate flexural capacity. Thus, the need for adequate design guidelines when flexurally strengthening reinforced concrete members with externally bonded reinforcement is clear. The development of an end debonding model in Chapter 4 is a necessary step in addressing that need.

CHAPTER 4

PREDICTION OF END DEBONDING

The prediction models introduced in Chapter 2 are assessed in this chapter to determine their effectiveness in predicting end debonding failure. The statistical analysis of the models, the evaluation of their sensitivity to various parameters, and the consideration of computational difficulty are recounted in the following sections.

4.1 Analytical Evaluation using Debonding Models

The two debonding prediction models proposed by Roberts (1989) and Colotti, Spadea, and Swamy (2004) were used to evaluate experimental data from the studies listed in Chapter 3. The normal and shear peeling stresses at ultimate failure for each test specimen were calculated using the model by Roberts (1989). Sample calculations are provided in Appendix C, and the results are tabulated in Appendix D. Because the studies reported by Yao and Teng (2007) and Oehlers and Moran (1990) did not present all of the necessary parameters for computations using Roberts' (1989) model, assumptions for these parameters were made based on customary industry practice. For the specimens in the study by Yao and Teng (2007), the modulus of elasticity of the external composite FRP was assumed to be 30% of the elastic modulus of its fibers (30% fiber volume). The adhesive in the study by Oehlers and Moran (1990) was assumed to have an average thickness of 1.5 mm (0.06 in.), an elastic modulus of 400 ksi, and a Poisson's ratio of 0.35. The validity of these assumptions was investigated with a parameter sensitivity study, as discussed in Section 4.2. Specimens from the studies by

Duthinh and Starnes (2004) and Oehlers (1992) could not be used to evaluate Roberts' peeling stress model (1989). Duthinh and Starnes (2004) provided end anchorage for each specimen's external reinforcement, which changed the boundary conditions for debonding prediction. Oehlers' (1992) study did not report sufficient information to allow the normal and shear peeling stresses for Roberts' (1989) model to be determined; an excessive number of assumptions would have been needed to be made in the computations. Finally, when the concrete compressive strengths were reported as cube compressive strengths in a study, they were converted to cylinder compressive strengths for consistency with practice in the United States. Table 3.1 provides the factors used to convert cube compressive strength to cylinder compressive strength.

In Figure 4.1, the ratio of the normal peeling stress, f_{peel}, to the concrete shear transfer strength, $\tau_{\text{int}} = 0.171\sqrt{f'_c}$ where f'_c is in MPa[10], is plotted for the specimens in the each of the studies. The concrete shear transfer strength was selected for comparison because approximately 90% of the computed values for the normal peeling stress were greater than the values for shear transfer strength. The statistical mean, standard deviation, and coefficient of variation (COV) were calculated for the ratios of the normal peeling stress to shear transfer strength. The data set was then examined using the Maximum Normed Residual (MNR) method outlined in ASTM D 7290-06 Standard Practice to determine any outliers. One outlier was removed from the set of 90 data points, and the statistical mean, standard deviation, and COV were recalculated.

[10] In English units: $\tau_{\text{int}} = 0.065\sqrt{f'_c}$ where f'_c is in ksi.

The model by Colotti et al. (2004) was used to compute the plate end shear at ultimate failure for the specimens in each of the studies from Chapter 3. Sample calculations are provided in Appendix E, and the results are tabulated in Appendix F. Because this model only predicts debonding failure and different formulae are presented for other failure modes, the evaluation of the model by Colotti et al. (2004) was limited to specimens which experienced plate end debonding failure. Specimens from the study by Duthinh and Starnes (2004) were again excluded from the evaluation due to changed boundary conditions. Specimens in which the external reinforcement terminated within constant moment regions of four-point bending tests, where the shears would be zero, were excluded as well. Unlike the model by Roberts (1989), no parameter assumptions had to be made when calculating the plate end shears. The experimental values of plate end shears at ultimate peeling failure were divided by the analytical values calculated from the model by Colotti et al. (2004) and were plotted in Figure 4.2. The mean, standard deviation, and COV were calculated for the ratios of experimental to theoretical plate end shears. This data set also was examined to identify any statistical outliers using the MNR method of ASTM D 7290-06 Standard Practice, but none were found.

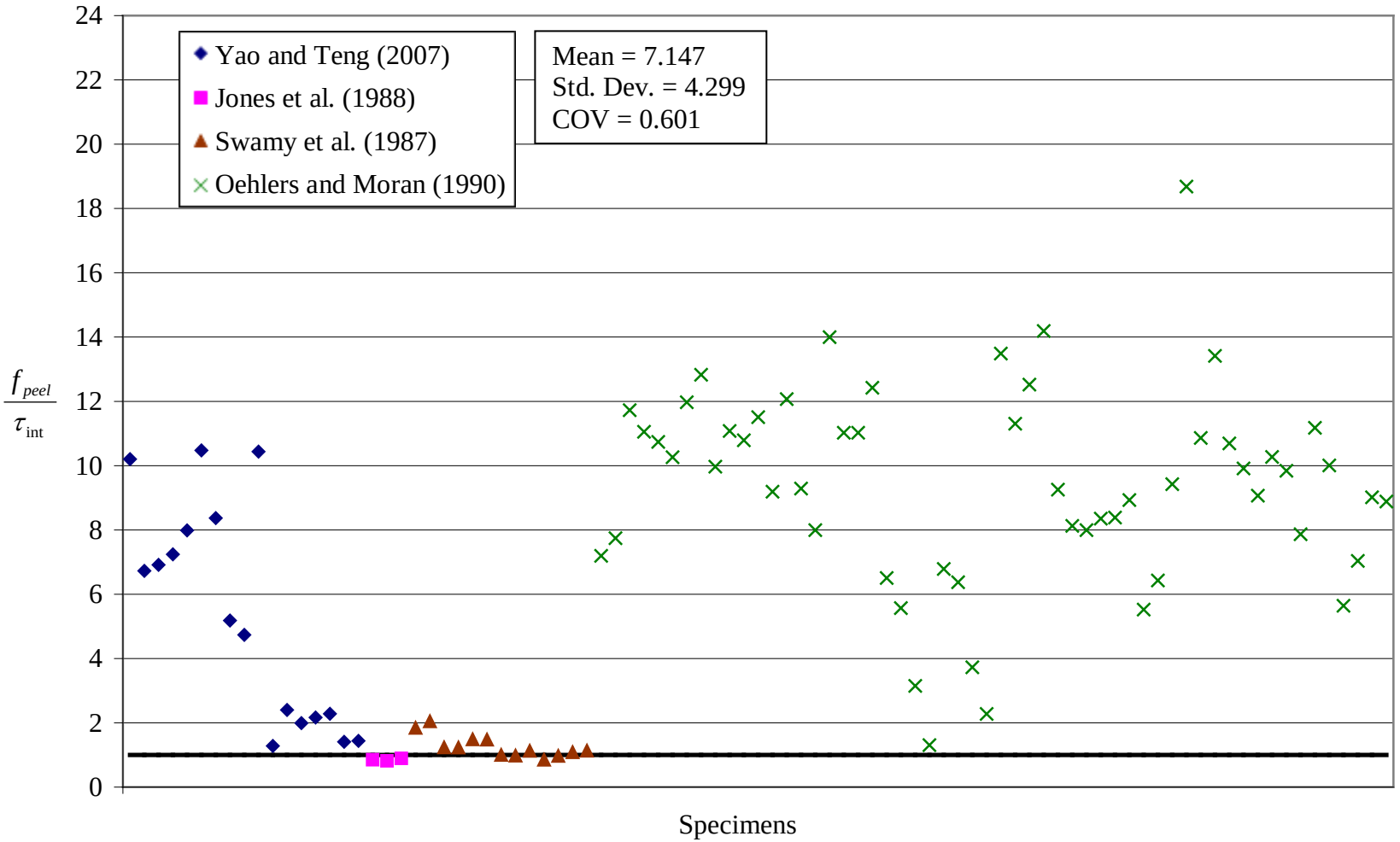

Figure 4.1. Failure Prediction using Normal Peeling Stress Model by Roberts (1989)

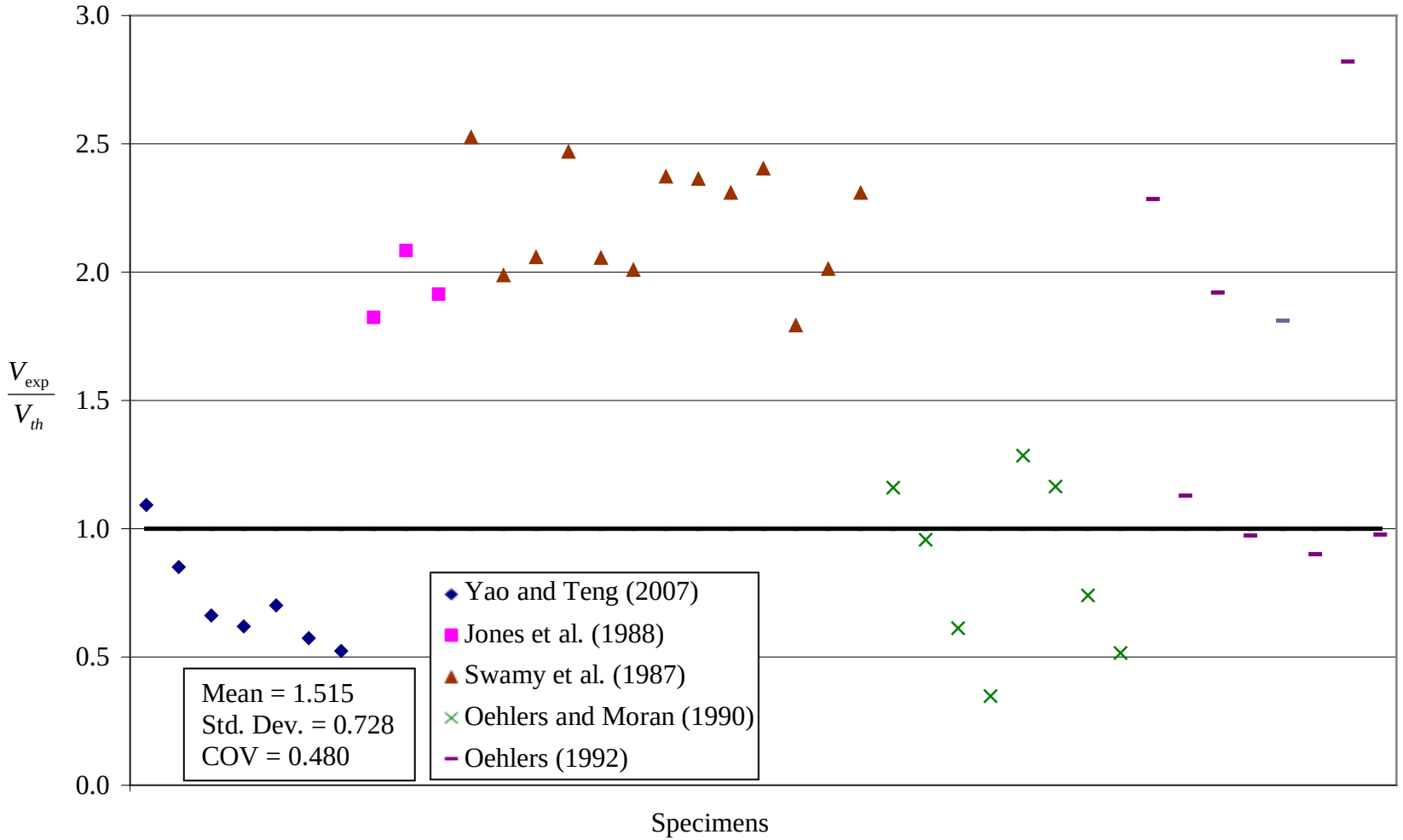

Figure 4.2. Failure Prediction using Plate End Shear Model by Colotti, Spadea, and Swamy (2004)

4.2 Parameter Sensitivity of Analytical Models

A sensitivity analysis of the analytical models with respect to various parameters may allow unknown specimen properties to be assumed without introducing significant error in the prediction of the point of end debonding failure. In addition, by investigating the sensitivity of the models to various parameters, the limitations of each model in predicting debonding failure may be assessed. Because no assumptions were made in calculating the peeling stresses and plate end shears for specimens of the 1987 study by Swamy et al., these specimens were selected for examining parametric sensitivity.

The figures in the following sub-sections depict the sensitivity of the models by Roberts (1989) and Colotti et al. (2004) to variation in their parameters. On the abscissa, the ratio of a parameter with respect to its original value reported in the study by Swamy et al. (1987) is plotted. On the ordinate is the ratio of the model's experimental value to its theoretical value at end debonding failure. A data point was placed where the ratio of the parameter with respect to its original specified value equaled one. In other words, the data point represents the actual experimental values found in the study by Swamy et al. (1987).

4.2.1 Roberts (1989)

4.2.1.1 Effect of Concrete Beam Properties on Peeling Stress

The geometric and material properties of the concrete beams were investigated for their effect on the peeling stress. Of the properties that were investigated - area of flexural tension reinforcement, concrete compressive strength, beam width, beam height, and concrete cover - the calculated normal peeling stress at debonding was most sensitive

to variations in the area of flexural tension reinforcement. Figure 4.3 shows that as the area increases, the calculated normal peeling stress at failure decreases significantly. Increases in the concrete compressive strength and beam width (Figures 4.4 and 4.5) have little impact on peeling stress; beam height is relatively more important (Figures 4.6). Figure 4.7 shows that an increase in the concrete cover increases the calculated normal peeling stress, a finding which is consistent with the results presented by Yao and Teng (2007).

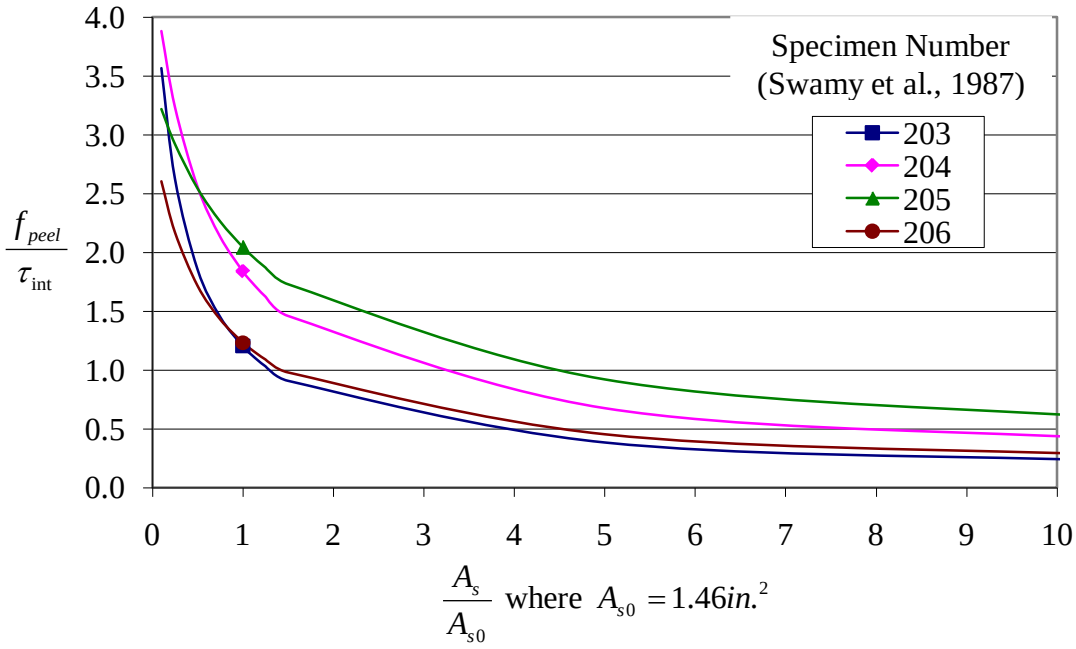

Figure 4.3. Sensitivity of Normal Peeling Stress with respect to Flexural Tension Reinforcement Area

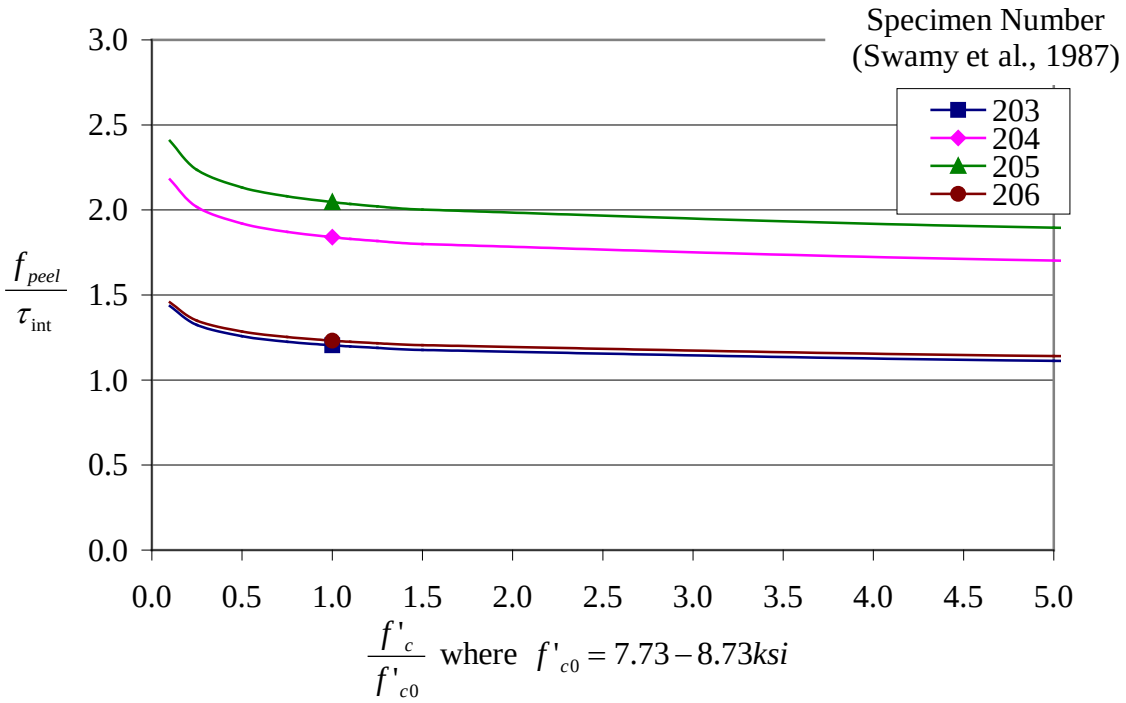

Figure 4.4. Sensitivity of Normal Peeling Stress with respect to Concrete Compressive Strength

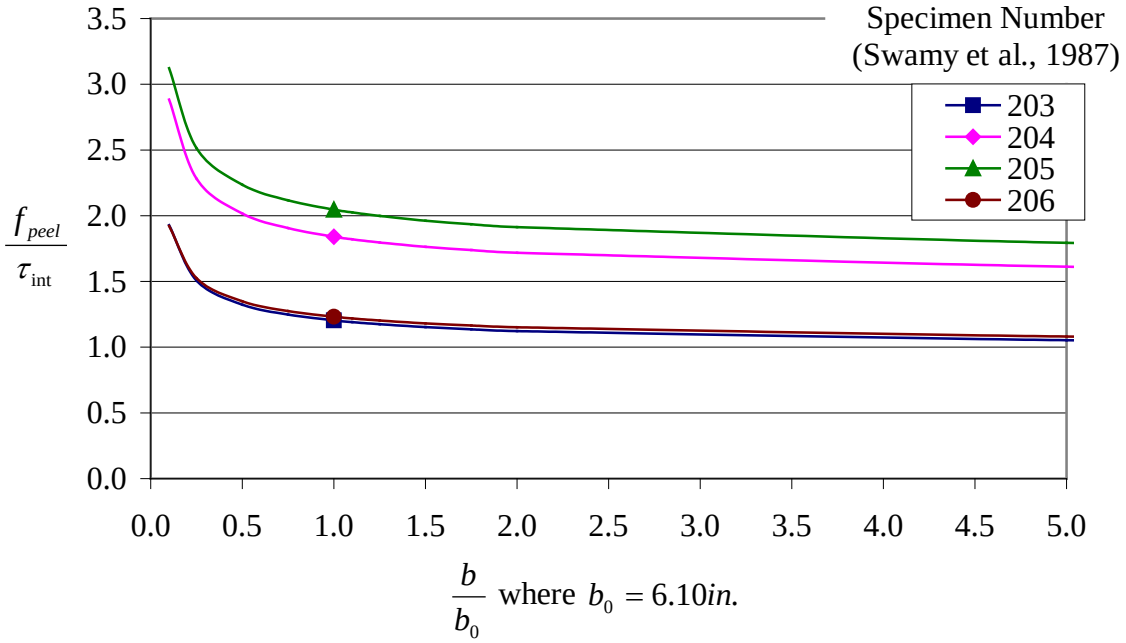

Figure 4.5. Sensitivity of Normal Peeling Stress with respect to Beam Width

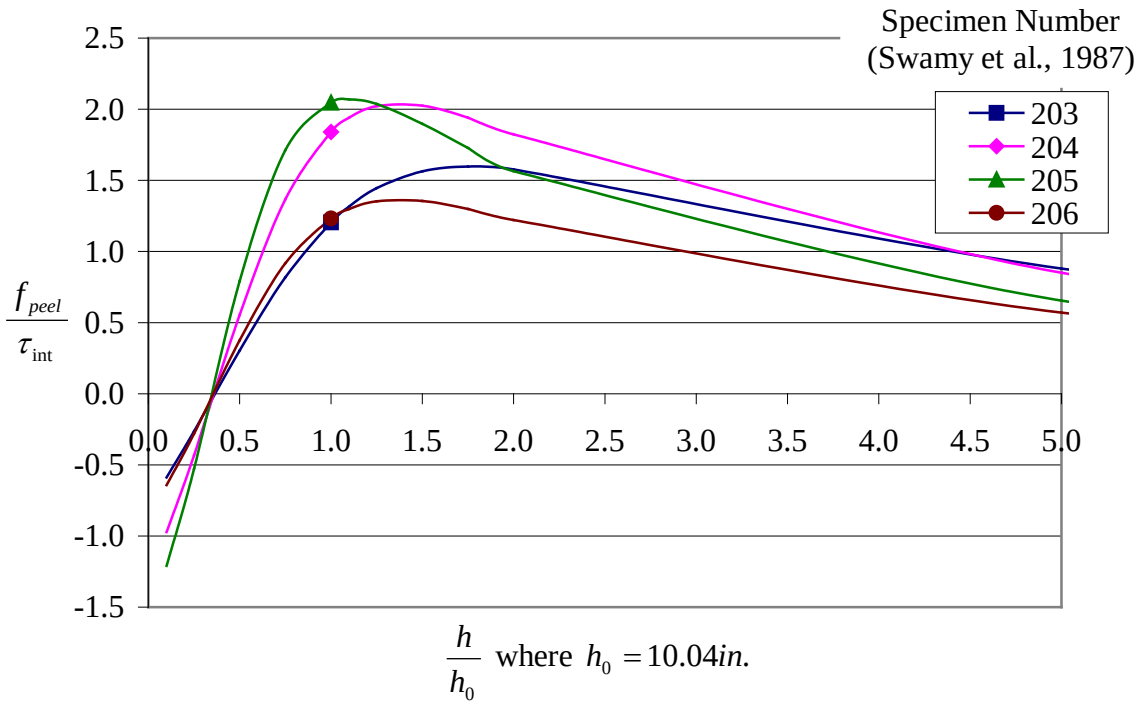

Figure 4.6. Sensitivity of Normal Peeling Stress with respect to Beam Height

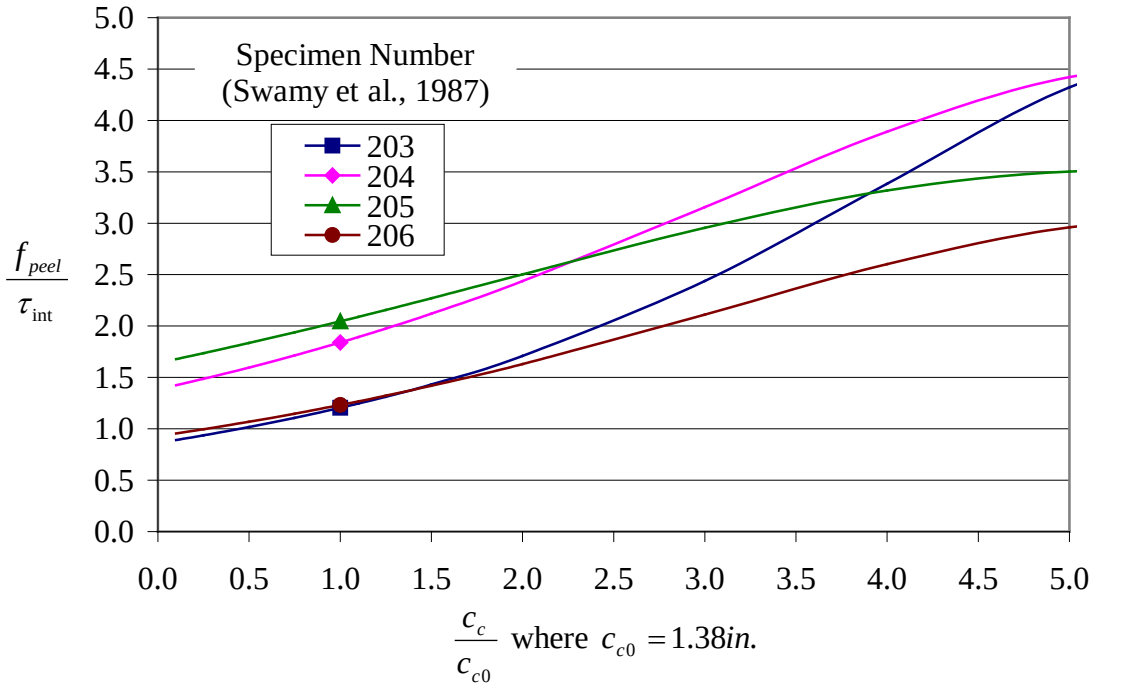

Figure 4.7. Sensitivity of Normal Peeling Stress with respect to Concrete Cover

4.2.1.2 Effect of External Reinforcement Properties on Peeling Stress

The properties of the external reinforcement were varied to determine the sensitivity of the calculated normal peeling stress with respect to the strength and stiffness of the external plate. Increases in plate thickness increased the normal peeling stress for debonding (Figure 4.8), which is consistent with the findings by Swamy et al. (1987). Conversely, increases in the plate width and the elastic modulus of the plate decreased the normal peeling stress (Figures 4.9 and 4.10).

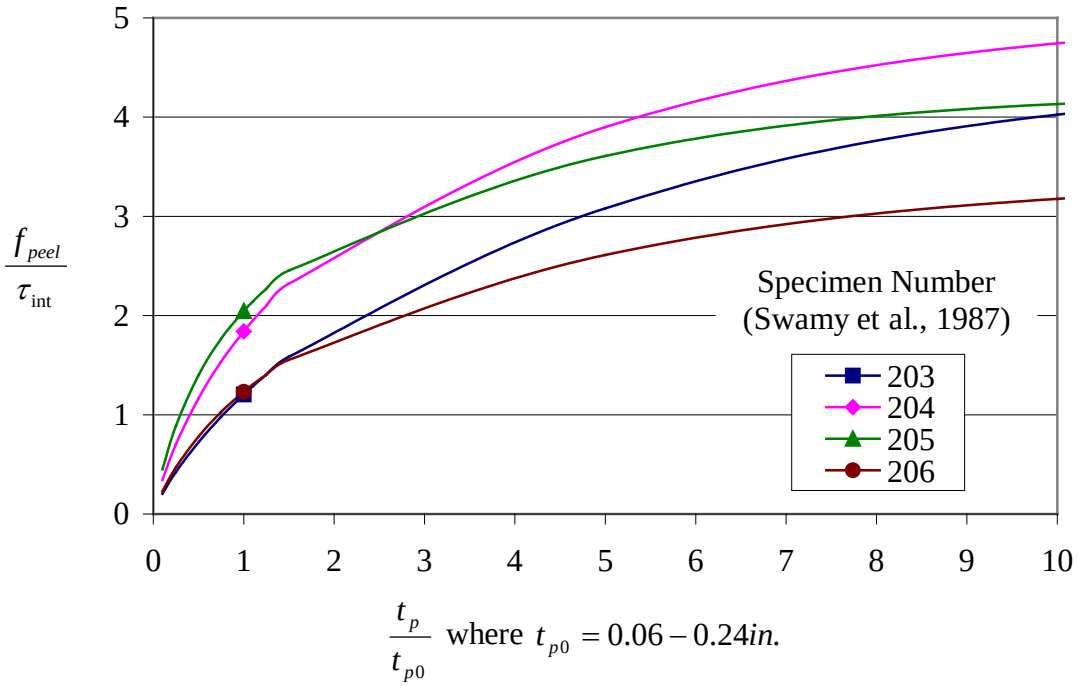

Figure 4.8. Sensitivity of Normal Peeling Stress with respect to Thickness of the External Reinforcement

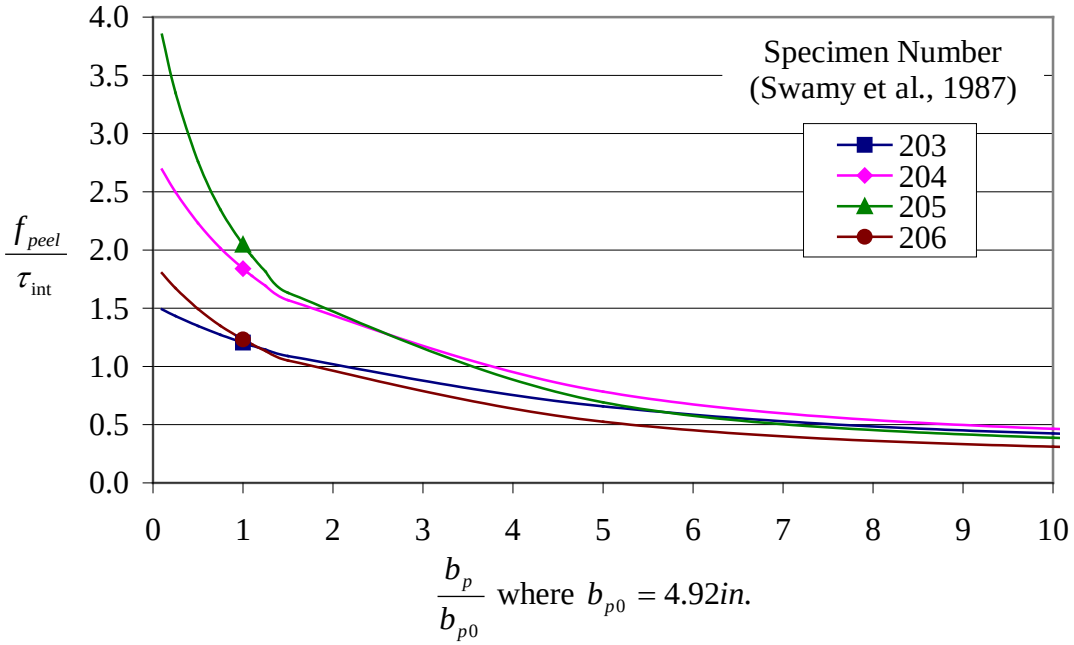

Figure 4.9. Sensitivity of Normal Peeling Stress with respect to Width of the External Reinforcement

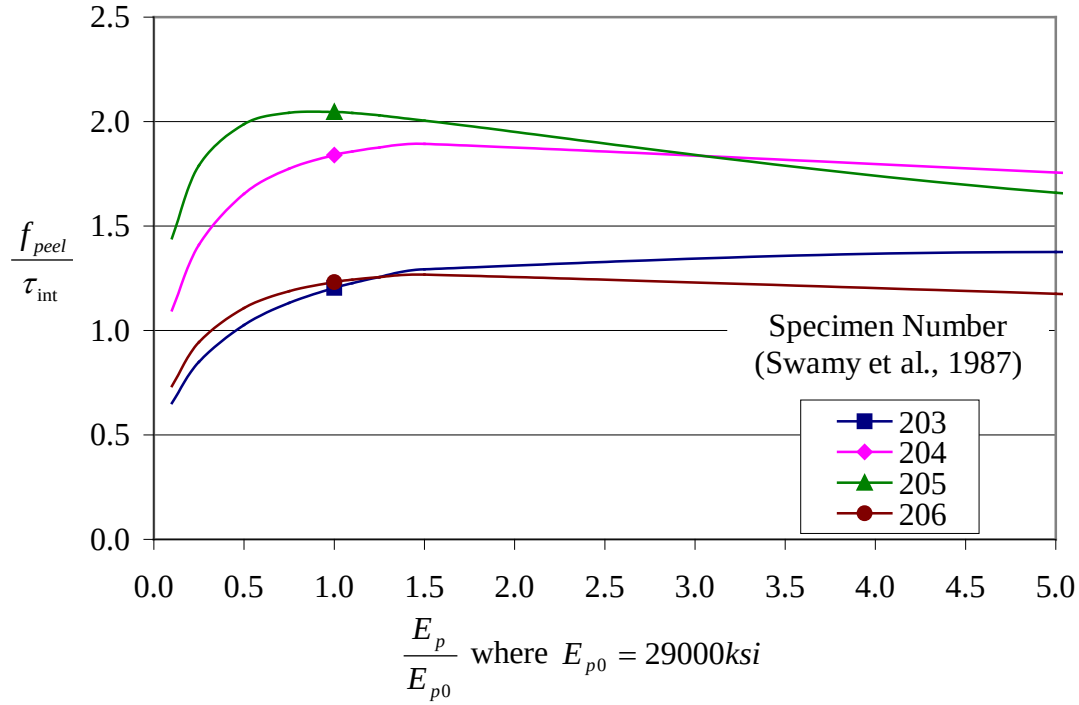

Figure 4.10. Sensitivity of Normal Peeling Stress with respect to the External Reinforcement Elastic Modulus

4.2.1.3 Effect of Adhesive Properties on Peeling Stress

The effect of the adhesive properties on the calculated normal peeling stress also was investigated. Using reasonable values for the elastic modulus of the adhesive (maximum of 3.45 GPa or 500 ksi), the calculated peeling stress increased slightly, as shown in Figure 4.11. Assuming that the lower limit for adhesive thickness is approximately 1.0 mm (0.04 in.), the normal peeling stress showed little variation with an increase in adhesive thickness (Figure 4.12), even up to five times the lower limit. It may be concluded that for all reasonable values of adhesive thickness, the normal peeling stress is insensitive to variations in the adhesive thickness. Since neither the adhesive thickness nor the elastic modulus of the adhesive appears to have a significant effect on the calculated normal peeling stress, the assumptions regarding these parameters that were necessary when evaluating the model by Roberts (1989) should have a negligible impact on the evaluation of the merits of that model.

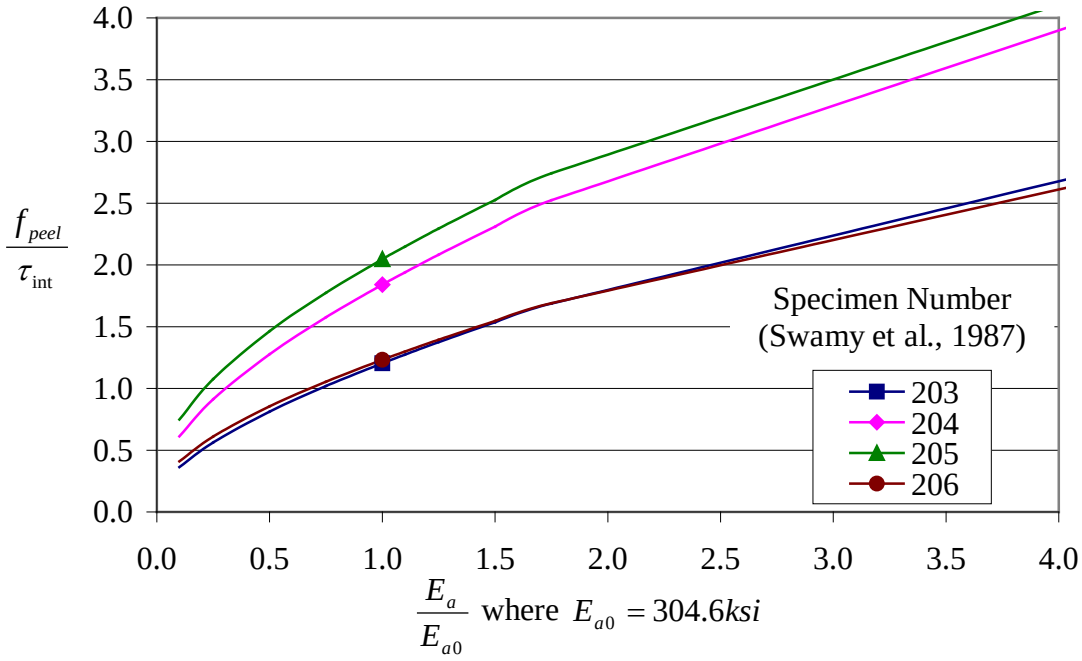

Figure 4.11. Sensitivity of Normal Peeling Stress with respect to the Elastic Modulus of the Adhesive

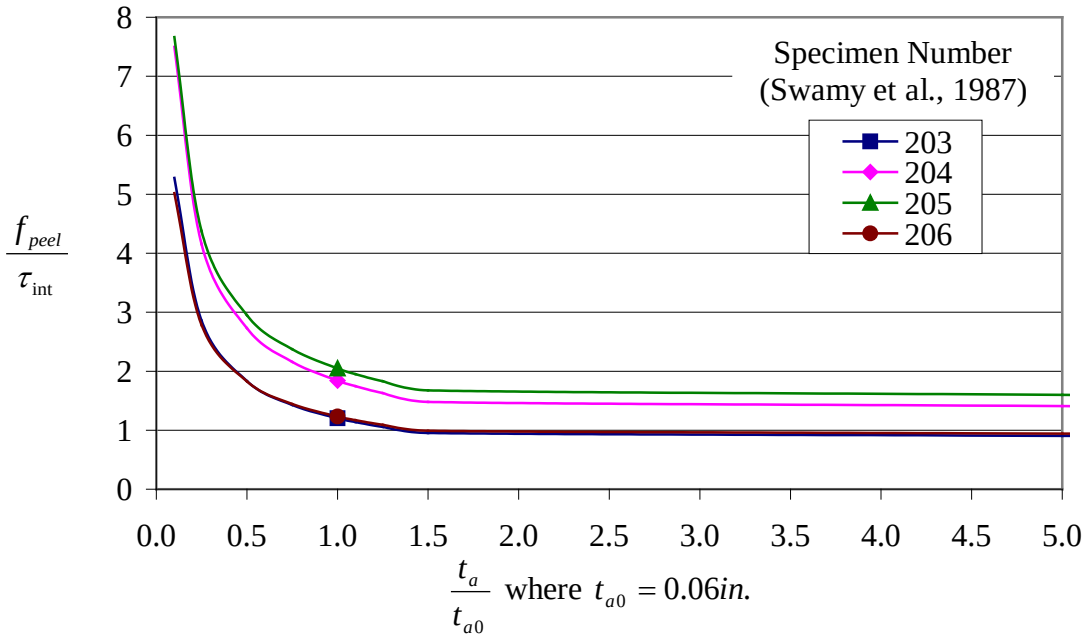

Figure 4.12. Sensitivity of Normal Peeling Stress with respect to the Thickness of the Adhesive

4.2.2 Colotti, Spadea, and Swamy (2004)

4.2.2.1 Effect of Concrete Beam Properties on Shear at Plate End

The properties of the concrete beam that were investigated were the concrete cover, area of longitudinal reinforcement, concrete compressive strength, area of shear reinforcement, shear reinforcement spacing, beam width, and beam height. Assuming that the tensile strength of the concrete (in psi units) is approximately $6.7\sqrt{f'_c}$ (ACI 318-08 Commentary Section R8.6.1), variations in the concrete compressive strength (Figure 4.13) and the stirrup spacing (Figure 4.14) had the most significant effects on the calculated shear at the plate end. As stirrup spacing increased, the calculated value of plate end shear at which debonding would occur decreased. As the concrete compressive strength increased, the tensile strength of the concrete increased, causing an increase in the calculated value for the debonding plate end shear.

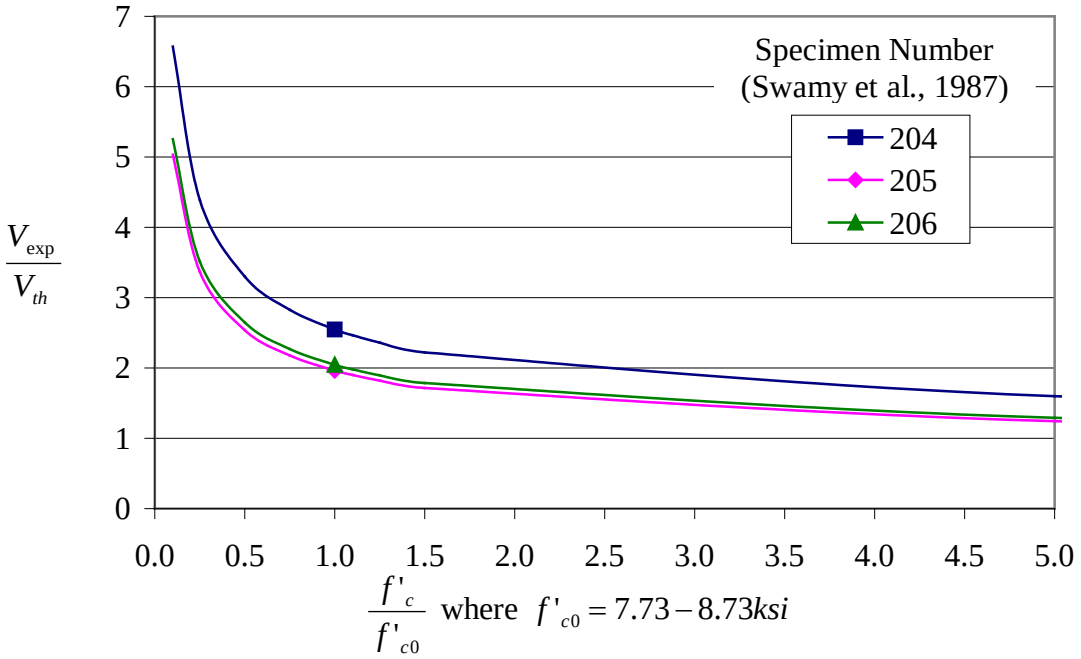

Figure 4.13. Sensitivity of Theoretical Plate End Shear with respect to Concrete Compressive Strength

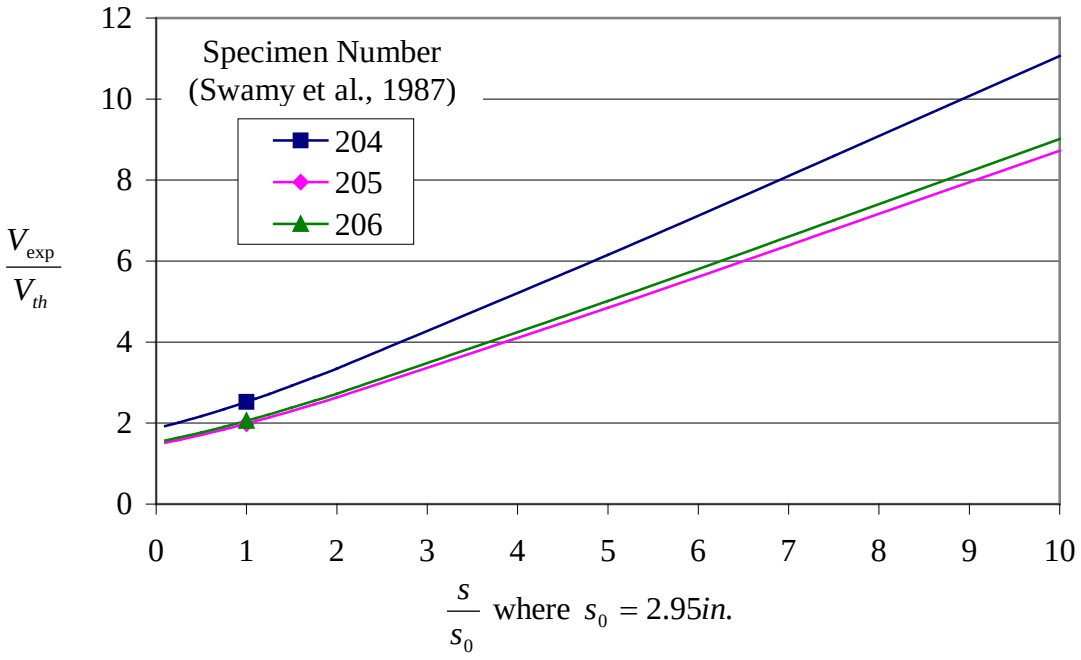

Figure 4.14. Sensitivity of Theoretical Plate End Shear with respect to Spacing of Transverse Reinforcement

For beams with smaller cross-sectional areas, the theoretical shear capacity is considerably reduced; with less contribution from the concrete to shear strength, the ratio of experimental to theoretical ultimate plate end shear is increased. This condition is apparent in Figures 4.15 and 4.16, which display the sensitivity of the theoretical shear with respect to beam width and beam height. Increases in beam cross-sectional area, though, do not have as significant an effect on the theoretical shear capacity of the beam. The sensitivity of the theoretical plate end shear with respect to the cross-sectional area of transverse reinforcement follows this same trend (Figure 4.17), which is to be expected.

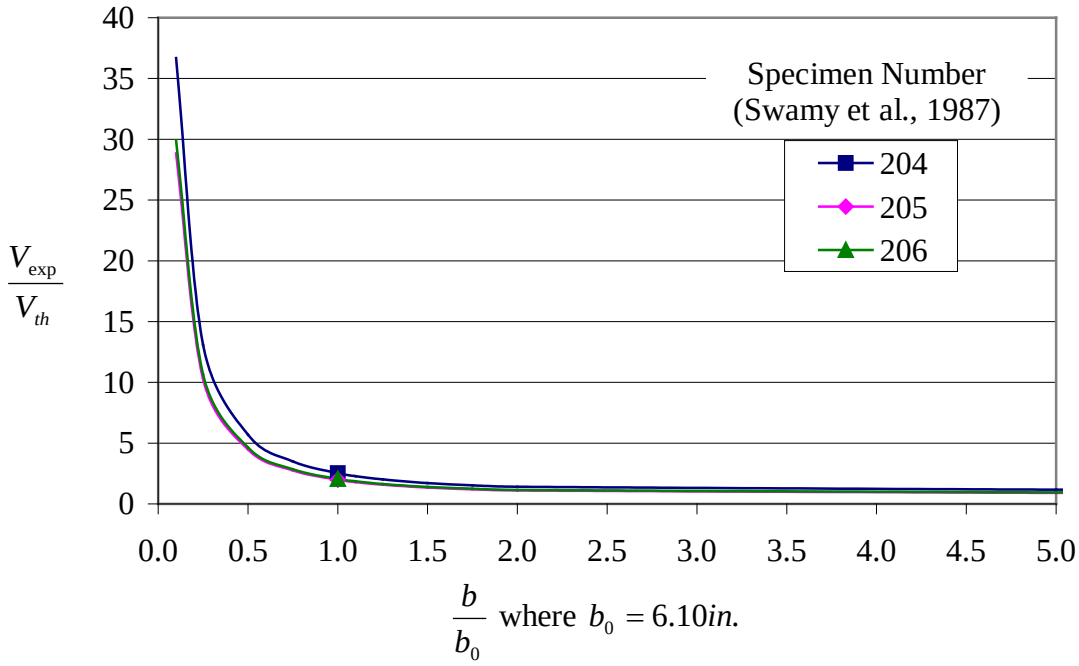

Figure 4.15. Sensitivity of Theoretical Plate End Shear with respect to Beam Width

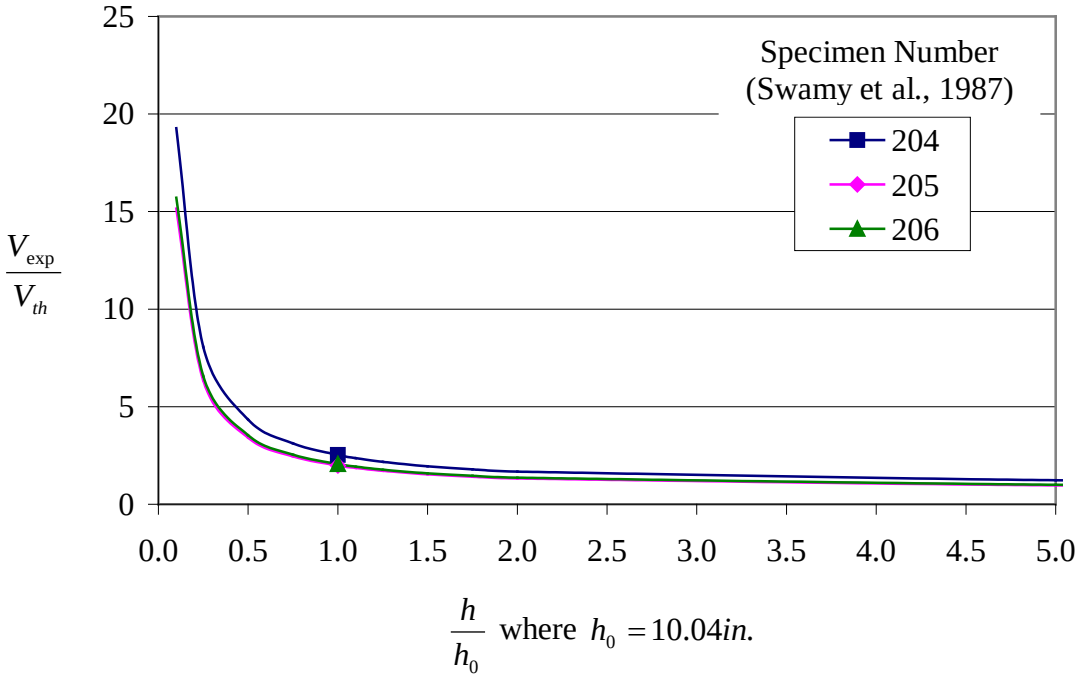

Figure 4.16. Sensitivity of Theoretical Plate End Shear with respect to Beam Height

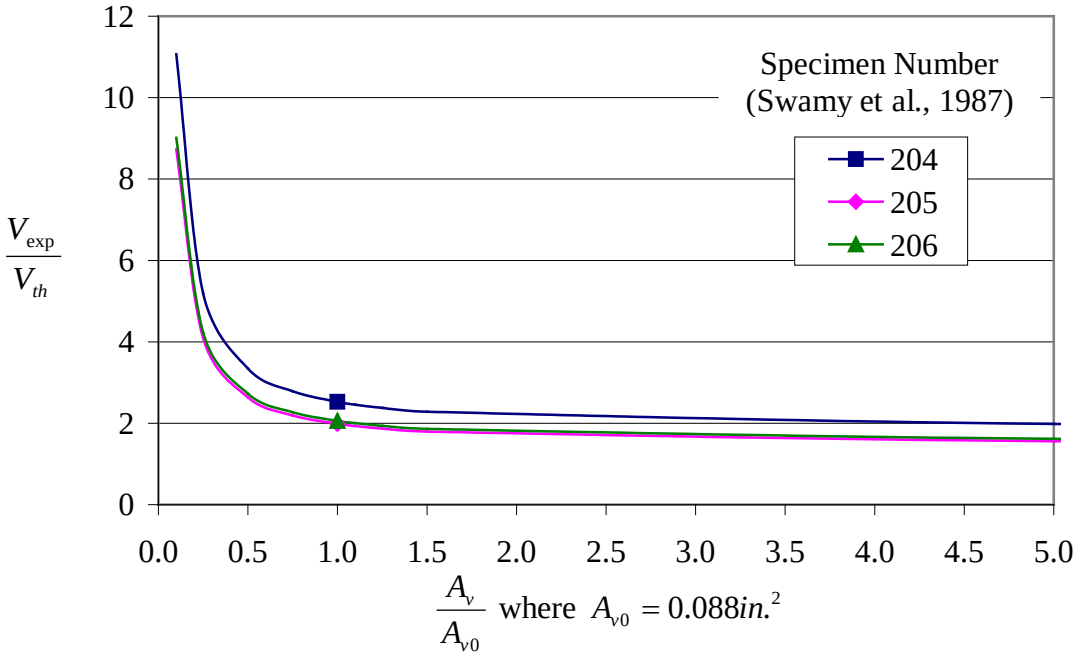

Figure 4.17. Sensitivity of Theoretical Plate End Shear with respect to Transverse Reinforcement Area

According to the model by Colotti et al. (2004), increasing the concrete cover and the area of flexural tension reinforcement decreases the value of the plate end shear at failure. The decrease in shear capacity with increased concrete cover (Figure 4.18) coincides with the results from the sensitivity analysis of Roberts' (1989) model, which suggested that an increase in the concrete cover would increase the interfacial shear and normal stresses, thereby increasing the likelihood of debonding. Yao and Teng had similar findings in their 2007 study. The theoretical plate end shear appears to be least sensitive to variations in the area of flexural tension reinforcement (Figure 4.19).

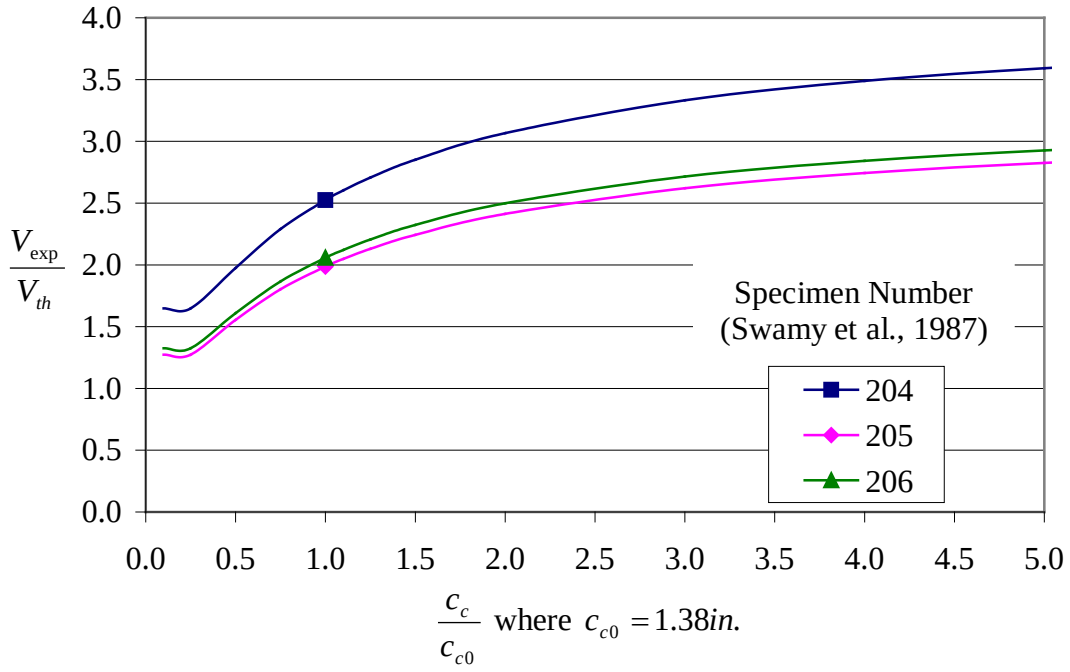

Figure 4.18. Sensitivity of Theoretical Plate End Shear with respect to Concrete Cover

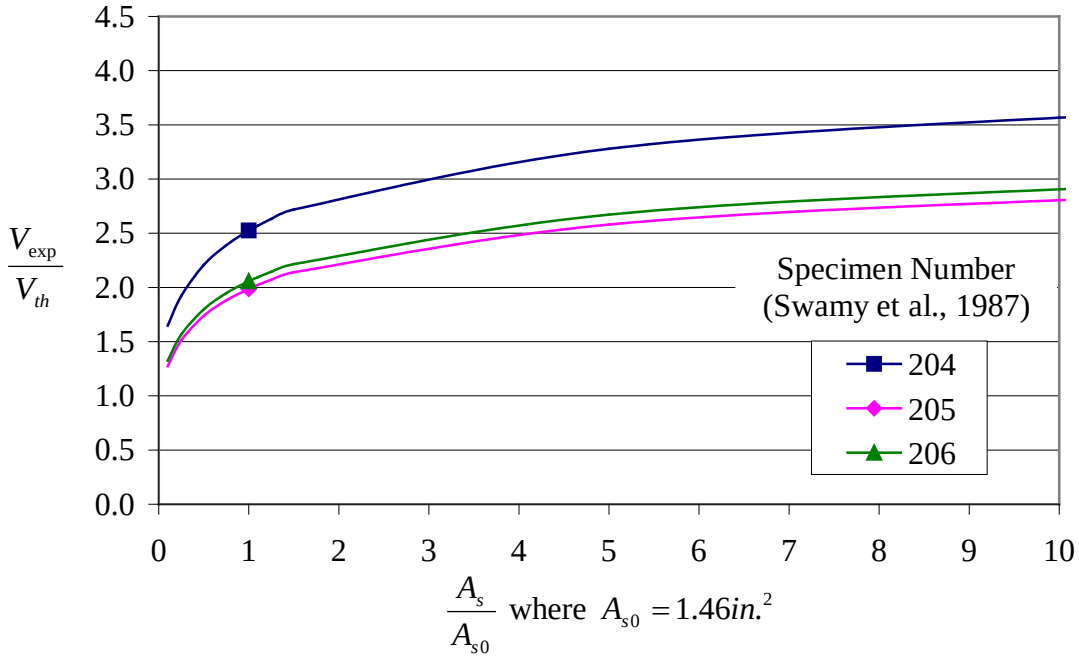

Figure 4.19. Sensitivity of Theoretical Plate End Shear with respect to Flexural Tension Reinforcement Area

4.2.2.2 Effect of External Reinforcement Properties on Shear at Plate End

The only parameters of the external plate that are accounted for in the calculation of the plate end shear are the width of the external reinforcement and its development length into the shear span. The external reinforcement width is used to find the limiting bond strength when debonding occurs without concrete cover separation. Since the limiting bond strength with concrete cover separation typically governs, the plate width has little or no effect on the calculated plate end shear (Figure 4.20), which is consistent with the findings by Yao and Teng (2007). The development length of the plate into the shear span is the only parameter of the external reinforcement to have an impact on the computed value of the plate end shear. As the development length approaches zero, the plate end shear also approaches zero, as might be expected (Figure 4.21).

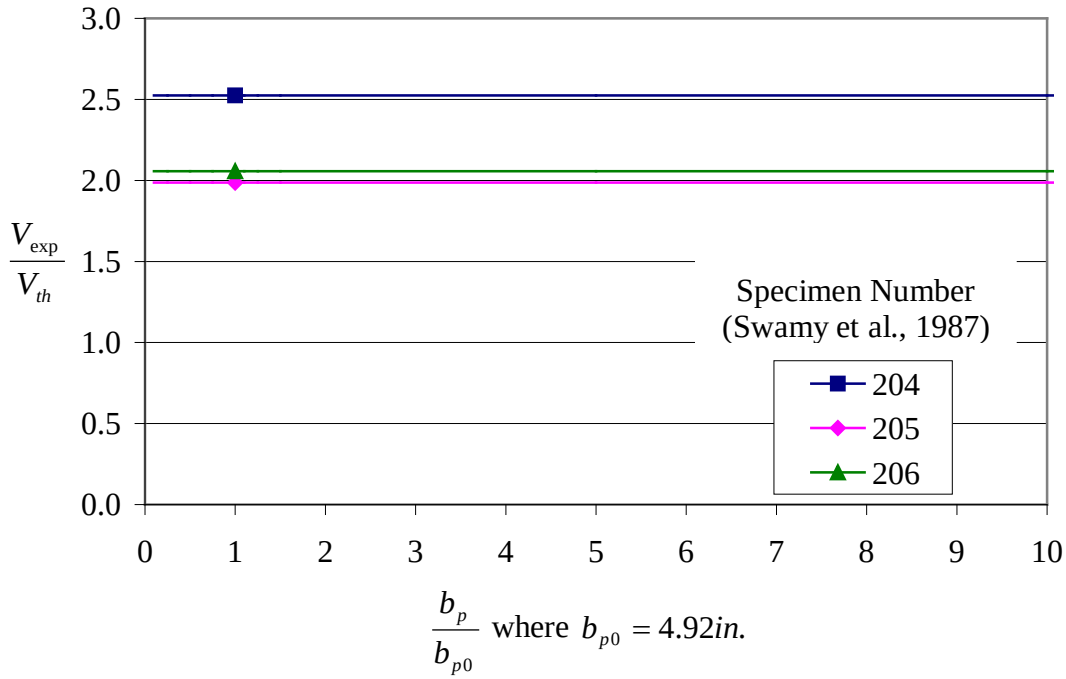

Figure 4.20. Sensitivity of Theoretical Plate End Shear with respect to Width of the External Reinforcement

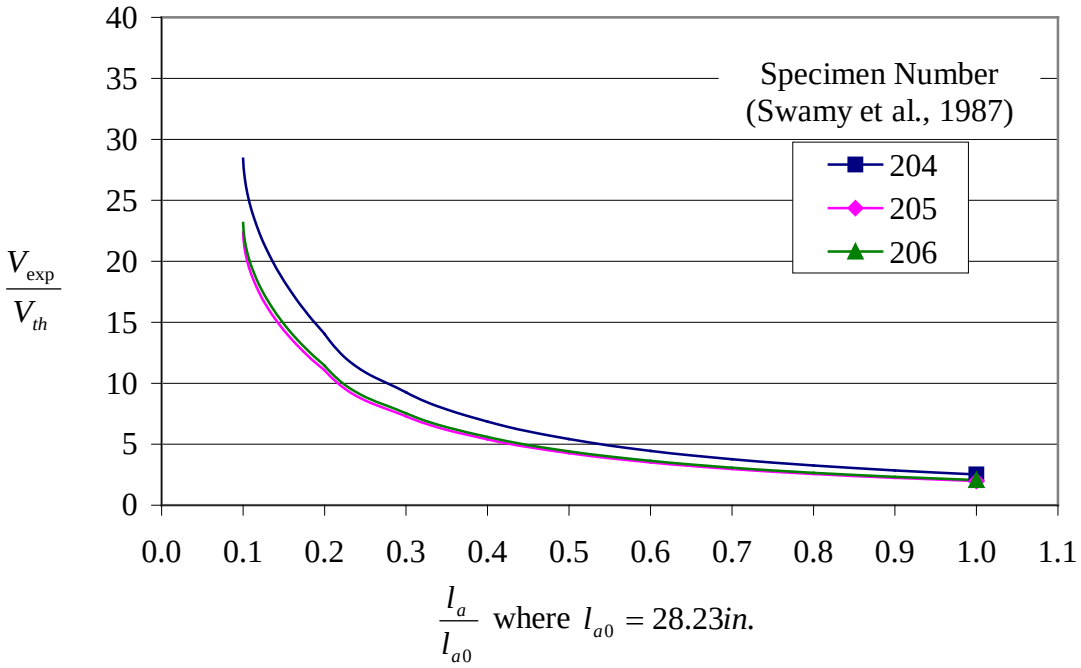

Figure 4.21. Sensitivity of Theoretical Plate End Shear with respect to the Length of External Reinforcement in the Shear Span

4.2.2.3 Effect of Adhesive Properties on Shear at Plate End

Properties of the adhesive are not taken into consideration in the model presented by Colotti, Spadea, and Swamy (2004). Therefore, a sensitivity analysis was not performed since the model assumes that the adhesive does not contribute to the bond strength at the concrete/external reinforcement interface.

4.3 Selection of Model

The two proposed models (Roberts, 1989; Colotti et al., 2004) for predicting premature debonding failure of reinforced concrete beams flexurally strengthened with external reinforcement both are candidates for use in engineering design practice. As described in Section 4.1, a statistical analysis was performed in which each model's ability to predict ultimate beam failure due to debonding with or without concrete cover separation was considered. The mean value for the ratios of the normal peeling stress, computed using Roberts' (1989) model, to the interfacial shear stress was relatively high at 7.147. Ideally, the mean value of the data set would be closer to 1.0. The standard deviation of this ratio was 4.299, and the coefficient of variation (COV) was 0.601, indicating a high degree of variability in the prediction capability of this model. The COV is a useful tool for comparison when comparing between data sets with different units and widely different means, such as these two data sets.

The ratios of the experimental to the theoretical plate end shear values, computed using the model by Colotti et al. (2004), were statistically evaluated as well. The mean value of this data set was 1.515 with a standard deviation of 0.728 and a coefficient of variation of 0.480. The COV is a dimensionless number which expresses the standard deviation in the context of the mean of the data. The COV for the data set from Roberts'

(1989) model was larger than the COV for the data set using the model by Colotti et al. (2004), indicating that model for plate end shear had less variability in its failure prediction. However, both variabilities are quite high when compared to customary engineering prediction models.

In addition to model predictability, the ease of computation must also be considered when selecting a model to predict ultimate beam failure due to debonding. Several attributes of the models may affect the ease of computation, such as the number of variables in each model, how well-defined the variables are, and which geometric or material properties of the beam specimens may be unknown or difficult to ascertain in a typical design situation. To determine the normal peeling stress at which debonding occurs using the model adopted from Roberts (1989), the moment of inertia for the cracked section of the externally reinforced concrete beam first must be found. While several steps are involved in computing the moment of inertia for a cracked section, this set of calculations is common in engineering practice and can typically be performed quickly. All of the variables in the subsequent steps of the formulation are characteristic, well-defined variables.

The model by Colotti et al. (2004) is more complex than the model by Roberts (1989) for several reasons. First, it requires the calculation of two different bond strengths, one for interfacial plate debonding failure and another for plate debonding failure with concrete cover separation. The two bond strengths must then be compared to determine the minimum, which will govern the design. Once the minimum bond strength is determined, then the plate end shear at ultimate debonding failure can be calculated. Extensive formulations are employed to generate the parameters in the plate end shear

calculation. These formulations incorporate numerous variables of their own, some of which are ill-defined or uncommon in engineering practice in the United States. For instance, in calculating the bond strength for debonding with concrete cover separation, the flexural crack spacing size must be known. A theoretical crack spacing size must be calculated through another formula presented in the paper by Colotti et al. (2004). Also, as noted in the sensitivity analyses of Section 4.2.2.2, the only properties of the external reinforcement which are accounted for in this model are the plate width and the plate development length into the shear span. In cases where the bond strength with concrete cover separation governs, only the development length of the external reinforcement participates in determining the theoretical plate end shear at debonding failure. The model neglects other parameters that Roberts' (1989) model considers, such as plate stiffness and properties of the adhesive. Lastly, the model by Colotti et al. (2004) is limited to the use of beams which have external reinforcement extending into the shear spans.

The model by Roberts (1989) has a higher conservative bias and variability in its failure prediction than the model by Colotti et al. (2004), but has practical advantages in executing the calculations for normal peeling stress over the calculations to find the plate end shear at debonding. The peeling stress calculations are straight-forward and consistent with engineering practice in the United States. In addition, the model incorporates properties of all components of an externally reinforced concrete beam. The model by Roberts (1989) is applicable for all externally reinforced concrete beams. It is not limited to beams which only have plates extending into the shear spans. For these reasons, the model by Roberts (1989) calculating the normal and shear peeling stress at

debonding failure is recommended for design. Proposed guidelines for its use in bridge rehabilitation are developed in the next chapter.

CHAPTER 5

RECOMMENDED GUIDELINES FOR FLEXURAL STRENGTHENING USING EXTERNALLY BONDED FRP REINFORCEMENT

This research was intended to provide the technical basis to support the reinforcement end peeling limit state established in the NCHRP Project 10-73 (Zureick et al., 2009) entitled *Guide Specification for the Design of Externally Bonded FRP Systems for Repair and Strengthening of Concrete Bridge Elements.* The *Guide Specification* outlines a procedure for design to prevent premature plate end debonding of simply supported reinforced concrete bridge beams and slabs that have been flexurally strengthened with externally bonded FRP reinforcement. An overview of the *Guide Specification,* as presented in the NCHRP Project 10-73 (Zureick et al., 2009), is reproduced below for convenience.

5.1 Design Basis

The *Guide Specification* presented in the NCHRP Project 10-73 (Zureick et al., 2009) for preventing premature plate end debonding failure is based on the work of Roberts (1989) and has been reformulated to be consistent with the *AASHTO LRFD Bridge Design Specification (2007)* format.

5.2 Design for Plate End Debonding Failure

5.2.1 Peeling Stress

The normal and shear stresses at the point of termination of the externally bonded FRP reinforcement shall be computed by:

$$f_{peel} = \tau_a \left[\left(\frac{3E_a}{E_p} \right) \frac{t_p}{t_a} \right]^{1/4} \tag{5.1}$$

$$\tau_a = \left[V_u + \left(\frac{G_a}{E_p t_p t_a} \right)^{1/2} M_u \right] \frac{t_p \left[h + \left(t_p / 2 \right) - y \right]}{I_T} \tag{5.2}$$

in which

$$E_a = 2G_a(1+\nu_a) \tag{5.3}$$

and

E_a = elastic modulus of the adhesive, ksi

E_p = elastic modulus of the external reinforcement, ksi

f_{peel} = normal peeling stress in the adhesive, ksi

G_a = shear modulus of the adhesive, ksi

h = depth of the reinforced concrete beam, in.

I_T = moment of inertia of an equivalent external reinforcement transformed section, neglecting any contribution of concrete in tension, in.^{4}

M_u = factored moment at the point of external plate termination, kip-in.

t_p = thickness of the external reinforcement, in.

t_a = thickness of the adhesive, in.

V_u = factored shear force at the point of external reinforcement termination, kips

y = distance from the extreme compression surface to the neutral axis of an equivalent concrete transformed section, neglecting any contribution of concrete in tension, in.

ν_a = Poisson's ratio of the adhesive, which may be taken as 0.35

τ_a = shear stress in the adhesive, ksi

5.2.2 Design Limits

The normal plate end peeling stress, f_{peel}, in the adhesive as computed in Equation (5.1), for a reinforced concrete beam with externally bonded FRP reinforcement shall be limited by:

$$f_{peel} < \tau_{\text{int}} \tag{5.4}$$

where

$$\tau_{\text{int}} = 0.065\sqrt{f'_c} \tag{5.5}$$

f'_c = cylinder compressive strength of concrete, ksi

τ_{int} = interfacial shear transfer strength, ksi

5.3 Development of Required Tension Force in Externally Bonded FRP Plate

Externally bonded plates shall be designed with adequate development length or end anchorage to develop the required tension force in the plate.

5.3.1 Development Length of Externally Bonded Reinforcement

The minimum development length of the externally bonded FRP reinforcement shall be sufficient to develop the full tension force required within the plate in the

maximum moment region. The minimum tension development length shall be determined as:

$$L_d = \frac{T_{FRP}}{\tau_{\text{int}} b_p} \tag{5.6}$$

b_p = width of external reinforcement, in.

L_d = minimum development length of external FRP reinforcement, in.

T_{FRP} = tensile force in the external FRP reinforcement corresponding to an FRP strain of 0.005, kips

If the adequate development length cannot be provided, then end anchorage shall be provided at the ends of the external FRP plate.

5.3.2 End Anchorage of Externally Bonded Reinforcement

End anchorage shall be provided to withstand the normal peeling force when development length requirements cannot be met. Permissible methods for providing end anchorage include, but are not limited to:

- Application of a transverse stainless steel plate with clamps.
- Bolting ends through grommets in the external FRP plate with multi-directional fibers.
- Wrapping the beam with an FRP wrap at the external FRP plate ends.

CHAPTER 6

CONCLUSIONS AND RECOMMENDATIONS

The aging transportation infrastructure of today coupled with constraints on public financial resources demands alternatives to bridge replacement for maintaining the safety and functionality of existing bridges. The upgrade of reinforced concrete bridge beams and slabs using externally bonded reinforcement is one of several techniques available for flexural strengthening. It is an effective, rapid, and economical means to increase the flexural capacity of bridge members for ultimate conditions. The research summarized in this thesis examined the performance of reinforced concrete members with externally bonded reinforcement. Through the evaluation of models to predict premature plate end debonding, this research addressed one of the challenges to flexural strengthening with externally bonded reinforcement.

6.1 Prediction of Plate End Debonding

When designing externally bonded reinforcement for bridge strengthening, the designer must consider all likely failure modes of the strengthened beam, recognizing that limit states that govern the design of a new bridge and a rehabilitated bridge may not be the same. Experimental studies reviewed in this thesis show that plate end debonding is a particularly important consideration in this mode of bridge strengthening and that measures must be taken in design to prevent this mode of failure from occurring. The formulation to predict plate end debonding in the present study, as adopted from Roberts (1989), presents a mechanics-based solution for design purposes. Unlike the model

proposed Colotti et al. (2004), Roberts' (1989) model accounts for all components of the composite beam: the reinforced concrete beam, the adhesive, and the external reinforcement. Whereas the model by Colotti et al. (2004) is not applicable under certain boundary conditions, e.g., if the external reinforcement does not extend beyond the constant moment region in four-point bending, Roberts' model (1989) is applicable under any given boundary conditions. Finally, when computing the normal and shear peeling stresses proposed by Roberts' (1989) model, the calculations are similar to those frequently found in engineering practice. In contrast, the Colotti et al. (2004) model depends on parameters which are uncommon to engineering practice in the United States. Therefore, the formulation adopted from Roberts' (1989) model would appear to be more readily implemented in the United States.

From the adaptation of Roberts' (1989) formulation for calculating the normal and shear peeling stresses, supported by several experimental studies, the *Guide Specification* for the NCHRP Project 10-73 (Zureick et al., 2009) was developed to predict and prevent plate end debonding for design purposes. The guidelines presented in Chapter 5 can be used to develop a specification for the Georgia Department of Transportation to prevent plate end debonding failure when using externally bonded reinforcement to flexurally strengthen reinforced concrete bridge beams.

6.2 Future Research

Further research experimentation may prove to be beneficial in evaluating the adaptation of Roberts' (1989) model to bridge strengthening. The model was developed primarily from experimental studies in which the externally bonded reinforcement consisted of steel plate. Moreover, few experimental programs have reported engineering

properties of the adhesive, necessitating a number of assumptions when evaluating the validity of Roberts' (1989) model. A future experimental program which uses FRP as external reinforcement and varies the adhesive properties would facilitate a better description of beam behavior given these conditions. Roberts' (1989) model could be evaluated using this type of experimental program to conclusively determine the accuracy of assumptions made for adhesive properties. Additional experiments may also exhibit any fallacies of the model that were not identified through the sensitivity studies and previous evaluations using other experimental programs. If Roberts' formulation (1989) can be validated with results from this experimental program, additional confidence would be provided that the *Guide Specification* can predict plate end debonding failure under various boundary conditions accurately.

In addition, future experimental studies on the effectiveness of different types of FRP plate end anchorage when peeling failure is a critical limit state would be advantageous. These studies could identify the most effective methods for anchoring externally bonded FRP plates to achieve composite beam behavior.

APPENDIX A

FLEXURAL STRENGTH SAMPLE CALCULATIONS

A.1 Jones, Swamy, Charif (1988)

A.1.1 Specimen F31 (Specimens F33, F34, F36, and F37 are similar to F31)

Reported Parameters:

$L = 2300mm = 90.55in.$ $a = 767mm = 30.20in.$

$b = 155mm = 6.10in.$ $t_p = 6mm = 0.24in.$

$h = 255mm = 10.04in.$ $b_p = 125mm = 4.92in.$

$d_s = 220mm = 8.66in.$ $E_s = 200GPa = 29000ksi$

$f'_c = 43.6MPa = 6.32ksi$ $f_{yp} = 246MPa = 35.68ksi$

$A_s = 942mm^2 = 1.46in.^2$ $E_p = 200GPa = 29000ksi$

$f_y = 430MPa = 62.37ksi$

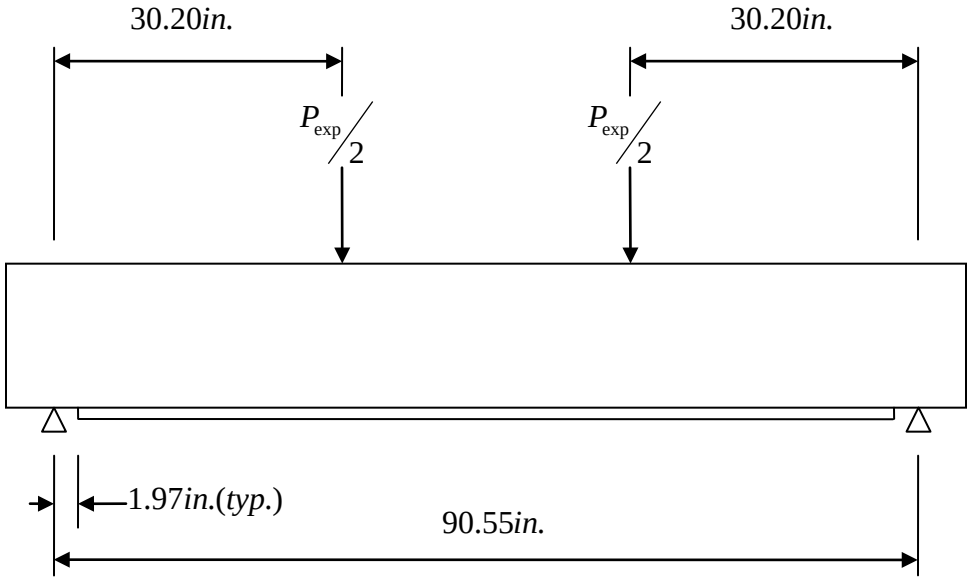

Figure A.1a. Specimen F31 Experimental Set-up used by Jones et al. (1988)

Calculate the modulus of elasticity of the concrete, where f'_c is in psi.

$E_c = 57{,}000\sqrt{f'_c}$

$E_c = 57{,}000\sqrt{6324} = 4{,}532{,}844\,psi = 4533ksi$

Find the strain, ε_0, in the concrete when the concrete stress, f_c, reaches its compressive strength, f'_c.

$$\varepsilon_0 = 1.71\left(\frac{f'_c}{E_c}\right)$$
$$\varepsilon_0 = 1.71\left(\frac{6.32}{4533}\right) = 0.002386$$

Assume a compression block depth, c. Determine the strain in the plate, ε_p, assuming that the beam fails due to concrete crushing in compression, where $\varepsilon_c = 0.003$.

$c = 5.05in.$ (assumed)

$$\varepsilon_p = 0.003\left(\frac{h-c}{c}\right)$$
$$\varepsilon_p = 0.003\left(\frac{10.04-5.05}{5.05}\right) = 0.002964$$

Check yielding of the steel plate.

$$\varepsilon_{yp} = \frac{f_{yp}}{E_p} = \frac{35.68}{29000} = 0.00123 < 0.002964$$ The steel plate has yielded.

Find the tension force in the plate, T_p.

$$T_p = b_p t_p f_{yp}$$
$$T_p = 4.92(0.24)(35.68) = 41.44kips$$

Calculate the strain in the internal steel reinforcement.

$$\varepsilon_s = 0.003\left(\frac{d_s - c}{c}\right)$$
$$\varepsilon_s = 0.003\left(\frac{8.66-5.05}{5.05}\right) = 0.002145$$

Check yielding of the internal reinforcement.

$$\varepsilon_{ys} = \frac{f_y}{E_s} = \frac{62.37}{29000} = 0.002151 > 0.002145$$ The internal reinforcement does not yield.

Find the tension force in the flexural tension reinforcement, T_s.

$$f_s = \varepsilon_s E_s$$
$$T_s = A_s f_s$$
$$T_s = 1.46(0.002145)(29000) = 90.83 kips$$

The total tensile force is

$$T = T_p + T_s = 41.436 + 90.826 = 132.26 kips$$

Find the concrete compression force to check force equilibrium, $C = T$.

$C = 0.9 f'_c \beta_1 cb$, where $\beta_1 = \dfrac{\ln\left[1+\left(\dfrac{\varepsilon_c}{\varepsilon_0}\right)^2\right]}{\varepsilon_c/\varepsilon_0}$

$$\beta_1 = \frac{\ln\left[1+\left(\dfrac{0.003}{0.002386}\right)^2\right]}{0.003/0.002386} = 0.754$$

$C = 0.9(6.32)(0.754)(5.05)(6.10) = 132.26 kips = T$ Force equilibrium checks.

Find k.

$$k = 1 - \frac{2\left[\left(\dfrac{\varepsilon_c}{\varepsilon_0}\right) - \arctan\left(\dfrac{\varepsilon_c}{\varepsilon_0}\right)\right]}{\left(\dfrac{\varepsilon_c}{\varepsilon_0}\right)^2 \beta_1}$$

$$k = 1 - \frac{2\left[\left(\dfrac{0.003}{0.002386}\right) - \arctan\left(\dfrac{0.003}{0.002386}\right)\right]}{\left(\dfrac{0.003}{0.002386}\right)^2 0.754} = 0.399$$

Find the theoretical ultimate moment in maximum moment region when concrete crushing occurs.

$$M_{th} = T_s(d_s - kc) + T_p(h - kc)$$
$$M_{th} = (90.83)(8.66 - 0.399 * 5.05) + (41.44)(10.04 - 0.399 * 5.05) = 936.33 kip - in.$$

Thus, the theoretical ultimate moment at the plate end (1.97 in. from the support) is

$$M_{th} = 936.33\left(\frac{1.97}{30.20}\right) = 61.04kip-in.\ \ (6.90kN-m)$$

Specimen F31 experienced premature failure by plate end debonding. The experimental ultimate moment, $M_{\exp}$, at the point of plate termination was 40.27 kip-in. (4.55 kN-m), which is 66% of the theoretical ultimate moment at the point of plate termination.

A.1.2 Specimen F32 (Specimen F35 is similar to F32)

Reported Parameters:

$L = 2300mm = 90.55in.$ $a = 767mm = 30.20in.$
$b = 155mm = 6.10in.$ $t_p = 6mm = 0.24in.$
$h = 255mm = 10.04in.$ $b_p = 125mm = 4.92in.$
$d_s = 220mm = 8.66in.$ $E_s = 200GPa = 29000ksi$
$f'_c = 43.6MPa = 6.32ksi$ $f_{yp} = 263MPa = 38.14ksi$
$A_s = 942mm^2 = 1.46in.^2$ $E_p = 200GPa = 29000ksi$
$f_y = 430MPa = 62.37ksi$

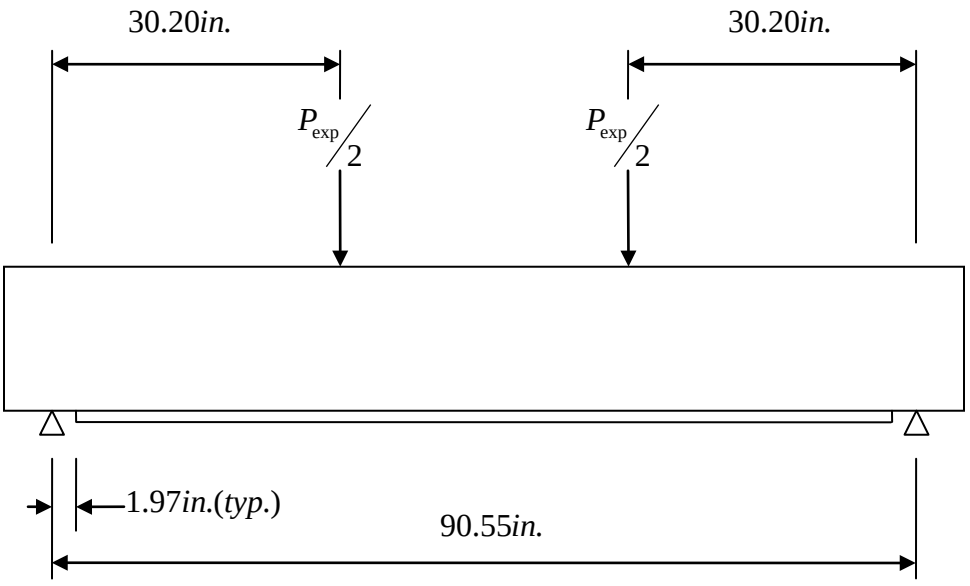

Figure A.1b. Specimen F32 Experimental Set-up used by Jones et al. (1988)

Calculate the modulus of elasticity of the concrete, where f'_c is in psi.

$$E_c = 57{,}000\sqrt{f'_c}$$
$$E_c = 57{,}000\sqrt{6324} = 4{,}532{,}844\,psi = 4533ksi$$

Find the strain, ε_0, in the concrete when the concrete stress, f_c, reaches its compressive strength, f'_c.

$$\varepsilon_0 = 1.71\left(\frac{f'_c}{E_c}\right)$$
$$\varepsilon_0 = 1.71\left(\frac{6.32}{4533}\right) = 0.002386$$

Assume a compression block depth, c. Determine the strain in the plate, ε_p, assuming that the beam fails due to concrete crushing in compression, where $\varepsilon_c = 0.003$.

$c = 5.091in.$ (assumed)

$$\varepsilon_p = 0.003\left(\frac{h-c}{c}\right)$$
$$\varepsilon_p = 0.003\left(\frac{10.04-5.091}{5.091}\right) = 0.002916$$

Check yielding of the steel plate.

$$\varepsilon_{yp} = \frac{f_{yp}}{E_p} = \frac{38.14}{29000} = 0.00132 < 0.002916$$ The steel plate has yielded.

Find the tension force in the plate, T_p.

$$T_p = b_p t_p f_{yp}$$
$$T_p = 4.92(0.24)(38.14) = 44.3kips$$

Calculate the strain in the internal steel reinforcement.

$$\varepsilon_s = 0.003\left(\frac{d_s-c}{c}\right)$$
$$\varepsilon_s = 0.003\left(\frac{8.66-5.091}{5.091}\right) = 0.002104$$

Check yielding of the internal reinforcement.

$$\varepsilon_{ys} = \frac{f_y}{E_s} = \frac{62.37}{29000} = 0.002151 > 0.002104$$ The internal reinforcement does not yield.

Find the tension force in the flexural tension reinforcement, T_s.

$$f_s = \varepsilon_s E_s$$
$$T_s = A_s f_s$$
$$T_s = 1.46(0.002104)(29000) = 89.07 kips$$

The total tensile force is

$$T = T_p + T_s = 44.3 + 89.07 = 133.37 kips$$

Find the concrete compression force to check force equilibrium, $C = T$.

$$C = 0.9 f'_c \beta_1 cb, \text{ where } \beta_1 = \frac{\ln\left[1 + \left(\frac{\varepsilon_c}{\varepsilon_0}\right)^2\right]}{\varepsilon_c / \varepsilon_0}$$

$$\beta_1 = \frac{\ln\left[1 + \left(\frac{0.003}{0.002386}\right)^2\right]}{0.003/0.002386} = 0.754$$

$C = 0.9(6.32)(0.754)(5.091)(6.10) = 133.34 kips = T$ Force equilibrium checks.

Find k.

$$k = 1 - \frac{2\left[\left(\frac{\varepsilon_c}{\varepsilon_0}\right) - \arctan\left(\frac{\varepsilon_c}{\varepsilon_0}\right)\right]}{\left(\frac{\varepsilon_c}{\varepsilon_0}\right)^2 \beta_1}$$

$$k = 1 - \frac{2\left[\left(\frac{0.003}{0.002386}\right) - \arctan\left(\frac{0.003}{0.002386}\right)\right]}{\left(\frac{0.003}{0.002386}\right)^2 0.754} = 0.399$$

Find the theoretical ultimate moment in maximum moment region when concrete crushing occurs.

$$M_{th} = T_s\left(d_s - kc\right) + T_p\left(h - kc\right)$$
$$M_{th} = \left(89.07\right)\left(8.66 - 0.399 * 5.091\right) + \left(44.3\right)\left(10.04 - 0.399 * 5.091\right) = 945.47 kip - in.$$

Thus, the theoretical ultimate moment at the plate end (1.97 in. from the support) is

$$M_{th} = 945.47\left(\frac{1.97}{30.20}\right) = 61.63 kip - in. \;\; (6.96 kN - m)$$

Specimen F32 experienced premature failure by plate end debonding. The experimental ultimate moment, $M_{\exp}$, at the point of plate termination was 46.02 kip-in. (5.20 kN-m), which is 75% of the theoretical ultimate moment at the point of plate termination.

APPENDIX B

REPORTED PARAMETERS

B.1 Swamy, Jones, and Bloxham (1987)

Table B.1a. Reported Properties of the Concrete Beams (Swamy et al., 1987)

Specimen Number	*b (in.)*	*h (in.)*	*d_s (in.)*	*L (in.)*	*a (in.)*	*f'_t (ksi)*	*f'_c (ksi)*
201	6.10	10.04	8.66	90.55	30.20	0.61	7.82
202	6.10	10.04	8.66	90.55	30.20	0.63	8.83
203	6.10	10.04	8.66	90.55	30.20	0.61	7.73
204	6.10	10.04	8.66	90.55	30.20	0.61	8.18
205	6.10	10.04	8.66	90.55	30.20	0.62	8.73
206	6.10	10.04	8.66	90.55	30.20	0.61	8.53
207	6.10	10.04	8.66	90.55	30.20	0.62	8.73
208	6.10	10.04	8.66	90.55	30.20	0.61	8.41
209	6.10	10.04	8.66	90.55	30.20	0.61	9.02
210	6.10	10.04	8.66	90.55	30.20	0.61	8.75
211	6.10	10.04	8.66	90.55	30.20	0.63	8.99
212	6.10	10.04	8.66	90.55	30.20	0.61	7.82
213	6.10	10.04	8.66	90.55	30.20	0.61	8.30
214	6.10	10.04	8.66	90.55	30.20	0.61	8.59
215	6.10	10.04	8.66	90.55	30.20	0.62	8.92
216	6.10	10.04	8.66	90.55	30.20	0.62	8.47
217	6.10	10.04	8.66	90.55	30.20	0.61	8.50
218	6.10	10.04	8.66	90.55	30.20	0.62	8.92
219	6.10	10.04	8.66	90.55	30.20	0.63	9.14
220	6.10	10.04	8.66	90.55	30.20	0.61	8.44
221	6.10	10.04	8.66	90.55	30.20	0.61	8.11
222	6.10	10.04	8.66	90.55	30.20	0.61	8.01
223	6.10	10.04	8.66	90.55	30.20	0.63	8.99
224	6.10	10.04	8.66	90.55	30.20	0.62	8.86

Table B.1b. Reported Properties of the Longitudinal and Shear Reinforcement (Swamy et al., 1987)

Specimen Number	A_s *(in.^{2})*	f_y *(ksi)*	A_v *(in.^{2})*	f_{yt} *(ksi)*	*s (in.)*	E_s *(ksi)*
201	1.46	61.64	0.088	36.26	2.95	29000
202	1.46	61.64	0.088	36.26	2.95	29000
203	1.46	61.64	0.088	36.26	2.95	29000
204	1.46	61.64	0.088	36.26	2.95	29000
205	1.46	61.64	0.088	36.26	2.95	29000
206	1.46	61.64	0.088	36.26	2.95	29000
207	1.46	61.64	0.088	36.26	2.95	29000
208	1.46	61.64	0.088	36.26	2.95	29000
209	1.46	61.64	0.088	36.26	2.95	29000
210	1.46	61.64	0.088	36.26	2.95	29000
211	1.46	61.64	0.088	36.26	2.95	29000
212	1.46	61.64	0.088	36.26	2.95	29000
213	1.46	61.64	0.088	36.26	2.95	29000
214	1.46	61.64	0.088	36.26	2.95	29000
215	1.46	61.64	0.088	36.26	2.95	29000
216	1.46	61.64	0.088	36.26	2.95	29000
217	1.46	61.64	0.088	36.26	2.95	29000
218	1.46	61.64	0.088	36.26	2.95	29000
219	1.46	61.64	0.088	36.26	2.95	29000
220	1.46	61.64	0.088	36.26	2.95	29000
221	1.46	61.64	0.088	36.26	2.95	29000
222	1.46	61.64	0.088	36.26	2.95	29000
223	1.46	61.64	0.088	36.26	2.95	29000
224	1.46	61.64	0.088	36.26	2.95	29000

Table B.1c. Reported Properties of the External Reinforcement and Adhesive (Swamy et al., 1987)

Specimen Number	*Plate Layers*	b_p *(in.)*	t_p* *(in.)*	f_{yp} *(ksi)*	E_p *(ksi)*	l_a *(in.)*	t_a *(in.)*	E_a *(ksi)*	v_a
201	--	--	--	--	--	--	--	--	--
202	--	--	--	--	--	--	0.12	304.6	0.33
203	1	4.92	0.06	34.23	29000	28.23	0.06	304.6	0.33
204	1	4.92	0.12	37.42	29000	28.23	0.06	304.6	0.33
205	1	4.92	0.24	35.97	29000	28.23	0.06	304.6	0.33
206	2	4.92	0.06	34.23	29000	28.23	0.06	304.6	0.33
207	1	4.92	0.06	34.23	29000	28.23	0.12	304.6	0.33
208	1	4.92	0.12	37.42	29000	28.23	0.12	304.6	0.33
209	1	4.92	0.24	35.97	29000	28.23	0.12	304.6	0.33
210	1	4.92	0.24	35.97	29000	28.23	0.12	304.6	0.33
211	1	4.92	0.06	34.23	29000	28.23	0.12	304.6	0.33
212	1	4.92	0.06	34.23	29000	28.23	0.12	304.6	0.33
213	2	4.92	0.06	34.23	29000	28.23	0.12	304.6	0.33
214	2	4.92	0.06	34.23	29000	28.23	0.12	304.6	0.33
215	1	4.92	0.12	37.42	29000	28.23	0.12	304.6	0.33
216	1	4.92	0.06	34.23	29000	28.23	0.24	304.6	0.33
217	1	4.92	0.12	37.42	29000	28.23	0.24	304.6	0.33
218	1	4.92	0.24	35.97	29000	28.23	0.24	304.6	0.33
219	1	4.92	0.24	35.97	29000	28.23	0.24	304.6	0.33
220	1	4.92	0.06	34.23	29000	28.23	0.22†	304.6	0.33
221	1	4.92	0.06	34.23	29000	28.23	0.12	304.6	0.33
222	1	4.92	0.06	34.23	29000	28.23	0.12	304.6	0.33
223	1	4.92	0.06	34.23	29000	28.23	0.12	304.6	0.33
224	1	4.92	0.12	37.42	29000	28.23	0.12	304.6	0.33

*Thickness per plate layer.

†Average adhesive thickness.

B.2 Jones, Swamy, and Charif (1988)

Table B.2a. Reported Properties of the Concrete Beams (Jones et al., 1988)

Specimen Number	*b (in.)*	*h (in.)*	*c_c (in.)*	*L (in.)*	*a (in.)*	*f'_t (ksi)*	*f'_c (ksi)*
F31	6.10	10.04	1.38	90.55	30.20	0.51	6.32
F32	6.10	10.04	1.38	90.55	30.20	0.51	6.32
F33	6.10	10.04	1.38	90.55	30.20	0.51	6.32
F34	6.10	10.04	1.38	90.55	30.20	0.51	6.32
F35	6.10	10.04	1.38	90.55	30.20	0.51	6.32
F36	6.10	10.04	1.38	90.55	30.20	0.51	6.32
F37	6.10	10.04	1.38	90.55	30.20	0.51	6.32

Table B.2b. Reported Properties of the Longitudinal and Shear Reinforcement (Jones et al., 1988)

Specimen Number	*A_s ($in.^2$)*	*f_y (ksi)*	*A_v ($in.^2$)*	*f_{yt} (ksi)*	*s (in.)*	*E_s (ksi)*
F31	1.46	62.37	0.088	46.99	2.95	29000
F32	1.46	62.37	0.088	46.99	2.95	29000
F33	1.46	62.37	0.088	46.99	2.95	29000
F34	1.46	62.37	0.088	46.99	2.95	29000
F35	1.46	62.37	0.088	46.99	2.95	29000
F36	1.46	62.37	0.088	46.99	2.95	29000
F37	1.46	62.37	0.088	46.99	2.95	29000

Table B.2c. Reported Properties of the External Reinforcement and Adhesive (Jones et al., 1988)

Specimen Number	*Plate Layers*	*b_p (in.)*	*t_p* (in.)*	*f_{yp} (ksi)*	*E_p (ksi)*	*l_a (in.)*	*t_a (in.)*	*E_a (ksi)*
F31	1	4.92	0.24	35.68	29000	28.23	0.06	40.45
F32	2	4.92	0.12	38.14	29000	28.23	0.06	40.45
F33	1	4.92	0.24	35.68	29000	28.23	0.06	40.45
F34	1	4.92	0.24	35.68	29000	28.23	0.06	40.45
F35	2	4.92	0.12	38.14	29000	28.23	0.06	40.45
F36	1	4.92	0.24	35.68	29000	28.23	0.06	40.45
F37	1	4.92	0.24	35.68	29000	28.23	0.06	40.45

∗Thickness per plate layer.

B.3 Oehlers and Moran (1990)

Table B.3a. Reported Properties of the Concrete Beams (Oehlers and Moran, 1990)

Specimen Number	*b (in.)*	*h (in.)*	*c_c (in.)*	*L (in.)*	*a* (in.)*	*f'_t (ksi)*	*f'_c (ksi)*
1/1	4.92	5.91	1.50	82.68	17.72	0.55	5.51
1/2	4.92	5.91	1.50	82.68	17.72	0.55	5.51
2/1	4.92	5.91	1.50	82.68	17.72	0.42	4.04
2/2	4.92	5.91	1.50	82.68	17.72	0.42	4.04
3/1	4.92	5.91	1.10	82.68	17.72	0.40	3.34
3/2	4.92	5.91	1.10	82.68	17.72	0.40	3.34
3/3	4.92	5.91	1.10	82.68	17.72	0.43	3.34
3/4	4.92	5.91	1.10	82.68	17.72	0.43	3.34
4/1	4.92	5.91	1.10	82.68	17.72	0.59	5.08
4/2	4.92	5.91	1.10	82.68	17.72	0.59	5.08
4/3	4.92	5.91	1.10	82.68	17.72	0.60	4.99
4/4	4.92	5.91	1.10	82.68	17.72	0.60	4.99
5/1	4.92	5.91	1.10	82.68	17.72	0.50	4.99
5/2	4.92	5.91	1.10	82.68	17.72	0.50	4.99
5/3	4.92	5.91	1.10	82.68	17.72	0.48	4.90
5/4	4.92	5.91	1.10	82.68	17.72	0.48	4.90
6/1	4.92	5.91	1.10	82.68	17.72	0.45	4.25
6/2	4.92	5.91	1.10	82.68	17.72	0.45	4.25
6/3	4.92	5.91	1.10	82.68	17.72	0.48	4.25
6/4	4.92	5.91	1.10	82.68	17.72	0.48	4.25
7/1	4.72	7.87	1.10	64.96	32.48	0.46	4.14
7/2	4.72	7.87	1.10	64.96	32.48	0.46	4.14
7/3	4.72	7.87	1.10	64.96	32.48	0.46	4.04
7/4	4.72	7.87	1.10	64.96	32.48	0.46	4.04
8/1	4.72	7.87	1.10	64.96	32.48	0.44	4.35
8/2	4.72	7.87	1.10	64.96	32.48	0.44	4.35
8/3	4.72	7.87	1.10	64.96	32.48	0.39	4.14
8/4	4.72	7.87	1.10	64.96	32.48	0.39	4.14
9/1	4.92	5.91	1.10	82.68	17.72	0.47	4.44
9/2	4.92	5.91	1.10	82.68	17.72	0.47	4.44
9/3	4.92	5.91	1.10	82.68	17.72	0.46	3.48
9/4	4.92	5.91	1.10	82.68	17.72	0.46	3.48
10/1	4.72	7.09	1.10	64.96	15.16	0.55	3.94
10/2	4.72	7.09	1.10	64.96	15.16	0.55	3.94
10/3	4.72	7.09	1.10	64.96	15.16	0.50	4.35
10/4	4.72	7.09	1.10	64.96	15.16	0.50	4.35
11/1	4.72	7.09	1.10	64.96	15.16	0.48	4.04
11/2	4.72	7.09	1.10	64.96	15.16	0.48	4.04
11/3	4.72	7.09	1.10	64.96	15.16	0.60	4.25

Table B.3a (continued).

Specimen Number	*b (in.)*	*h (in.)*	c_c *(in.)*	*L (in.)*	*a* (in.)*	f'_t *(ksi)*	f'_c *(ksi)*
11/4	4.72	7.09	1.10	64.96	15.16	0.60	4.25
12/1	4.72	7.09	1.10	64.96	15.16	0.49	3.63
12/2	4.72	7.09	1.10	64.96	15.16	0.49	3.63
12/3	4.72	7.09	1.10	64.96	15.16	0.54	4.25
12/4	4.72	7.09	1.10	64.96	15.16	0.54	4.25
13/6	4.72	7.87	0.71	98.43	21.65	0.48	4.80
13/7	4.72	9.45	0.71	98.43	21.65	0.51	4.71
13/9	4.72	6.30	0.71	70.87	13.78	0.66	5.22
13/10	4.72	6.30	0.71	70.87	13.78	0.66	5.22
13/11	4.72	6.30	0.71	70.87	13.78	0.70	4.14
13/13	4.72	6.30	1.50	70.87	15.75	0.49	4.35
13/14	4.72	6.30	1.50	70.87	15.75	0.49	4.35
13/15	4.72	6.30	1.57	70.87	15.75	0.46	3.94
13/16	4.72	6.30	1.57	70.87	15.75	0.46	3.94
13/17	4.72	6.30	2.28	70.87	15.75	0.46	4.90
13/18	4.72	6.30	2.28	70.87	15.75	0.46	4.90
13/19	4.72	6.30	1.42	70.87	15.75	0.48	4.90
13/20	4.72	6.30	1.42	70.87	15.75	0.48	4.90

*From data presented by Moran (1988).

Table B.3b. Reported Properties of the Longitudinal and Shear Reinforcement (Oehlers and Moran, 1990)

Specimen Number	d_b *(in.)*	f_y* *(ksi)*	A_v* *(in.^{2})*	f_{yt}* *(ksi)*	s* *(in.)*
1/1	0.63	66.72	0.156	36.26	1.97
1/2	0.63	66.72	0.156	36.26	1.97
2/1	0.63	66.72	0.156	36.26	2.76
2/2	0.63	66.72	0.156	36.26	2.76
3/1	0.63	66.72	0.088	36.26	1.97
3/2	0.63	66.72	0.088	36.26	1.97
3/3	0.63	66.72	0.088	36.26	1.97
3/4	0.63	66.72	0.088	36.26	1.97
4/1	0.63	66.72	0.088	36.26	1.97
4/2	0.63	66.72	0.088	36.26	1.97
4/3	0.63	66.72	0.088	36.26	1.97
4/4	0.63	66.72	0.088	36.26	1.97
5/1	0.63	66.72	0.088	36.26	1.97
5/2	0.63	66.72	0.088	36.26	1.97
5/3	0.63	66.72	0.088	36.26	1.97
5/4	0.63	66.72	0.088	36.26	1.97
6/1	0.63	66.72	0.088	36.26	1.97
6/2	0.63	66.72	0.088	36.26	1.97
6/3	0.63	66.72	0.088	36.26	1.97
6/4	0.63	66.72	0.088	36.26	1.97
7/1	0.63	66.72	0.088	36.26	1.97
7/2	0.63	66.72	0.088	36.26	1.97
7/3	0.63	66.72	0.088	36.26	1.97
7/4	0.63	66.72	0.088	36.26	1.97
8/1	0.63	66.72	0.088	36.26	1.97
8/2	0.63	66.72	0.088	36.26	1.97
8/3	0.63	66.72	0.088	36.26	1.97
8/4	0.63	66.72	0.088	36.26	1.97
9/1	0.63	66.72	0.088	36.26	1.97
9/2	0.63	66.72	0.088	36.26	1.97
9/3	0.63	66.72	0.088	36.26	1.97
9/4	0.63	66.72	0.088	36.26	1.97
10/1	0.63	66.72	0.088	36.26	1.97
10/2	0.63	66.72	0.088	36.26	1.97
10/3	0.63	66.72	0.088	36.26	1.97
10/4	0.63	66.72	0.088	36.26	1.97
11/1	0.63	66.72	0.088	36.26	1.97
11/2	0.63	66.72	0.088	36.26	1.97
11/3	0.63	66.72	0.088	36.26	1.97
11/4	0.63	66.72	0.088	36.26	1.97
12/1	0.63	66.72	0.088	36.26	1.97
12/2	0.63	66.72	0.088	36.26	1.97

Table B.3b (continued).

Specimen Number	d_b *(in.)*	f_y* *(ksi)*	A_v* *(in.^{2})*	f_{yt}* *(ksi)*	s* *(in.)*
12/3	0.63	66.72	0.088	36.26	1.97
12/4	0.63	66.72	0.088	36.26	1.97
13/6	0.63	66.72	0.156	36.26	2.76
13/7	0.63	66.72	0.156	36.26	2.76
13/9	0.63	66.72	0.156	36.26	2.76
13/10	0.63	66.72	0.156	36.26	2.76
13/11	0.63	66.72	0.156	36.26	2.76
13/13	0.63	66.72	0.156	36.26	2.76
13/14	0.63	66.72	0.156	36.26	2.76
13/15	0.79	66.72	0.156	36.26	2.76
13/16	0.79	66.72	0.156	36.26	2.76
13/17	0.63	66.72	0.156	36.26	2.76
13/18	0.63	66.72	0.156	36.26	2.76
13/19	0.47	66.72	0.156	36.26	2.76
13/20	0.47	66.72	0.156	36.26	2.76

*From data presented by Moran (1988).

Table B.3c. Reported Properties of the External Reinforcement and Adhesive (Oehlers and Moran, 1990)

Specimen Number	b_p *(in.)*	t_p *(in.)*	f_{yp} *(ksi)*	l_a* *(in.)*
1/1	4.92	0.12	36.26	0
1/2	4.92	0.12	36.26	0
2/1	4.92	0.20	36.26	0
2/2	4.92	0.20	36.26	0
3/1	4.92	0.12	36.26	0
3/2	4.92	0.12	36.26	0
3/3	4.92	0.12	36.26	0
3/4	4.92	0.12	36.26	0
4/1	4.92	0.20	36.26	0
4/2	4.92	0.20	36.26	0
4/3	4.92	0.20	36.26	0
4/4	4.92	0.20	36.26	0
5/1	4.92	0.20	36.26	0
5/2	4.92	0.20	36.26	0
5/3	4.92	0.20	36.26	0
5/4	4.92	0.20	36.26	0
6/1	4.92	0.20	36.26	0
6/2	4.92	0.20	36.26	0
6/3	4.92	0.20	36.26	0
6/4	4.92	0.20	36.26	0
7/1	4.72	0.20	36.26	14.07
7/2	4.72	0.20	36.26	17.72
7/3	4.72	0.20	36.26	23.62
7/4	4.72	0.20	36.26	27.56
8/1	4.72	0.20	36.26	14.07
8/2	4.72	0.20	36.26	17.72
8/3	4.72	0.20	36.26	19.69
8/4	4.72	0.20	36.26	23.62
9/1	4.92	0.12	36.26	0
9/2	4.92	0.12	36.26	0
9/3	4.92	0.12	36.26	0
9/4	4.92	0.12	36.26	0
10/1	4.72	0.39	36.26	0
10/2	4.72	0.39	36.26	0
10/3	4.72	0.26	36.26	0
10/4	4.72	0.26	36.26	0
11/1	4.72	0.12	36.26	0
11/2	4.72	0.12	36.26	0
11/3	4.72	0.59	36.26	0
11/4	4.72	0.59	36.26	0
12/1	3.94	0.39	36.26	0
12/2	1.97	0.39	36.26	0

Table B.3c (continued).

Specimen Number	b_p *(in.)*	t_p *(in.)*	f_{yp} *(ksi)*	l_a* *(in.)*
12/3	0.98	0.39	36.26	0
12/4	2.95	0.39	36.26	0
13/6	4.72	0.20	36.26	0
13/7	4.72	0.20	36.26	0
13/9	4.72	0.08	36.26	0
13/10	4.72	0.08	36.26	0
13/11	4.72	0.20	36.26	0
13/13	4.72	0.08	36.26	0
13/14	4.72	0.20	36.26	0
13/15	4.72	0.08	36.26	0
13/16	4.72	0.20	36.26	0
13/17	4.72	0.24	36.26	0
13/18	4.72	0.08	36.26	0
13/19	4.72	0.08	36.26	0
13/20	4.72	0.20	36.26	0

*The length of the external reinforcement, l_a, from the location of maximum moment into the shear span was computed from data presented by Moran (1988).

B.4 Oehlers (1992)

Table B.4a. Reported Properties of the Concrete Beams (Oehlers, 1992)

Specimen Number	*b (in.)*	*h (in.)*	d_s *(in.)*	*a (in.)*	f'_t *(ksi)*	f'_c *(ksi)*
2/2/N	5.12	6.89	5.79	21.65	0.62	6.82
2/2/S	5.12	6.89	5.79	21.65	0.62	6.82
2/3/N	5.12	6.89	5.79	21.65	0.62	6.82
2/3/S	5.12	6.89	5.79	21.65	0.62	6.82
2/4/N	5.12	6.89	5.79	21.65	0.62	6.82
2/4/S	5.12	6.89	5.79	21.65	0.62	6.82
5/1/N	5.12	6.89	5.79	21.65	0.68	7.11
5/1/S	5.12	6.89	5.79	21.65	0.68	7.11

Table B.4b. Reported Properties of the Longitudinal and Shear Reinforcement (Oehlers, 1992)

Specimen Number	d_b *(in.)*	f_y *(ksi)*	A_v *(in.^{2})*	f_{yt} *(ksi)*	*s (in.)*
2/2/N	0.63	64.40	0.04	82.38	2.95
2/2/S	0.63	64.40	0.04	82.38	2.95
2/3/N	0.63	64.40	0.09	74.11	2.95
2/3/S	0.63	64.40	0.09	74.11	2.95
2/4/N	0.63	64.40	0.09	74.11	1.77
2/4/S	0.63	64.40	0.09	74.11	1.77
5/1/N	0.63	64.40	0.09	74.11	1.77
5/1/S	0.63	64.40	0.09	74.11	1.77

Table B.4c. Reported Properties of the External Reinforcement and Adhesive (Oehlers, 1992)

Specimen Number	b_p *(in.)*	t_p *(in.)*	f_{yp} *(ksi)*	l_a *(in.)*
2/2/N	5.12	0.20	39.45	9.84
2/2/S	5.12	0.20	39.45	18.70
2/3/N	5.12	0.20	39.45	9.84
2/3/S	5.12	0.20	39.45	18.70
2/4/N	5.12	0.20	39.45	9.84
2/4/S	5.12	0.20	39.45	18.70
5/1/N	5.12	0.20	39.45	5.91
5/1/S	5.12	0.20	39.45	15.75

B.5 Duthinh and Starnes (2004)

Table B.5a. Reported Properties of the Concrete Beams (Duthinh and Starnes, 2004)

Specimen Number	b *(in.)*	h *(in.)*	d_s *(in.)*	L *(in.)*	a *(in.)*	f'_c *(ksi)*
4a	5.98	18.11	16.34	108.27	32.09	6.14
4b	5.98	17.99	16.26	108.27	32.09	6.19
5	6.14	18.11	16.30	108.27	32.09	6.14
6	5.98	17.99	16.14	108.27	32.09	6.02
7N	5.98	17.99	16.06	108.27	32.09	6.08
8N	6.18	18.11	15.98	108.27	32.09	6.09
9	6.26	17.99	15.94	108.27	32.09	6.21
10	5.98	17.99	15.87	108.27	32.09	6.21

Table B.5b. Reported Properties of the Longitudinal and Shear Reinforcement (Duthinh and Starnes, 2004)

Specimen Number	A_s *(in.^{2})*	f_y *(ksi)*	A_v *(in.^{2})*	f_{yt} *(ksi)*	s *(in.)*
4a	0.39	62.37	0.22	60.19	3.94
4b	0.39	62.80	0.22	60.19	3.94
5	0.62	73.39	0.22	60.19	3.94
6	0.88	65.70	0.22	60.19	3.94
7N	1.20	68.02	0.22	60.19	3.94
8N	1.58	67.30	0.22	60.19	3.94
9	2.0	65.70	0.22	60.19	3.94
10	2.54	65.70	0.22	60.19	3.94

Table B.5c. Reported Properties of the External Reinforcement and Adhesive (Duthinh and Starnes, 2004)

Specimen Number	b_p *(in.)*	t_p *(in.)*	E_p *(ksi)*	l_a *(in.)*	t_a *(in.)*
4a	1.97	0.05	22481	30.12	0.12
4b	3.94	0.05	22481	30.12	0.12
5	1.97	0.05	22481	30.12	0.12
6	1.97	0.05	22481	30.12	0.12
7N	1.97	0.05	22481	30.12	0.12
8N	1.97	0.05	22481	30.12	0.12
9	--	--	--	--	--
10	--	--	--	--	--

B.6 Yao and Teng (2007)

Table B.6a. Reported Properties of the Concrete Beams (Yao and Teng, 2007)

Specimen Number	*b (in.)*	*h (in.)*	c_c *(in.)*	*L (in.)*	*a (in.)*	f'_t *(ksi)*	f'_c *(ksi)*
CS-C10-A	5.95	9.95	0.67	59.06	19.69	0.58	3.24
CS-C50-A	5.93	9.95	2.22	59.06	19.69	0.39	4.51
CS-A	5.91	9.95	1.42	59.06	19.69	0.45	3.70
CS-L1-A	5.92	9.95	1.52	59.06	19.69	0.49	4.29
CS-L3-A	5.95	9.96	1.42	59.06	19.69	0.51	3.93
CS-W50-A	5.93	10.05	1.48	59.06	19.69	0.47	4.58
CS-W100-A	5.93	10.0	1.59	59.06	19.69	0.47	4.42
CP-A	5.95	9.95	1.38	59.06	19.69	0.56	4.35
SP-A	5.95	9.97	1.56	59.06	19.69	0.54	4.19
GS-A	5.95	9.93	1.56	59.06	19.69	0.63	4.52
CS-NS-B	5.93	9.95	1.46	59.06	19.69	0.39	4.36
CS-C10-B	5.95	9.95	0.67	59.06	19.69	0.58	3.24
CS-C50-B	5.93	9.95	2.22	59.06	19.69	0.39	4.51
CS-B	5.91	9.95	1.42	59.06	19.69	0.45	3.70
CS-L1-B	5.92	9.95	1.52	59.06	19.69	0.49	4.29
CS-L3-B	5.95	9.96	1.42	59.06	19.69	0.51	3.93
CS-W50-B	5.93	10.05	1.48	59.06	19.69	0.47	4.58
CS-W100-B	5.93	10.0	1.59	59.06	19.69	0.47	4.42
CP-B	5.95	9.95	1.38	59.06	19.69	0.56	4.35
SP-B	5.95	9.97	1.56	59.06	19.69	0.54	4.19
GS-B	5.95	9.93	1.56	59.06	19.69	0.63	4.52

Table B.6b. Reported Properties of the Longitudinal and Shear Reinforcement (Yao and Teng, 2007)

Specimen Number	A_s *(in.^{2})*	f_y *(ksi)*	A_v *(in.^{2})*	f_{yt} *(ksi)*	*s (in.)*	E_s *(ksi)*
CS-C10-A	0.24	77.74	0.24	77.74	3.94	28863
CS-C50-A	0.24	76.0	0.24	77.74	3.94	29153
CS-A	0.24	77.74	0.24	77.74	3.94	28863
CS-L1-A	0.24	77.74	0.24	77.74	3.94	28863
CS-L3-A	0.24	77.74	0.24	77.74	3.94	28863
CS-W50-A	0.24	77.74	0.24	77.74	3.94	28863
CS-W100-A	0.24	77.74	0.24	77.74	3.94	28863
CP-A	0.24	77.74	0.24	77.74	3.94	28863
SP-A	0.24	77.74	0.24	77.74	3.94	28863
GS-A	0.24	77.74	0.24	77.74	3.94	28863
CS-NS-B	0.24	76.0	0.24	76.0	29.53	29153
CS-C10-B	0.24	77.74	0.24	77.74	3.94	28863
CS-C50-B	0.24	76.0	0.24	77.74	3.94	29153
CS-B	0.24	77.74	0.24	77.74	3.94	28863
CS-L1-B	0.24	77.74	0.24	77.74	3.94	28863
CS-L3-B	0.24	77.74	0.24	77.74	3.94	28863
CS-W50-B	0.24	77.74	0.24	77.74	3.94	28863
CS-W100-B	0.24	77.74	0.24	77.74	3.94	28863
CP-B	0.24	77.74	0.24	77.74	3.94	28863
SP-B	0.24	77.74	0.24	77.74	3.94	28863
GS-B	0.24	77.74	0.24	77.74	3.94	28863

Table B.6c. Reported Properties of the External Reinforcement and Adhesive (Yao and Teng, 2007)

Specimen Number	b_p *(in.)*	t_p *(in.)*	f_{yp} *(ksi)*	E_p* *(ksi)*	l_a *(in.)*	t_a *(in.)*
CS-C10-A	5.83	0.073	--	37130	0	0.08
CS-C50-A	5.83	0.073	--	37130	0	0.08
CS-A	5.83	0.069	--	37130	0	0.08
CS-L1-A	5.83	0.040	--	37130	0	0.08
CS-L3-A	5.83	0.104	--	37130	0	0.08
CS-W50-A	1.97	0.079	--	37130	0	0.08
CS-W100-A	3.94	0.077	--	37130	0	0.08
CP-A	5.83	0.047	--	23931	0	0.08
SP-A	5.83	0.079	22.92	25237	0	0.08
GS-A	5.83	0.066	--	3263	0	0.08
CS-NS-B	5.83	0.067	--	37130	17.72	0.08
CS-C10-B	5.83	0.073	--	37130	17.72	0.08
CS-C50-B	5.83	0.073	--	37130	17.72	0.08
CS-B	5.83	0.069	--	37130	17.72	0.08
CS-L1-B	5.83	0.040	--	37130	17.72	0.08
CS-L3-B	5.83	0.104	--	37130	17.72	0.08
CS-W50-B	1.97	0.079	--	37130	17.72	0.08
CS-W100-B	3.94	0.077	--	37130	17.72	0.08
CP-B	5.83	0.047	--	23931	17.72	0.08
SP-B	5.83	0.079	22.92	25237	17.72	0.08
GS-B	5.83	0.066	--	3263	17.72	0.08

*For all specimens except SP-A/B and GS-A/B, fiber properties are listed.

APPENDIX C

ROBERTS' (1989) PEELING STRESS MODEL SAMPLE CALCULATIONS

C.1 Swamy, Jones, and Bloxham (1987)

C.1.1 Specimen 204

Reported Parameters:

$L = 2300mm = 90.55in.$ $a = 767mm = 30.20in.$

$b = 155mm = 6.10in.$ $t_p = 3mm = 0.118in.$

$h = 255mm = 10.04in.$ $b_p = 125mm = 4.92in.$

$d_s = 220mm = 8.66in.$ $E_p = 200GPa = 29000ksi$

$f'_c = 56.4MPa = 8.18ksi$ $t_a = 1.5mm = 0.059in.$

$A_s = 942mm^2 = 1.46in.^2$ $E_a = 2.1GPa = 304.6ksi$

$E_s = 200GPa = 29000ksi$ $\upsilon_a = 0.33$

Calculate the modulus of elasticity of the concrete, where f'_c is in psi.

$$E_c = 57{,}000\sqrt{f'_c}$$

$$E_c = 57{,}000\sqrt{8181} = 5{,}155{,}600\,psi = 5156ksi$$

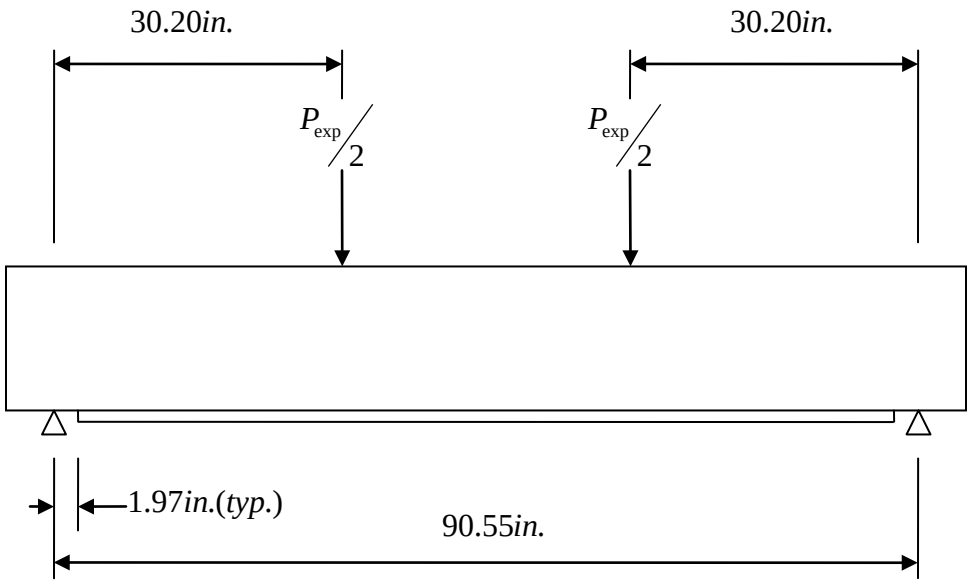

Figure C.1. Specimen 204 Experimental Set-up used by Swamy et al. (1987)

Calculate the location of the neutral axis at a distance, y, from the top of the cross section using the formulas below. Then, compute the moment of inertia, I_T, for a cracked section.

$$y = \frac{-B + \sqrt{B^2 + 4AC}}{2A}$$

where $A = b/2$, $B = \frac{E_s}{E_c}A_s + \frac{E_p}{E_c}t_p b_p$, and $C = \frac{E_s}{E_c}A_s d_s + \frac{E_p}{E_c}t_p b_p\left(h + \frac{t_p}{2}\right)$

$$A = \frac{6.10}{2} = 3.05in.$$
$$B = \frac{29000}{5156}(1.46) + \frac{29000}{5156}(0.118)(4.92) = 11.48in.^2$$
$$C = \frac{29000}{5156}(1.46)(8.66) + \frac{29000}{5156}(0.118)(4.92)\left(10.04 + \frac{0.118}{2}\right) = 104.12in.^3$$

$$y = \frac{-(11.48) + \sqrt{(11.48)^2 + 4(3.05)(104.12)}}{2(3.05)} = 4.26in.$$

$$I_T = \left(\frac{E_c}{E_p}\right)\left(\frac{by^3}{3}\right) + \left(\frac{E_s}{E_p}\right)A_s(d_s - y)^2 + t_p b_p\left(h + \frac{t_p}{2} - y\right)^2$$
$$I_T = \left(\frac{5156}{29000}\right)\left(\frac{6.10(4.26)^3}{3}\right) + \left(\frac{29000}{29000}\right)(1.46)(8.66 - 4.26)^2$$
$$+ (0.118)(4.92)\left(10.04 + \frac{0.118}{2} - 4.26\right)^2$$
$$I_T = 76.03in.^4$$

Compute the adhesive shear modulus, G_a, and the interfacial shear transfer strength, τ_{int}.

$$G_a = \frac{E_a}{2(1+\nu_a)}$$
$$G_a = \frac{304.6}{2(1+0.33)} = 114.50ksi$$

$$\tau_{\text{int}} = 0.065\sqrt{f'_c}$$
$$\tau_{\text{int}} = 0.065\sqrt{8.181} = 0.186ksi$$

Now, using the ultimate load at peeling failure of $P_{\exp} = 60.70 kips$, the normal peeling stress, f_{peel}, can be computed from the equations:

$$\tau_a = \left[V_{\exp} + \left(\frac{G_a}{E_p t_p t_a} \right)^{1/2} M_{\exp} \right] \frac{t_p \left[h + \left(t_p / 2 \right) - y \right]}{I_T}$$

$$f_{peel} = \tau_a \left[\left(\frac{3E_a}{E_p} \right) \frac{t_p}{t_a} \right]^{1/4}$$

$$\tau_a = \left[30.35 + \left(\frac{114.50}{29000(0.118)(0.059)} \right)^{1/2} 59.74 \right] \frac{0.118 \left(10.04 + \frac{0.118}{2} - 4.26 \right)}{76.03} = 0.683 ksi$$

$$f_{peel} = 0.683 \left[\left(\frac{3(304.6)}{29000} \right) \frac{0.118}{0.059} \right]^{1/4} = 0.342 ksi \quad (2.36 MPa)$$

$$f_{peel} = 0.342 ksi > \tau_{\text{int}} = 0.186 ksi$$

Specimen 204 failed by plate end debonding with concrete cover separation.

C.2 Jones, Swamy, and Charif (1988)

C.2.1 Specimen F32

Reported Parameters:

$L = 2300mm = 90.55in.$ $a = 767mm = 30.20in.$

$b = 155mm = 6.10in.$ $t_p = 2*3mm = 6mm = 0.236in.$

$h = 255mm = 10.04in.$ $b_p = 125mm = 4.92in.$

$d_s = 220mm = 8.66in.$ $E_p = 200GPa = 29000ksi$

$f'_c = 43.6MPa = 6.32ksi$ $t_a = 1.5mm = 0.059in.$

$A_s = 942mm^2 = 1.46in.^2$ $E_a = 278.9MPa = 40.45ksi$

$E_s = 200GPa = 29000ksi$

Assumed Parameters:

$\upsilon_a = 0.35$

Calculate the modulus of elasticity of the concrete, where f'_c is in psi.

$E_c = 57{,}000\sqrt{f'_c}$

$E_c = 57{,}000\sqrt{6324} = 4{,}532{,}844\,psi = 4533ksi$

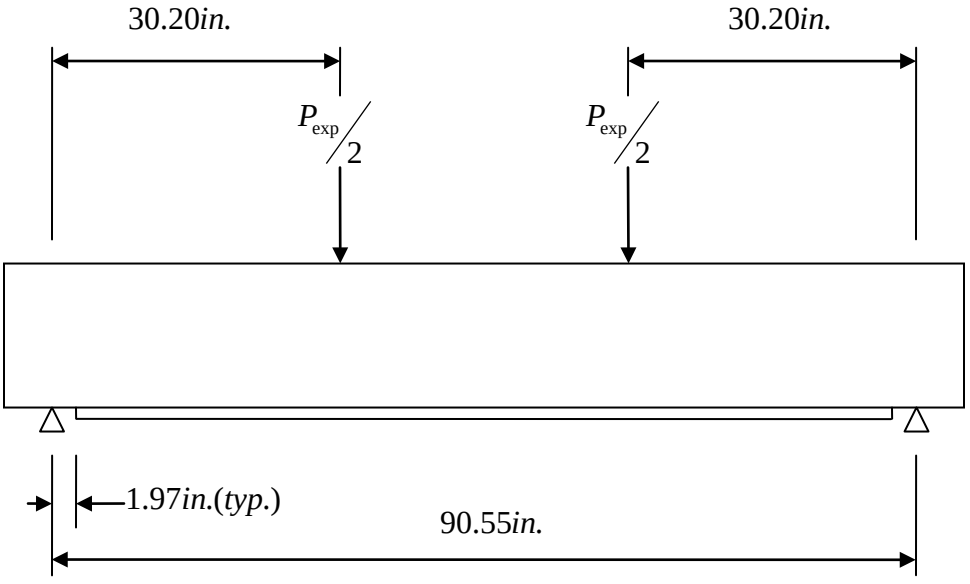

Figure C.2. Specimen F32 Experimental Set-up used by Jones et al. (1988)

Calculate the location of the neutral axis at a distance, y, from the top of the cross section using the formulas below. Then, compute the moment of inertia, I_T, for a cracked section.

$$y = \frac{-B + \sqrt{B^2 + 4AC}}{2A}$$

where $A = b/2$, $B = \frac{E_s}{E_c}A_s + \frac{E_p}{E_c}t_p b_p$, and $C = \frac{E_s}{E_c}A_s d_s + \frac{E_p}{E_c}t_p b_p\left(h + \frac{t_p}{2}\right)$

$$A = \frac{6.10}{2} = 3.05in.$$
$$B = \frac{29000}{4533}(1.46) + \frac{29000}{4533}(0.236)(4.92) = 16.78in.^2$$
$$C = \frac{29000}{4533}(1.46)(8.66) + \frac{29000}{4533}(0.236)(4.92)\left(10.04 + \frac{0.236}{2}\right) = 156.47in.^3$$

$$y = \frac{-(16.78) + \sqrt{(16.78)^2 + 4(3.05)(156.47)}}{2(3.05)} = 4.92in.$$

$$I_T = \left(\frac{E_c}{E_p}\right)\left(\frac{by^3}{3}\right) + \left(\frac{E_s}{E_p}\right)A_s\left(d_s - y\right)^2 + t_p b_p\left(h + \frac{t_p}{2} - y\right)^2$$
$$I_T = \left(\frac{4533}{29000}\right)\left(\frac{6.10(4.92)^3}{3}\right) + \left(\frac{29000}{29000}\right)(1.46)(8.66 - 4.92)^2$$
$$+ (0.236)(4.92)\left(10.04 + \frac{0.236}{2} - 4.92\right)^2$$
$$I_T = 90.18in.^4$$

Compute the adhesive shear modulus, G_a, assuming a Poisson's ratio of $\upsilon_a = 0.35$, and the interfacial shear transfer strength, τ_{int}.

$$G_a = \frac{E_a}{2(1+\nu_a)}$$
$$G_a = \frac{40.451}{2(1+0.35)} = 14.98ksi$$

$$\tau_{\text{int}} = 0.065\sqrt{f'_c}$$
$$\tau_{\text{int}} = 0.065\sqrt{6.324} = 0.163ksi$$

Now, using the ultimate load at peeling failure of $P_{\exp} = 46.76 kips$, the normal peeling stress, f_{peel}, can be computed from the equations:

$$\tau_a = \left[V_{\exp} + \left(\frac{G_a}{E_p t_p t_a} \right)^{1/2} M_{\exp} \right] \frac{t_p \left[h + \left(t_p / 2 \right) - y \right]}{I_T}$$

$$f_{peel} = \tau_a \left[\left(\frac{3E_a}{E_p} \right) \frac{t_p}{t_a} \right]^{1/4}$$

$$\tau_a = \left[23.38 + \left(\frac{14.98}{29000(0.236)(0.059)} \right)^{1/2} 46.02 \right] \frac{0.236\left(10.04 + \frac{0.236}{2} - 4.92 \right)}{90.18} = 0.442 ksi$$

$$f_{peel} = 0.442 \left[\left(\frac{3(40.45)}{29000} \right) \frac{0.236}{0.059} \right]^{1/4} = 0.134 ksi \quad (0.92 MPa)$$

$$f_{peel} = 0.134 ksi < \tau_{\text{int}} = 0.163 ksi$$

Specimen F32 failed by plate end debonding.

C.3 Oehlers and Moran (1990)

C.3.1 Specimen 8/4

Reported Parameters:

$L = 1650mm = 64.96in.$ $a = 825mm = 32.48in.$

$b = 120mm = 4.72in.$ $t_p = 5mm = 0.197in.$

$h = 200mm = 7.87in.$ $b_p = 120mm = 4.72in.$

$A_s = 402mm^2 = 0.62in.^2$ $d_s = 172mm = 6.77in.$

$f'_c = 28.57MPa = 4.14ksi$

Assumed Parameters:

$E_s = 200GPa = 29000ksi$ $E_p = 200GPa = 29000ksi$

$E_a = 2.76GPa = 400ksi$ $t_a = 1.5mm = 0.059in.$

Calculate the modulus of elasticity of the concrete, where f'_c is in psi.

$$E_c = 57{,}000\sqrt{f'_c}$$

$$E_c = 57{,}000\sqrt{4143.57} = 3{,}669{,}123psi = 3669ksi$$

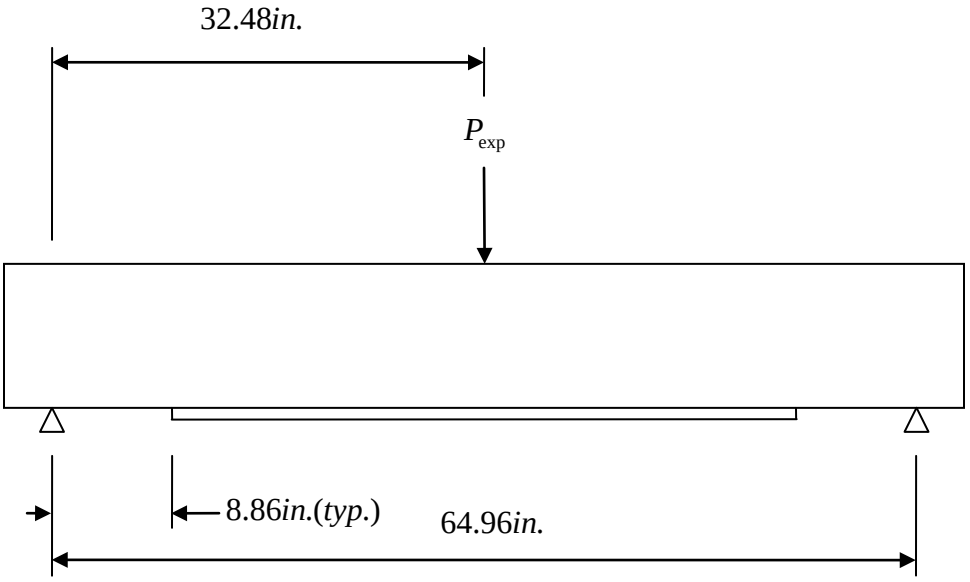

Figure C.3. Specimen 8/4 Experimental Set-up used by Oehlers and Moran (1990)

Calculate the location of the neutral axis at a distance, y, from the top of the cross section using the formulas below. Then, compute the moment of inertia, I_T, for a cracked section.

$$y = \frac{-B + \sqrt{B^2 + 4AC}}{2A}$$

where $A = b/2$, $B = \frac{E_s}{E_c}A_s + \frac{E_p}{E_c}t_p b_p$, and $C = \frac{E_s}{E_c}A_s d_s + \frac{E_p}{E_c}t_p b_p\left(h + \frac{t_p}{2}\right)$

$$A = \frac{4.72}{2} = 2.36in.$$
$$B = \frac{29000}{3669}(0.62) + \frac{29000}{3669}(0.197)(4.72) = 12.28in.^2$$
$$C = \frac{29000}{3669}(0.62)(6.77) + \frac{29000}{3669}(0.197)(4.72)\left(7.87 + \frac{0.197}{2}\right) = 91.95in.^3$$

$$y = \frac{-(12.28) + \sqrt{(12.28)^2 + 4(2.36)(91.95)}}{2(2.36)} = 4.16in.$$

$$I_T = \left(\frac{E_c}{E_p}\right)\left(\frac{by^3}{3}\right) + \left(\frac{E_s}{E_p}\right)A_s(d_s - y)^2 + t_p b_p\left(h + \frac{t_p}{2} - y\right)^2$$
$$I_T = \left(\frac{3669}{29000}\right)\left(\frac{4.72(4.16)^3}{3}\right) + \left(\frac{29000}{29000}\right)(0.62)(6.77 - 4.16)^2$$
$$+ (0.197)(4.74)\left(7.87 + \frac{0.197}{2} - 4.16\right)^2$$
$$I_T = 32.11in.^4$$

Compute the adhesive shear modulus, G_a, assuming a Poisson's ratio of $\upsilon_a = 0.35$, and the interfacial shear transfer strength, τ_{int}.

$$G_a = \frac{E_a}{2(1+\nu_a)}$$
$$G_a = \frac{400}{2(1+0.35)} = 148.15ksi$$

$$\tau_{\text{int}} = 0.065\sqrt{f'_c}$$
$$\tau_{\text{int}} = 0.065\sqrt{4.144} = 0.132ksi$$

Now, using the ultimate load at peeling failure of $P_{\exp} = 6.158 kips$, the normal peeling stress, f_{peel}, can be computed from the equations:

$$\tau_a = \left[V_{\exp} + \left(\frac{G_a}{E_p t_p t_a} \right)^{1/2} M_{\exp} \right] \frac{t_p \left[h + \left(t_p / 2 \right) - y \right]}{I_T}$$

$$f_{peel} = \tau_a \left[\left(\frac{3E_a}{E_p} \right) \frac{t_p}{t_a} \right]^{1/4}$$

$$\tau_a = \left[3.08 + \left(\frac{148.15}{29000(0.197)(0.059)} \right)^{1/2} 27.28 \right] \frac{0.197\left(7.87 + \frac{0.197}{2} - 4.16 \right)}{32.11} = 0.495 ksi$$

$$f_{peel} = 0.495 \left[\left(\frac{3(400)}{29000} \right) \frac{0.197}{0.059} \right]^{1/4} = 0.301 ksi \quad (2.08 MPa)$$

$$f_{peel} = 0.301 ksi > \tau_{\text{int}} = 0.132 ksi$$

Specimen 8/4 failed by plate end debonding with concrete cover separation.

C.4 Yao and Teng (2007)

C.4.1 Specimen CS-A

Reported Parameters:

$L = 1500mm = 59.06in.$ $a = 500mm = 19.69in.$

$b = 150.2mm = 5.91in.$ $t_p = 1.74mm = 0.069in.$ (average)

$h = 252.7mm = 9.95in.$ $b_p = 148mm = 5.83in.$

$d_s = 216.7mm = 8.53in.$ $t_a = 2mm = 0.079in.$

$f'_c = 25.5MPa = 3.70ksi$ $E_a = 2.69GPa = 390ksi$ (from manufacturer)

$A_s = 157mm^2 = 0.24in.^2$ $E_s = 199GPa = 28863ksi$

Assumed Parameters:

$\upsilon_a = 0.35$ $E_p = 76.8GPa = 11139ksi$ (30% fiber volume)

Calculate the modulus of elasticity of the concrete, where f'_c is in psi.

$$E_c = 57{,}000\sqrt{f'_c}$$

$$E_c = 57{,}000\sqrt{6398.57} = 3{,}466{,}505psi = 3467ksi$$

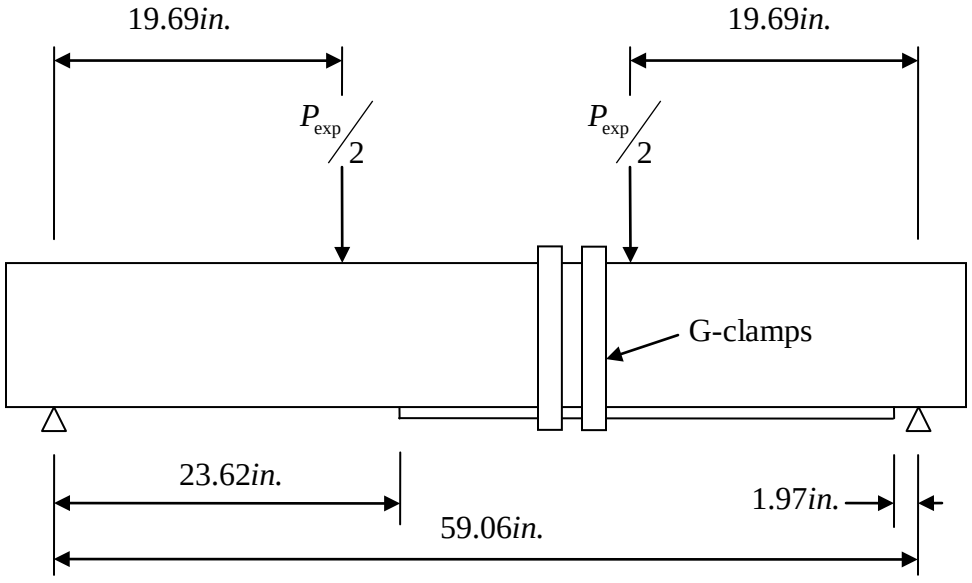

Figure C.4a. Specimen CS-A Experimental Set-up used by Yao and Teng (2007)

Calculate the location of the neutral axis at a distance, y, from the top of the cross section using the formulas below. Then, compute the moment of inertia, I_T, for a cracked section.

$$y = \frac{-B + \sqrt{B^2 + 4AC}}{2A}$$

where $A = b/2$, $B = \frac{E_s}{E_c}A_s + \frac{E_p}{E_c}t_p b_p$, and $C = \frac{E_s}{E_c}A_s d_s + \frac{E_p}{E_c}t_p b_p\left(h + \frac{t_p}{2}\right)$

$$A = \frac{5.91}{2} = 2.96in.$$
$$B = \frac{28863}{3467}(0.24) + \frac{11139}{3467}(0.069)(5.83) = 3.32in.^2$$
$$C = \frac{28863}{3467}(0.24)(8.51) + \frac{11139}{3467}(0.069)(5.83)\left(9.95 + \frac{0.069}{2}\right) = 30.17n.^3$$

$$y = \frac{-(3.32) + \sqrt{(3.32)^2 + 4(2.96)(30.17)}}{2(2.96)} = 2.68in.$$

$$I_T = \left(\frac{E_c}{E_p}\right)\left(\frac{by^3}{3}\right) + \left(\frac{E_s}{E_p}\right)A_s\left(d_s - y\right)^2 + t_p b_p\left(h + \frac{t_p}{2} - y\right)^2$$
$$I_T = \left(\frac{3467}{11139}\right)\left(\frac{5.91(2.68)^3}{3}\right) + \left(\frac{28863}{11139}\right)(0.24)(8.51 - 2.68)^2$$
$$+ (0.069)(5.83)\left(9.95 + \frac{0.069}{2} - 2.68\right)^2$$
$$I_T = 54.69in.^4$$

Compute the adhesive shear modulus, G_a, assuming a Poisson's ratio of $\upsilon_a = 0.35$, and the interfacial shear transfer strength, τ_{int}.

$$G_a = \frac{E_a}{2(1+\nu_a)}$$
$$G_a = \frac{390}{2(1+0.35)} = 144.44ksi$$

$$\tau_{\text{int}} = 0.065\sqrt{f'_c}$$
$$\tau_{\text{int}} = 0.065\sqrt{3.699} = 0.125ksi$$

Now, using the ultimate load at peeling failure of $P_{\exp} = 11.26 kips$, the normal peeling stress, f_{peel}, can be computed from the equations:

$$\tau_a = \left[V_{\exp} + \left(\frac{G_a}{E_p t_p t_a} \right)^{1/2} M_{\exp} \right] \frac{t_p \left[h + \left(t_p / 2 \right) - y \right]}{I_T}$$

$$f_{peel} = \tau_a \left[\left(\frac{3E_a}{E_p} \right) \frac{t_p}{t_a} \right]^{1/4}$$

$$\tau_a = \left[0 + \left(\frac{144.44}{11139(0.069)(0.079)} \right)^{1/2} 110.86 \right] \frac{0.069\left(9.95 + \frac{0.069}{2} - 2.68 \right)}{54.69} = 1.572 ksi$$

$$f_{peel} = 1.572 \left[\left(\frac{3(390)}{11139} \right) \frac{0.069}{0.079} \right]^{1/4} = 0.864 ksi \quad (5.96 MPa)$$

$$f_{peel} = 0.864 ksi > \tau_{\text{int}} = 0.125 ksi$$

Specimen CS-A failed by plate end debonding with concrete cover separation.

C.4.2 Specimen SP-A

Reported Parameters:

$L = 1500 mm = 59.06 in.$ $a = 500 mm = 19.69 in.$

$b = 151.2 mm = 5.95 in.$ $t_p = 2 mm = 0.079 in.$

$h = 253.3 mm = 9.97 in.$ $b_p = 148 mm = 5.83 in.$

$d_s = 213.8 mm = 8.42 in.$ $E_p = 174 GPa = 25237 ksi$

$f'_c = 28.855 MPa = 4.19 ksi$ $t_a = 2 mm = 0.079 in.$

$A_s = 157 mm^2 = 0.24 in.^2$ $E_a = 2.69 GPa = 390 ksi$ (from manufacturer)

$E_s = 199 GPa = 28863 ksi$

Assumed Parameters:

$\upsilon_a = 0.35$

Calculate the modulus of elasticity of the concrete, where f'_c is in psi.

$$E_c = 57{,}000\sqrt{f'_c}$$
$$E_c = 57{,}000\sqrt{4185} = 3{,}687{,}420\,psi = 3687\,ksi$$

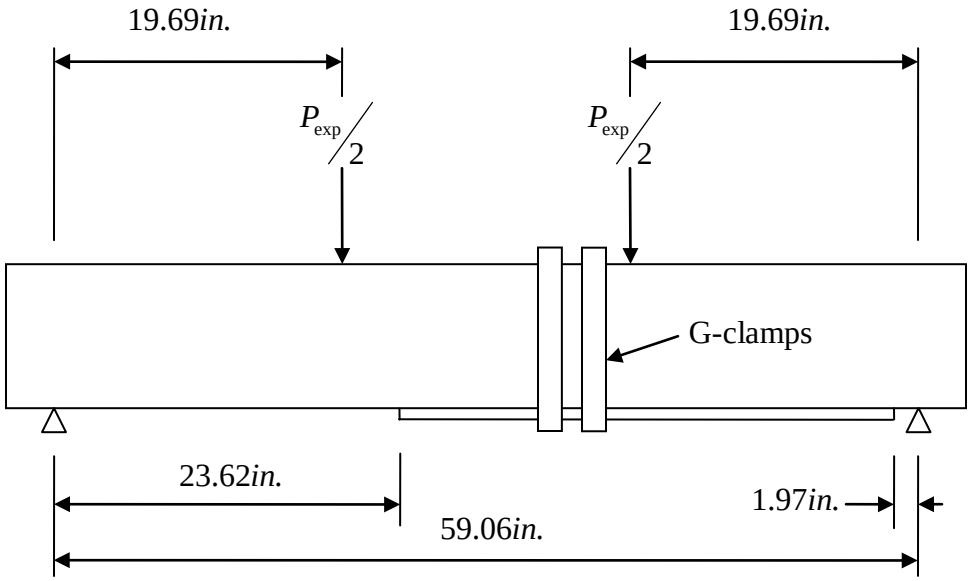

Figure C.4b. Specimen SP-A Experimental Set-up used by Yao and Teng (2007)

Calculate the location of the neutral axis at a distance, y, from the top of the cross section using the formulas below. Then, compute the moment of inertia, I_T, for a cracked section.

$$y = \frac{-B + \sqrt{B^2 + 4AC}}{2A}$$

where $A = b/2$, $B = \frac{E_s}{E_c}A_s + \frac{E_p}{E_c}t_p b_p$, and $C = \frac{E_s}{E_c}A_s d_s + \frac{E_p}{E_c}t_p b_p\left(h + \frac{t_p}{2}\right)$

$$A = \frac{5.95}{2} = 2.98in.$$
$$B = \frac{28863}{3687}(0.24) + \frac{25237}{3687}(0.079)(5.83) = 5.05in.^2$$

$$C = \frac{28863}{3687}(0.24)(8.42) + \frac{25237}{3687}(0.079)(5.83)\left(9.97 + \frac{0.079}{2}\right) = 47.55in.^3$$

$$y = \frac{-(5.05) + \sqrt{(5.05)^2 + 4(2.98)(47.55)}}{2(2.98)} = 3.24in.$$

$$I_T = \left(\frac{E_c}{E_p}\right)\left(\frac{by^3}{3}\right) + \left(\frac{E_s}{E_p}\right)A_s(d_s - y)^2 + t_p b_p\left(h + \frac{t_p}{2} - y\right)^2$$

$$I_T = \left(\frac{3687 * 5.95(3.24)^3}{3 * 25237}\right) + \left(\frac{28863(0.24)}{25237}\right)(8.42 - 3.24)^2$$

$$+ (0.079 * 5.83)\left(9.97 + \frac{0.079}{2} - 3.24\right)^2$$

$$I_T = 38.36in.^4$$

Compute the adhesive shear modulus, G_a, assuming a Poisson's ratio of $\upsilon_a = 0.35$, and the interfacial shear transfer strength, τ_{int}.

$$G_a = \frac{E_a}{2(1+\nu_a)}$$

$$G_a = \frac{390}{2(1+0.35)} = 144.44ksi$$

$$\tau_{\text{int}} = 0.065\sqrt{f'_c}$$

$$\tau_{\text{int}} = 0.065\sqrt{4.185} = 0.133ksi$$

Now, using the ultimate load at peeling failure of $P_{\text{exp}} = 10.32kips$, the normal peeling stress, f_{peel}, can be computed from the equations:

$$\tau_a = \left[V_{\text{exp}} + \left(\frac{G_a}{E_p t_p t_a}\right)^{1/2} M_{\text{exp}}\right]\frac{t_p\left[h + \left(t_p/2\right) - y\right]}{I_T}$$

$$f_{peel} = \tau_a\left[\left(\frac{3E_a}{E_p}\right)\frac{t_p}{t_a}\right]^{1/4}$$

$$\tau_a = \left[0 + \left(\frac{144.44}{25237(0.079)(0.079)}\right)^{1/2} 101.56\right] \frac{0.079\left(9.972 + \frac{0.079}{2} - 3.24\right)}{38.36} = 1.357 ksi$$

$$f_{peel} = 1.357\left[\left(\frac{3(390)}{25237}\right)\frac{0.079}{0.079}\right]^{1/4} = 0.630 ksi \quad (4.34 MPa)$$

$$f_{peel} = 0.630 ksi > \tau_{\text{int}} = 0.133 ksi$$

Specimen SP-A failed by plate end debonding with concrete cover separation.

C.4.3 Specimen CS-W100-B

Reported Parameters:

$L = 1500 mm = 59.06 in.$	$a = 500 mm = 19.69 in.$
$b = 150.6 mm = 5.93 in.$	$t_p = 1.95 mm = 0.077 in.$ (average)
$h = 254 mm = 10.0 in.$	$b_p = 100 mm = 3.94 in.$
$d_s = 213.5 mm = 8.41 in.$	$t_a = 2 mm = 0.079 in.$
$f'_c = 30.5 MPa = 4.42 ksi$	$E_a = 2.69 GPa = 390 ksi$ (from manufacturer)
$A_s = 157 mm^2 = 0.24 in.^2$	$E_s = 199 GPa = 28863 ksi$

Assumed Parameters:

$\upsilon_a = 0.35$	$E_p = 76.8 GPa = 11139 ksi$ (30% fiber volume)

Calculate the modulus of elasticity of the concrete, where f'_c is in psi.

$$E_c = 57{,}000\sqrt{f'_c}$$

$$E_c = 57{,}000\sqrt{4423.1} = 3{,}790{,}875 psi = 3791 ksi$$

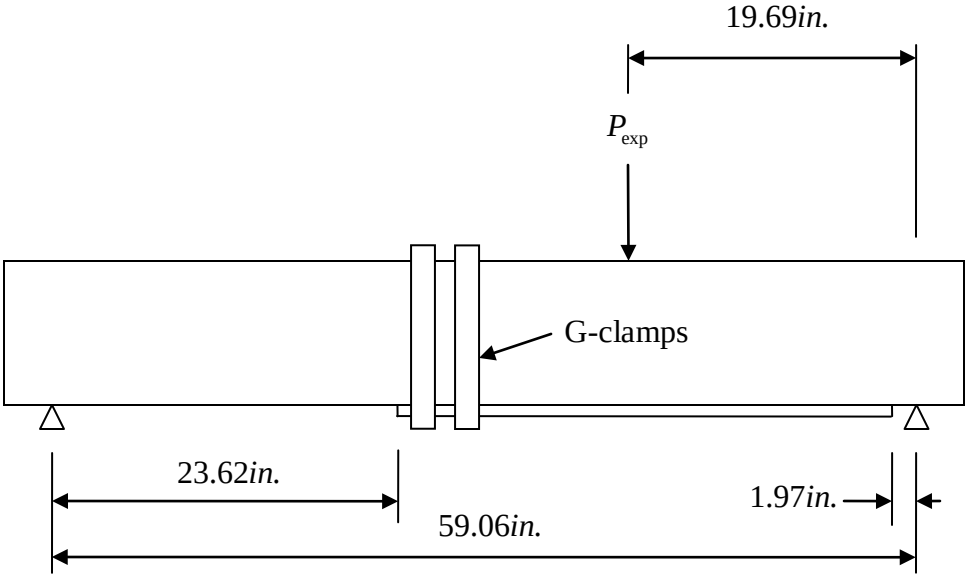

Figure C.4c. Specimen CS-W100-B Experimental Set-up used by Yao and Teng (2007)

Calculate the location of the neutral axis at a distance, y, from the top of the cross section using the formulas below. Then, compute the moment of inertia, I_T, for a cracked section.

$$y = \frac{-B + \sqrt{B^2 + 4AC}}{2A}$$

where $A = b/2$, $B = \frac{E_s}{E_c}A_s + \frac{E_p}{E_c}t_p b_p$, and $C = \frac{E_s}{E_c}A_s d_s + \frac{E_p}{E_c}t_p b_p\left(h + \frac{t_p}{2}\right)$

$$A = \frac{5.93}{2} = 2.96in.$$
$$B = \frac{28863}{3791}(0.24) + \frac{11139}{3791}(0.077)(3.94) = 2.75in.^2$$
$$C = \frac{28863}{3791}(0.24)(8.41) + \frac{11139}{3791}(0.077)(3.94)\left(10.0 + \frac{0.077}{2}\right) = 24.56in.^3$$

$$y = \frac{-(2.75) + \sqrt{(2.75)^2 + 4(2.96)(24.56)}}{2(2.96)} = 2.45in.$$

$$I_T = \left(\frac{E_c}{E_p}\right)\left(\frac{by^3}{3}\right) + \left(\frac{E_s}{E_p}\right)A_s\left(d_s - y\right)^2 + t_p b_p\left(h + \frac{t_p}{2} - y\right)^2$$

$$I_T = \left(\frac{37901 * 5.93(2.45)^3}{3 * 11139}\right) + \left(\frac{28863(0.24)}{11139}\right)(8.41 - 2.45)^2$$

$$+ (0.077 * 3.94)\left(10.0 + \frac{0.077}{2} - 2.45\right)^2$$

$$I_T = 49.66 in.^4$$

Compute the adhesive shear modulus, G_a, assuming a Poisson's ratio of $\upsilon_a = 0.35$, and the interfacial shear transfer strength, τ_{int}.

$$G_a = \frac{E_a}{2(1+\nu_a)}$$

$$G_a = \frac{390}{2(1+0.35)} = 144.44 ksi$$

$$\tau_{\text{int}} = 0.065\sqrt{f'_c}$$

$$\tau_{\text{int}} = 0.065\sqrt{4.423} = 0.137 ksi$$

Now, using the ultimate load at peeling failure of $P_{\text{exp}} = 18.16 kips$, the normal peeling stress, f_{peel}, can be computed from the equations:

$$\tau_a = \left[V_{\text{exp}} + \left(\frac{G_a}{E_p t_p t_a}\right)^{1/2} M_{\text{exp}}\right]\frac{t_p\left[h + \left(t_p/2\right) - y\right]}{I_T}$$

$$f_{peel} = \tau_a\left[\left(\frac{3E_a}{E_p}\right)\frac{t_p}{t_a}\right]^{1/4}$$

$$\tau_a = \left[12.11 + \left(\frac{144.44}{11139(0.077)(0.079)}\right)^{1/2} 23.84\right]\frac{0.077\left(10.0 + \frac{0.077}{2} - 2.45\right)}{49.66} = 0.552 ksi$$

$$f_{peel} = 0.552\left[\left(\frac{3(390)}{11139}\right)\frac{0.0768}{0.079}\right]^{1/4} = 0.312 ksi \;\; (2.15 MPa)$$

$$f_{peel} = 0.312 ksi > \tau_{\text{int}} = 0.137 ksi$$

Specimen CS-W100-B failed by plate end debonding with concrete cover separation.

APPENDIX D

PEELING STRESS VALUES USING ROBERTS' (1989) MODEL

D.1 Swamy, Jones, and Bloxham (1987)

Table D.1. Peeling Stress Values using Roberts' (1989) Model with Experiments Conducted by Swamy et al. (1987)

Specimen Number	P_{exp} *(kips)*	τ_{int} *(ksi)*	τ_a *(ksi)*	f_{peel} *(ksi)*
201*	52.16	0.182	--	--
202*	55.08	0.193	--	--
203	60.70	0.181	0.517	0.218
204	60.70	0.186	0.683	0.342
205	47.88	0.192	0.660	0.393
206	49.46	0.190	0.555	0.234
207	58.90	0.192	0.399	0.141
208	59.35	0.189	0.550	0.232
209	49.46	0.195	0.578	0.290
210	48.33	0.192	0.566	0.284
211	56.88	0.195	0.385	0.136
212	55.75	0.182	0.380	0.135
213	56.88	0.187	0.528	0.187
214	56.88	0.190	0.527	0.187
215	56.20	0.194	0.519	0.219
216	58.90	0.189	0.330	0.098
217	57.78	0.190	0.455	0.161
218	43.61	0.194	0.447	0.188
219	49.46	0.196	0.506	0.213
220	59.12	0.189	0.339	0.103
221	60.25	0.185	0.410	0.145
222	60.25	0.184	0.410	0.145
223	59.35	0.195	0.401	0.142
224	56.20	0.193	0.520	0.219

*Specimens 201 and 202 did not have external reinforcement.

D.2 Jones, Swamy, and Charif (1988)

Table D.2. Peeling Stress Values using Roberts' (1989) Model with Experiments Conducted by Jones et al. (1988)

Specimen Number	P_{exp} *(kips)*	τ_{int} *(ksi)*	τ_a *(ksi)*	f_{peel} *(ksi)*
F31	40.92	0.163	0.387	0.139
F32	46.76	0.163	0.442	0.134
F33	42.94	0.163	0.406	0.146
F34	49.68	0.163	0.470	0.169
F35	51.03	0.163	0.483	0.146
F36	64.07	0.163	0.606	0.218
F37	63.62	0.163	0.602	0.216

D.3 Oehlers and Moran (1990)

Table D.3. Peeling Stress Values using Roberts' (1989) Model with Experiments Conducted by Oehlers and Moran (1990)

Specimen Number	P_{exp} *(kips)*	τ_{int} *(ksi)*	τ_a *(ksi)*	f_{peel} *(ksi)*
1/1	9.19	0.153	2.047	1.098
1/2	9.89	0.153	2.203	1.182
2/1	12.19	0.131	2.514	1.532
2/2	11.49	0.131	2.369	1.444
3/1	11.29	0.119	2.377	1.275
3/2	10.79	0.119	2.271	1.218
3/3	12.59	0.119	2.650	1.421
3/4	13.49	0.119	2.839	1.523
4/1	12.59	0.146	2.396	1.460
4/2	13.99	0.146	2.662	1.622
4/3	13.49	0.145	2.570	1.566
4/4	14.39	0.145	2.741	1.670
5/1	11.49	0.145	2.189	1.334
5/2	15.09	0.145	2.874	1.752
5/3	11.49	0.144	2.191	1.335
5/4	9.89	0.144	1.887	1.150
6/1	15.99	0.134	3.077	1.875
6/2	12.59	0.134	2.423	1.477
6/3	12.59	0.134	2.423	1.477
6/4	14.19	0.134	2.731	1.664
7/1	9.16	0.132	1.412	0.861
7/2	9.59	0.132	1.209	0.737
7/3	8.39	0.131	0.675	0.411
7/4	5.61	0.131	0.280	0.171
8/1	9.81	0.136	1.509	0.920
8/2	11.28	0.136	1.418	0.864
8/3	7.30	0.132	0.809	0.493
8/4	6.16	0.132	0.495	0.301
9/1	16.69	0.137	3.444	1.847
9/2	13.99	0.137	2.887	1.549
9/3	13.49	0.121	2.831	1.518
9/4	15.29	0.121	3.208	1.721
10/1	14.36	0.129	1.647	1.194
10/2	12.61	0.129	1.446	1.048
10/3	13.08	0.136	1.666	1.084
10/4	13.66	0.136	1.740	1.132
11/1	14.36	0.131	2.042	1.095
11/2	15.30	0.131	2.175	1.167

Table D.3 (continued).

Specimen Number	P_{exp} *(kips)*	τ_{int} *(ksi)*	τ_a *(ksi)*	f_{peel} *(ksi)*
11/3	9.23	0.134	0.922	0.740
11/4	10.74	0.134	1.074	0.861
12/1	12.15	0.124	1.610	1.167
12/2	14.83	0.124	3.191	2.312
12/3	19.15	0.134	6.005	4.352
12/4	12.38	0.134	2.007	1.455
13/6	19.95	0.142	3.136	1.911
13/7	19.54	0.141	2.476	1.509
13/9	22.61	0.149	3.038	1.473
13/10	20.68	0.149	2.779	1.347
13/11	16.83	0.132	2.229	1.359
13/13	14.16	0.136	2.753	1.334
13/14	10.12	0.136	1.750	1.067
13/15	17.20	0.129	2.975	1.442
13/16	12.81	0.129	2.117	1.290
13/17	7.08	0.144	1.272	0.812
13/18	8.88	0.144	2.088	1.012
13/19	11.91	0.144	2.675	1.296
13/20	11.47	0.144	2.096	1.277

D.4 Yao and Teng (2007)

Table D.4. Peeling Stress Values using Roberts' (1989) Model with Experiments Conducted by Yao and Teng (2007)

Specimen Number	P_{exp} *(kips)*	τ_{int} *(ksi)*	τ_a *(ksi)*	f_{peel} *(ksi)*
CS-C10-A	16.95	0.117	2.134	1.193
CS-C50-A	10.70	0.138	1.664	0.929
CS-A	11.26	0.125	1.572	0.864
CS-L1-A	15.24	0.135	2.031	0.975
CS-L3-A	12.16	0.129	1.687	1.029
CS-W50-A	12.36	0.139	2.555	1.457
CS-W100-A	11.96	0.137	2.022	1.144
CP-A	10.21	0.136	1.257	0.703
SP-A	10.32	0.133	1.357	0.630
GS-A	17.18	0.138	1.950	1.443
CS-NS-B	13.04	0.136	0.319	0.174
CS-C10-B	22.35	0.117	0.502	0.281
CS-C50-B	18.64	0.138	0.517	0.289
CS-B	18.32	0.125	0.453	0.249
CS-L1-B	16.82	0.135	0.373	0.179
CS-L3-B	17.65	0.129	0.458	0.279
CS-W50-B	16.03	0.139	0.597	0.340
CS-W100-B	18.17	0.137	0.552	0.312
CP-B	17.09	0.136	0.342	0.191
SP-B	15.35	0.133	0.412	0.191
GS-B	18.43	0.138	0.328	0.242

APPENDIX E

COLOTTI, SPADEA, AND SWAMY'S (2004) PLATE END SHEAR MODEL SAMPLE CALCULATIONS

E.1 Oehlers (1992)

E.1.1 Specimen 2/2/S

Reported Parameters:

$b = 130mm = 5.12in.$ $b_p = 130mm = 5.12in.$

$h = 175mm = 6.89in.$ $l_a = 475mm = 18.70in.$

$d_s = 147mm = 5.79in.$ $a = 550mm = 21.65in.$

$A_s = 402mm^2 = 0.62in.^2$ $d_b = 16mm = 0.63in.$

$f'_c = 47MPa = 6.82ksi$ $A_v = 25.1mm^2 = 0.039in.^2$

$f'_t = 4.3MPa = 0.62ksi$ $f_{yt} = 568MPa = 82.38ksi$

$c_c = 28mm = 1.10in.$ $s = 75mm = 2.95in.$

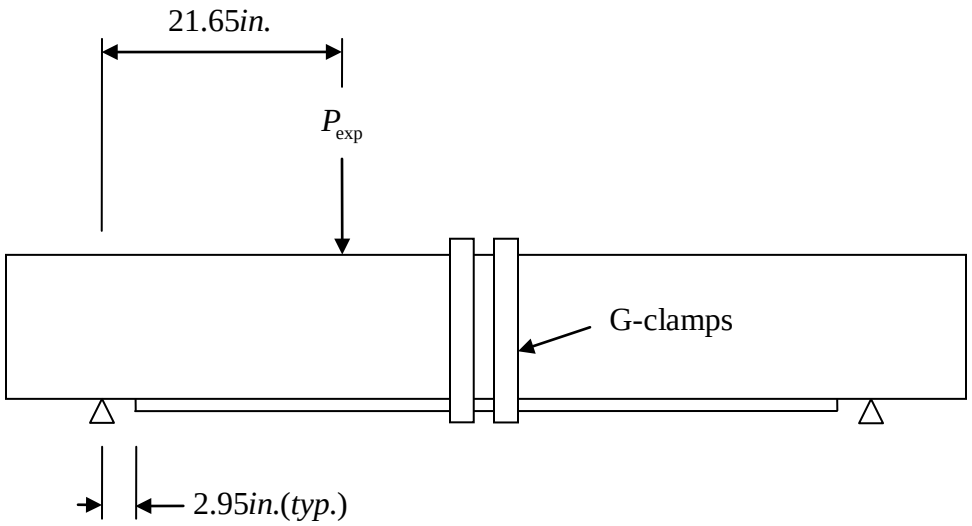

Figure E.1a. Specimen 2/2/S Experimental Set-up used by Oehlers (1992)

$$V_{th} = p_y d\left[\phi + \alpha - \sqrt{(\phi+\alpha)^2 - 2\phi\beta}\right] \;;\quad p_y > 0$$

where $\alpha = \frac{a}{d}$, $\beta = \frac{l_a}{d}$, and $\phi = \frac{U_y}{p_y}$

Calculate the strength of the transverse reinforcement, p_y.

$$p_y = \frac{A_v f_{yt}}{s}$$
$$p_y = \frac{0.039(82.38)}{2.95} = 1.09 kip/in.$$

The bond strength, U_y, is the minimum of the two equations:

1) $U_y = b_m[0.40175 + 0.06(f'_c - 2.9)]$ for $f'_c > 2.9 ksi$

2) $U_y = \frac{f'_t l_c b}{6 c_c}$

For the first bond strength equation, calculate the effective width of the plate-adhesive interface, b_m.

$$b_m = \frac{(b + b_p)}{2}$$
$$b_m = \frac{(5.12 + 5.12)}{2} = 5.12 in.$$

For the second bond strength equation, if tensile strength of the concrete, f'_t, is not specified, it may be taken as

$f'_t = 0.2049 * f_{ce}^{2/3}$ where $f_{ce} = \nu_c f'_c$ and $\nu_c = 0.7$

Since tensile strength of the concrete was reported as 0.624 ksi, this value will be used in computing the bond strength. Now, the crack spacing size, l_c, may be calculated as

$l_c = 1.9685 + 0.25 k_1 k_2 d_b / \rho_r$ where $k_1 = 0.8$ and $k_2 = 0.5$.

The effective tensile steel reinforcement ratio, ρ_r, and the crack spacing size, l_c, are

$$\rho_r = \frac{A_{se}}{2.5 b c_c} \text{ where } A_{se} = \frac{1}{2} A_s$$
$$\rho_r = \frac{1/2(0.62)}{2.5(5.12)(1.10)} = 0.022$$

$$l_c = 1.9685 + 0.25(0.8)(0.5)(0.63)/(0.022) = 4.82 in.$$

Now, determine the bond strength, U_y.

1) $U_y = 5.12\left[0.40175 + 0.06(6.82 - 2.9)\right] = 3.26 kip/in.$

2) $U_y = \dfrac{(0.62)(4.82)(5.12)}{6(1.10)} = 2.33 kip/in.$

$U_y = \min(3.26, 2.33) = 2.33 kip/in.$

Calculate the parameters, $\alpha = \dfrac{a}{d}$, $\beta = \dfrac{l_a}{d}$, and $\phi = \dfrac{U_y}{p_y}$, where $d = 0.9h$.

$$\alpha = \frac{21.65}{0.9(6.89)} = 3.49$$
$$\beta = \frac{18.70}{0.9(6.89)} = 3.02$$
$$\phi = \frac{2.33}{1.09} = 2.14$$

Find the theoretical shear load, V_{th}, at the plate end when debonding occurs.

$$V_{th} = 0.9(1.09)(6.89)\left[2.14 + 3.49 - \sqrt{(2.14 + 3.49)^2 - 2(2.14)(3.02)}\right] = 8.73 kips$$

$V_{th} = 8.73 kips = 38.8 kN$ Matches the theoretical results from Colotti et al. (2004).

Specimen 2/2/S failed by plate end debonding. The experimental ultimate shear force, $V_{\exp}$, at the point of plate termination was 9.85 kips (43.8 kN).

E.1.2 Specimen 2/4/S

Reported Parameters:

$b = 130mm = 5.12in.$	$b_p = 130mm = 5.12in.$
$h = 175mm = 6.89in.$	$l_a = 475mm = 18.70in.$
$d_s = 147mm = 5.79in.$	$a = 550mm = 21.65in.$
$A_s = 402mm^2 = 0.62in.^2$	$d_b = 16mm = 0.63in.$
$f'_c = 47MPa = 6.82ksi$	$A_v = 56.55mm^2 = 0.088in.^2$
$f'_t = 4.3MPa = 0.62ksi$	$f_{yt} = 511MPa = 74.11ksi$
$c_c = 28mm = 1.10in.$	$s = 45mm = 1.77in.$

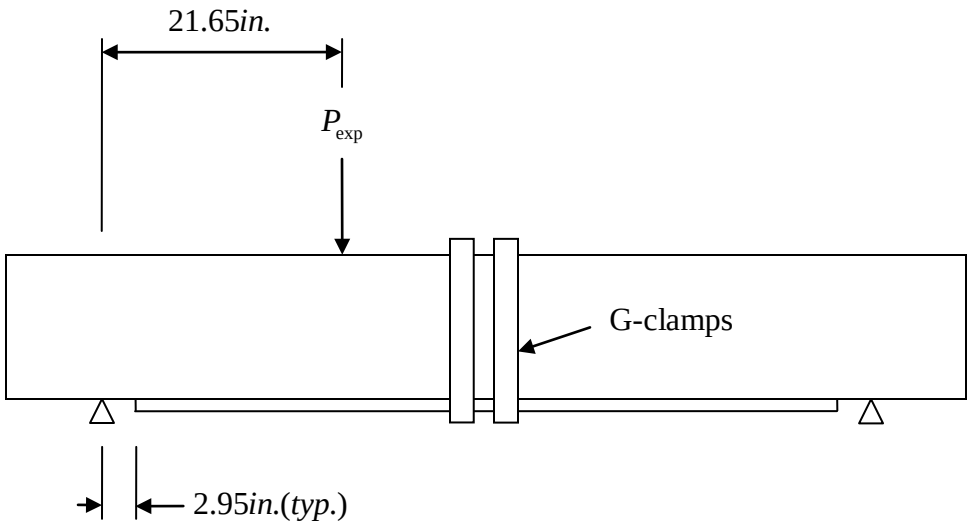

Figure E.1b. Specimen 2/4/S Experimental Set-up used by Oehlers (1992)

$$V_{th} = p_y d\left[\phi + \alpha - \sqrt{(\phi+\alpha)^2 - 2\phi\beta}\right] \;;\quad p_y > 0$$

$$\text{where } \alpha = \frac{a}{d},\ \beta = \frac{l_a}{d}, \text{ and } \phi = \frac{U_y}{p_y}$$

Calculate the strength of the transverse reinforcement, p_y.

$$p_y = \frac{A_v f_{yt}}{s}$$

$$p_y = \frac{0.088(74.11)}{1.77} = 3.67 kip/in.$$

The bond strength, U_y, is the minimum of the two equations:

1) $U_y = b_m\left[0.40175 + 0.06(f'_c - 2.9)\right]$ for $f'_c > 2.9 ksi$

2) $U_y = \dfrac{f'_t\, l_c b}{6c_c}$

For the first bond strength equation, calculate the effective width of the plate-adhesive interface, b_m.

$$b_m = \frac{(b + b_p)}{2}$$

$$b_m = \frac{(5.12 + 5.12)}{2} = 5.12in.$$

For the second bond strength equation, if tensile strength of the concrete, f'_t, is not specified, it may be taken as

$f'_t = 0.2049 * f_{ce}^{2/3}$ where $f_{ce} = \nu_c f'_c$ and $\nu_c = 0.7$

Since tensile strength of the concrete was reported as 0.62 ksi, this value will be used in computing the bond strength. Now, the crack spacing size, l_c, may be calculated as

$l_c = 1.9685 + 0.25 k_1 k_2 d_b / \rho_r$ where $k_1 = 0.8$ and $k_2 = 0.5$.

The effective tensile steel reinforcement ratio, ρ_r, and the crack spacing size, l_c, are

$$\rho_r = \frac{A_{se}}{2.5 b c_c} \text{ where } A_{se} = \frac{1}{2} A_s$$
$$\rho_r = \frac{1/2(0.62)}{2.5(5.12)(1.10)} = 0.022$$

$$l_c = 1.9685 + 0.25(0.8)(0.5)(0.63)/(0.022) = 4.82in.$$

Now, determine the bond strength, U_y.

1) $U_y = 5.12[0.40175 + 0.06(6.82 - 2.9)] = 3.26 kip/in.$
2) $U_y = \frac{(0.62)(4.82)(5.12)}{6(1.10)} = 2.33 kip/in.$

$U_y = \min(3.26, 2.33) = 2.33 kip/in.$

Calculate the parameters, $\alpha = \frac{a}{d}$, $\beta = \frac{l_a}{d}$, and $\phi = \frac{U_y}{p_y}$, where $d = 0.9h$.

$$\alpha = \frac{21.65}{0.9(6.89)} = 3.49$$
$$\beta = \frac{18.70}{0.9(6.89)} = 3.02$$
$$\phi = \frac{2.33}{3.67} = 0.63$$

Find the theoretical shear load, V_{th}, at the plate end when debonding occurs.

$$V_{th} = 0.9(3.67)(6.89)\left[0.63 + 3.49 - \sqrt{(0.63 + 3.49)^2 - 2(2.14)(3.02)}\right] = 11.21 kips$$

$V_{th} = 11.21 kips = 49.87 kN$ Matches the theoretical results from Colotti et al. (2004).

Specimen 2/4/S failed by plate end debonding. The experimental ultimate shear force, $V_{\exp}$, at the point of plate termination was 10.09 kips (44.9 kN).

APPENDIX F

PLATE END SHEAR VALUES USING COLOTTI, SPADEA, AND SWAMY'S (2004) MODEL

F.1 Swamy, Jones, and Bloxham (1987)

Table F.1. Plate End Shear Values using Colotti et al. (2004) Model with Experiments Conducted by Swamy et al. (1987)

Specimen Number	P_{exp} *(kips)*	V_{exp} *(kips)*	U_y *(kip/in.)*	V_{th} *(kips)*	$\frac{V_{exp}}{V_{th}}$
201*	52.16	26.08	--	--	--
202*	55.08	27.54	--	--	--
203	60.70	30.35	1.91	11.99	2.53
204	60.70	30.35	1.92	12.02	2.52
205	47.88	23.94	1.93	12.05	1.99
206	49.46	24.73	1.92	12.02	2.06
207	58.90	29.45	1.94	12.11	2.43
208	59.35	29.67	1.92	12.02	2.47
209	49.46	24.73	1.92	12.04	2.05
210	48.33	24.17	1.92	12.04	2.01
211	56.88	28.44	1.96	12.19	2.33
212	55.75	27.88	1.90	11.94	2.33
213	56.88	28.44	1.91	11.99	2.37
214	56.88	28.44	1.92	12.04	2.36
215	56.20	28.10	1.95	12.17	2.31
216	58.90	29.45	1.93	12.05	2.44
217	57.78	28.89	1.92	12.02	2.40
218	43.61	21.81	1.95	12.17	1.79
219	49.46	24.73	1.98	12.29	2.01
220	59.12	29.56	1.92	12.02	2.46
221	60.25	30.12	1.92	12.0	2.51
222	60.25	30.12	1.90	11.96	2.52
223	59.35	29.67	1.97	12.25	2.42
224	56.20	28.10	1.95	12.17	2.31

*Specimens 201 and 202 did not have external reinforcement.

F.2 Jones, Swamy, and Charif (1988)

Table F.2. Plate End Shear Values using Colotti et al. (2004) Model with Experiments Conducted by Jones et al. (1988)

Specimen Number	P_{exp} *(kips)*	V_{exp} *(kips)*	U_y *(kip/in.)*	V_{th} *(kips)*	$\frac{V_{exp}}{V_{th}}$
F31	40.92	20.46	1.61	11.22	1.82
F32	46.76	23.38	1.61	11.22	2.08
F33	42.94	21.47	1.61	11.22	1.91
F34	49.68	24.84	1.61	11.22	2.21
F35	51.03	25.52	1.61	11.22	2.27
F36	64.07	32.04	1.61	11.22	2.86
F37	63.62	31.81	1.61	11.22	2.84

F.3 Oehlers and Moran (1990)

Table F.3. Plate End Shear Values using Colotti et al. (2004) Model with Experiments Conducted by Oehlers and Moran (1990)

Specimen Number	P_{exp} *(kips)*	V_{exp} *(kips)*	U_y *(kip/in.)*	V_{th} *(kips)*	$\frac{V_{exp}}{V_{th}}$
1/1	9.19	0.0	1.71	0.0	--
1/2	9.89	0.0	1.71	0.0	--
2/1	12.19	0.0	1.46	0.0	--
2/2	11.49	0.0	1.46	0.0	--
3/1	11.29	0.0	1.41	0.0	--
3/2	10.79	0.0	1.41	0.0	--
3/3	12.59	0.0	1.49	0.0	--
3/4	13.49	0.0	1.49	0.0	--
4/1	12.59	0.0	2.06	0.0	--
4/2	13.99	0.0	2.06	0.0	--
4/3	13.49	0.0	2.11	0.0	--
4/4	14.39	0.0	2.11	0.0	--
5/1	11.49	0.0	1.75	0.0	--
5/2	15.09	0.0	1.75	0.0	--
5/3	11.49	0.0	1.69	0.0	--
5/4	9.89	0.0	1.69	0.0	--
6/1	15.99	0.0	1.59	0.0	--
6/2	12.59	0.0	1.59	0.0	--
6/3	12.59	0.0	1.67	0.0	--
6/4	14.19	0.0	1.67	0.0	--
7/1	9.16	4.58	1.50	3.95	1.16
7/2	9.59	4.80	1.50	5.01	0.96
7/3	8.39	4.20	1.52	6.86	0.61
7/4	5.61	2.81	1.52	8.08	0.35
8/1	9.81	4.91	1.44	3.82	1.29
8/2	11.28	5.64	1.44	4.85	1.16
8/3	7.30	3.65	1.30	4.94	0.74
8/4	6.16	3.08	1.30	5.98	0.52
9/1	16.69	0.0	1.63	0.0	--
9/2	13.99	0.0	1.63	0.0	--
9/3	13.49	0.0	1.62	0.0	--
9/4	15.29	0.0	1.62	0.0	--
10/1	14.36	0.0	1.79	0.0	--
10/2	12.61	0.0	1.79	0.0	--
10/3	13.08	0.0	1.65	0.0	--
10/4	13.66	0.0	1.65	0.0	--
11/1	14.36	0.0	1.57	0.0	--
11/2	15.30	0.0	1.57	0.0	--

Table F.3 (continued).

Specimen Number	P_{exp} *(kips)*	V_{exp} *(kips)*	U_y *(kip/in.)*	V_{th} *(kips)*	$\frac{V_{exp}}{V_{th}}$
11/3	9.23	0.0	1.97	0.0	--
11/4	10.74	0.0	1.97	0.0	--
12/1	12.15	0.0	1.62	0.0	--
12/2	14.83	0.0	1.49	0.0	--
12/3	19.15	0.0	1.38	0.0	--
12/4	12.38	0.0	1.76	0.0	--
13/6	19.95	0.0	1.94	0.0	--
13/7	19.54	0.0	2.06	0.0	--
13/9	22.61	0.0	2.56	0.0	--
13/10	20.68	0.0	2.56	0.0	--
13/11	16.83	0.0	2.25	0.0	--
13/13	14.16	0.0	1.44	0.0	--
13/14	10.12	0.0	1.44	0.0	--
13/15	17.20	0.0	1.17	0.0	--
13/16	12.81	0.0	1.17	0.0	--
13/17	7.08	0.0	1.18	0.0	--
13/18	8.88	0.0	1.18	0.0	--
13/19	11.91	0.0	1.73	0.0	--
13/20	11.47	0.0	1.73	0.0	--

F.4 Oehlers (1992)

Table F.4. Plate End Shear Values using Colotti et al. (2004) Model with Experiments Conducted by Oehlers (1992)

Specimen Number	P_{exp} *(kips)*	V_{exp} *(kips)*	U_y *(kip/in.)*	V_{th} *(kips)*	$\frac{V_{exp}}{V_{th}}$
2/2/N	9.85	9.85	2.33	4.31	2.28
2/2/S	9.85	9.85	2.33	8.73	1.13
2/3/N	10.09	10.09	2.33	5.26	1.92
2/3/S	10.16	10.16	2.33	10.44	0.97
2/4/N	10.36	10.36	2.33	5.72	1.81
2/4/S	10.09	10.09	2.33	11.21	0.90
5/1/N	10.32	10.32	2.54	3.66	2.82
5/1/S	9.87	9.87	2.54	10.10	0.98

*****Although the failure load was not reported, the failure load and shear load at the plate end were assumed to be the same.

F.5 Yao and Teng (2007)

Table F.5. Plate End Shear Values using Colotti et al. (2004) Model with Experiments Conducted by Yao and Teng (2007)

Specimen Number	P_{exp} *(kips)*	V_{exp} *(kips)*	U_y *(kip/in.)*	V_{th} *(kips)*	$\frac{V_{exp}}{V_{th}}$
CS-C10-A	16.95	0.0	2.48	0.0	--
CS-C50-A	10.70	0.0	2.18	0.0	--
CS-A	11.26	0.0	2.64	0.0	--
CS-L1-A	15.24	0.0	2.85	0.0	--
CS-L3-A	12.16	0.0	2.73	0.0	--
CS-W50-A	12.36	0.0	1.98	0.0	--
CS-W100-A	11.96	0.0	2.43	0.0	--
CP-A	10.21	0.0	2.88	0.0	--
SP-A	10.32	0.0	2.82	0.0	--
GS-A	17.18	0.0	2.94	0.0	--
CS-NS-B	13.04	8.69	2.36	7.96	1.09
CS-C10-B	22.35	14.90	2.48	17.52	0.85
CS-C50-B	18.64	12.42	2.18	15.63	0.79
CS-B	18.32	12.22	2.64	18.46	0.66
CS-L1-B	16.82	11.21	2.85	19.70	0.57
CS-L3-B	17.65	11.77	2.73	19.0	0.62
CS-W50-B	16.03	10.69	1.98	14.51	0.74
CS-W100-B	18.17	12.11	2.43	17.28	0.70
CP-B	17.09	11.39	2.88	19.87	0.57
SP-B	15.35	10.24	2.82	19.57	0.52
GS-B	18.43	12.29	2.94	20.18	0.61

REFERENCES

AASHTO. (2007). *AASHTO LRFD Bridge Design Specification Fourth Edition.* American Association of State Highway and Transportation Officials, Washington, D.C.

ACI Committee 318. (2005). "Building Code Requirements for Structural Concrete and Commentary." *ACI 318-05*, American Concrete Institute, Detroit, Michigan.

ACI Committee 318. (2008). "Building Code Requirements for Structural Concrete and Commentary." *ACI 318-08*, American Concrete Institute, Detroit, Michigan.

ACI Committee 440. (2008). "Guide for the Design and Construction of Externally Bonded FRP Systems for Strengthening Concrete Structures." *ACI 440-08*, American Concrete Institute, Detroit, Michigan.

Arduini, M. and Nanni, A. (1997). "Behavior of precracked RC beams strengthened with carbon FRP sheet." *Journal of Composites for Construction*. American Society of Civil Engineers, 1(2), 63-70.

ASTM Standard D3039/D3039 M. (2008). "Standard Test Method for Tensile Properties of Polymer Matrix Composite Materials." ASTM International, West Conshohocken, PA, www.astm.org.

ASTM Standard D7290. (2006). "Standard Practice for Evaluating Material Property Characteristic Values for Polymeric Composites for Civil Engineering Structural Applications." ASTM International, West Conshohocken, PA, www.astm.org.

Colotti, Vincenzo et al. (2004). "Structural Model to Predict the Failure Behavior of Plated Reinforced Concrete Beams." *Journal of Composites for Construction.* American Society of Civil Engineers, 8(2), 104-122.

"Conversion between Cube and Cylinder Strengths." Retrieved May 18, 2009, from http://www.logicsphere.com/products/firstmix/hlp/html/stre4s9w.htm

Duthinh, Dat and Starnes, Monica. (2004). "Strength and Ductility of Concrete Beams Reinforced with Carbon Fiber-Reinforced Polymer Plates and Steel." *Journal of Composites for Construction.* American Society of Civil Engineers, 8(1), 59-69.

GangaRao, H. V. S. et al. (2007). *Reinforced concrete design with FRP composites.* Boca Raton: CRC Press.

Hollaway, L. C. and Leeming, M.B. (1999). *Strengthening of Reinforced Concrete Structures - Using Externally Bonded FRP Composites in Structural and Civil Engineering.* Cambridge, England: Woodhead Publishing Limited.

Jones, R. et al. (1988). "Plate Separation and Anchorage of Reinforced Concrete Beams Strengthened by Epoxy-Bonded Steel Plates." *The Structural Engineer*, 66(5), 85-94.

Malek, A.M. et al. (1998). "Prediction of failure load of R/C beams strengthened with FRP plate due to stress concentration at the plate end." *ACI Structural Journal*. American Concrete Institute, 95(1), 142-152.

Moran, John P. (1988, June). "Separation of Externally Bonded Steel Plates from Reinforced Concrete Beams in Flexure." A thesis submitted to the National University of Ireland in candidature for the degree of Master of Engineering Science, University College Cork, Cork, Ireland.

Oehlers, D. J. and Moran, J.P. (1990). "Premature Failure of Externally Plated Reinforced Concrete Beams." *Journal of Structural Engineering*. American Society of Civil Engineers, 116(4), 978-995.

Oehlers, D.J. and Seracino, R. (2004). *Design of FRP and Steel Plated RC Structures: Retrofitting Beams and Slabs for Strength, Stiffness and Ductility*. UK: Elsevier.

Roberts, T. M. (1989). "Approximate Analysis of Shear and Normal Stress Concentrations in the Adhesive Layer of Plated RC Beams." *The Structural Engineer*, 67(12), 229-233.

Saadatmanesh, Hamid and Ehsani, Mohammad R. (1991). "RC beams strengthened with GFRP plates, I: Experimental Study." *Journal of Structural Engineering*. American Society of Civil Engineers, 117(11), 3417-3433.

Spadea, G. et al. (1998). "Structural behaviour of composite RC beams with externally bonded CFRP." *Journal of Composites for Construction*. American Society of Civil Engineers, 2(3), 132-137.

Swamy, R. N. et al. (1986). "Shear adhesion properties of epoxy resin adhesive." *Proceedings of International Symposium*, 741-755.

Swamy, R. N. et al. (1987). "Structural Behavior of Reinforced Concrete Beams Strengthened by Epoxy-Bonded Steel Plates." *The Structural Engineer*, 65A(2), 59-68.

Swamy, R.N. et al. (1999). "Strengthening for shear of RC beams by external plate bonding." *Structural Engineering*, 77(12), 19-30.

Teng, J.G. et al. (2002). *FRP-Strengthened RC Structures*. UK: John Wiley and Sons, Ltd.

Teng, J.G. et al. (2003). "Intermediate Crack Induced Debonding in RC Beams and Slabs." *Construction and Building Materials*, 17(6/7), 447-462.

Teng, J.G. et al. (2004). "Recent Research on Intermediate Crack Induced Debonding in FRP Strengthened Beams." *Proceedings of the 4th International Conference on Advanced Composite Materials for Bridges and Structures*. Calgary.

Todeschini, C.E. et al. (1964). "Behavior of concrete columns reinforced with high strength steels." *ACI Structural Journal*. American Concrete Institute, 61(6), 701-716.

Wang, N. et al. (In press). "Reliability Based Evaluation of Flexural Members Strengthened with Externally Fiber Reinforced Polymer Composites." *Journal of Structural Engineering*. American Society of Civil Engineers, 136.

Wang, N. et al. (2009). "Condition assessment of existing bridge structures: Report of Task 1 – Appraisal of state-of-the-art of bridge condition assessment." GDOT Project RP05-01._(ftp://ftp.dot.state.ga.us/DOTFTP/Anonymous-Public/Research_Projects/)

Yao, J. and Teng, J.G. (2007). "Plate End Debonding in FRP-Plated RC beams-I: Experiments." *Engineering Structures*, 29, 2457-2471.

Yao, Jian. (2004, October). "Debonding Failures in RC Beams and Slabs Strengthened with FRP Plates." A thesis submitted in partial fulfillment of the requirements for the degree of Doctor of Philosophy, The Hong Kong Polytechnic University, Hong Kong, China.

Zureick, A. et al. (2002). "Strengthening of reinforced concrete bridge deck slabs with shop-manufactured carbon composite plates." Final Report prepared for Georgia Department of Transportation and the Federal Highway Administration, Structural Engineering, Mechanics, and Materials Research Report No. 02-3, Georgia Institute of Technology. (http://reports.ce.gatech.edu/documents/Zureick_Kahn_and_Kim_2001.pdf)

Zureick, Abdul-Hamid et al. (2009). "Guide Specification for the Design of Bonded FRP Systems for Repair and Strengthening of Concrete Bridge Elements." Final Report prepared for National Cooperative Highway Research Program Transportation Research Board National Research Council, *NCHRP Project 10-73*.